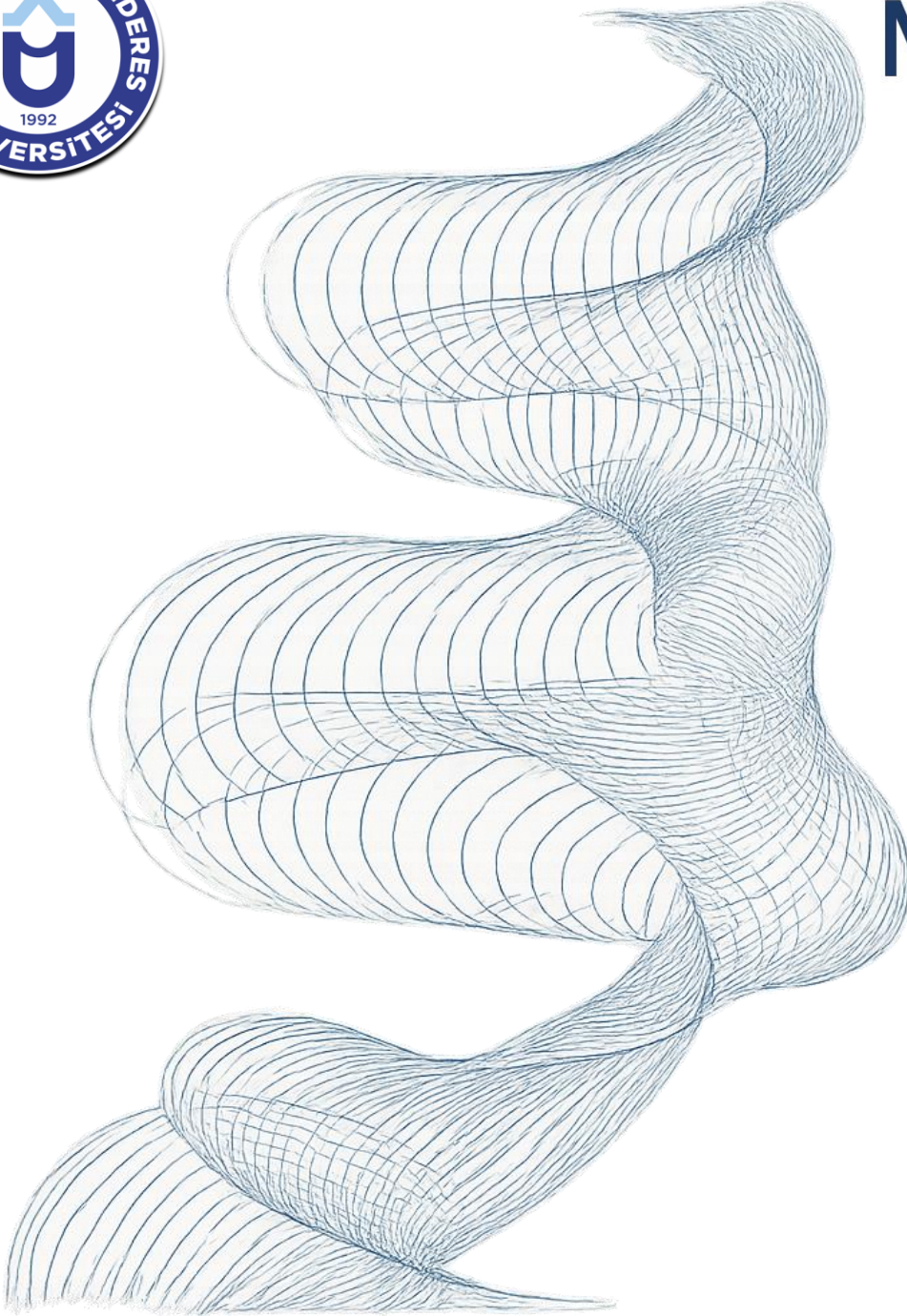


MEANDROS

MEDICAL AND DENTAL

JOURNAL



Year: 2025 June
Volume : 26
Issue: 2

**THE OFFICIAL JOURNAL OF AYDIN ADNAN MENDERES UNIVERSITY
FACULTIES OF MEDICINE AND DENTISTRY**

Citation Abbreviation: Meandros Med and Dental J
Formerly: Adnan Menderes Tıp Fakültesi Dergisi

© 2025 Meandros Medical and Dental Journal
e-ISSN: 2149-9063



<https://dergipark.org.tr/en/pub/meandrosmdj>



EDITORIAL BOARD

Editor in Chief

Seda ÖRENAY BOYACIOĞLU

Aydın Adnan Menderes University Faculty of Medicine,
Department of Medical Genetics, Aydın, Türkiye ORCID:
0000-0003-1651-1940

Associate Editors

Esra TALAY ÇEVLİK

Aydın Adnan Menderes University Faculty of Dentistry,
Department of Prosthodontics, Aydın, Türkiye ORCID:
0000-0002-8898-6710

Mahmut Alp KILIÇ

Aydın Adnan Menderes University Faculty of Medicine,
Department of Biophysics, Aydın, Türkiye ORCID: 0000-
0003-2645-1988

Secretary & Layout Editors

Umut Kerem KOLAÇ

Aydın Adnan Menderes University Faculty of Medicine,
Department of Medical Biology, Aydın, Türkiye ORCID:
0000-0003-0266-9069

Bakiye GÖKER BAĞCA

Aydın Adnan Menderes University Faculty of Medicine,
Department of Medical Biology, Aydın, Türkiye ORCID:
0000-0002-5714-7455

İlkim Pınar SARAL

Aydın Adnan Menderes University Faculty of Dentistry,
Department of Endodontics, Aydın, Türkiye ORCID:
0000-0003-1278-7464

Hüseyin ŞEKER

Aydın Adnan Menderes University Faculty of Dentistry,
Department of Prosthodontics, Aydın, Türkiye ORCID:
0000-0002-6690-3267

Issue Editors

Seda ÖRENAY BOYACIOĞLU

Aydın Adnan Menderes University Faculty of
Medicine, Department of Medical Genetics, Aydın,
Türkiye ORCID: 0000-0003-1651-1940

Mahmut Alp KILIÇ

Aydın Adnan Menderes University Faculty of
Medicine, Department of Biophysics, Aydın, Türkiye
ORCID: 0000-0003-2645-1988

Bakiye GÖKER BAĞCA

Aydın Adnan Menderes University Faculty of
Medicine, Department of Medical Biology, Aydın,
Türkiye ORCID: 0000-0002-5714-7455

Hicran DÖNMEZ ÖZKAN

Aydın Adnan Menderes University Faculty of
Dentistry, Department of Clinical Sciences,
Department of Endodontics, Aydın, Türkiye
ORCID:0000-0002-4495-2746

Yener OKUTAN

Aydın Adnan Menderes University Faculty of
Dentistry, Department of Clinical Sciences,
Department of Prosthetic Dentistry, Aydın, Türkiye,
ORCID:0000-0002-7188-4929

Kadriye ULU GÜZEL

Aydın Adnan Menderes University Faculty of
Dentistry, Department of Pedodontics, Aydın,
Türkiye, ORCID:0000-0002-3129-8490

Gökhan CESUR

Aydın Adnan Menderes University Faculty of
Medicine, Department of Physiology, Aydın, Türkiye,
ORCID: 0000-0002-6943-7521

Yazgı AY ÜNÜVAR

Aydın Adnan Menderes University Faculty of
Dentistry, Department of Ortodontics, Aydın, Türkiye,
ORCID: 0000-0002-1455-9855

CONTENTS

136	Gastrointestinal Manifestations Of Mature B Cell Neoplasms: Single Center Experiences From The Collective Perspective Of Hematology And Pathology <i>Ufuk DEMİRCİ, Busem BİNBÖĞA KURT, Tuğcan Alp KIRKIZLAR, Hakkı Onur KIRKIZLAR, Elif Gülsüm ÜMİT, Fulya ÖZ PUYAN, Ahmet Muzaffer DEMİR</i>
144	Arm And Leg Dominance Does Not Affect Functional Balance Tests <i>Emre SÖYLEMEZ, Mehmet CAN</i>
151	The Impact of Increased Platelet Count On Erythrocyte Aggregation in Obese Individuals Without Cardiovascular Disease <i>Serpil ÇEÇEN, Zozan GÜLEKEN</i>
157	Objective Lens Densitometry Evaluation Using Scheimpflug Topography in Children After Covid- 19 Infection <i>Onur KALAY, Ayşe İpek AKYÜZ ÜNSAL, Erol ERKAN, Sayime AYDIN EROĞLU, Sinan BEKMEZ, Esin TUNCA KIRIKKAYA, İmran KURT ÖMÜRLÜ</i>
164	Effect of Extended Polymerization Times on the Degree of Conversion and Microhardness of Resin Composites <i>Tuğçe ERDEM, Sezer DEMİRBUĞ, Hacer BALKAYA</i>
170	Evaluation of the Connections of Different Type of Abutments to the Implant Body Under Mastication <i>Yezdan Dilan ERKCAN, Mehmet Ali KILIÇARSLAN, Bora AKAT, Burak BILECENOĞLU, Kaan ORHAN</i>
177	Psychological Comparison of Adults with Dizziness: Depression, Anxiety, and Somatization in Typical vs. Abnormal Vestibular Test Results <i>Hanifi KORKMAZ, Ahmet KUTLUHAN, Banu MUJDECİ, Erkan KARATAŞ</i>
185	Investigation of the Effect Of 25(Oh)D3 Levels on the Disease Severity and the Course of the Treatment in Active Pulmonary Tuberculosis Patients <i>Esmâ Seda AKALIN KARACA, Gönenç ORTAKÖYLÜ</i>
193	Evaluation of the Effectiveness of Different Cleaning Methods for Removable Space Maintainers <i>Ceren SAĞLAM, Dilşah ÇOĞULU, Ayla Beyza ÇENGEL, Yasemin YİĞİT, Ataç UZEL</i>
199	The Success of Post-Endodontic Restorations Using Different Restorative Materials: A Two year Follow-Up Study <i>Sait GÜLLÜ, Emre ÇULHA, Uğur AYDIN, Muazzez Naz BAŞTÜRK ÖZER</i>
206	A Comparative Analysis of Angular Cephalometric Measurements Using Vistadent and Nemoceph Digital Software <i>Fundagül BİLGİÇ ZORTUK, Eyüp Burak KÜÇÜK</i>
211	Clinicopathological Significance of Immunohistochemical Pd-L1 and Androgen Receptor Expressions in Triple Negative Breast Cancers <i>Büşra EKİNCİ, Nesibe KAHRAMAN ÇETİN, İbrahim Halil ERDOĞDU, İbrahim METEOĞLU</i>
219	Temperature Change in the Pulp Chamber Induced by Different Light Curing Units in Simulated Deep Cavities <i>Yağmur KILIÇ, Mustafa Mert TULGAR</i>
226	Diagnostic Value of Circulating miRNA-16-5P and miRNA -221-3P in Thyroid Cancer <i>Esin OKTAY, Merve Bıyıklı ALEMDAR, Bilgin DEMİR, İbrahim Halil ERDOĞDU, Nesibe Kahraman ÇETİN, İmran Kurt ÖMÜRLÜ, Engin GÜNEY, Mustafa Gökhan ÜNSAL5</i>

Research Article

GASTROINTESTINAL MANIFESTATIONS OF MATURE B CELL NEOPLASMS: SINGLE CENTER EXPERIENCES FROM THE COLLECTIVE PERSPECTIVE OF HEMATOLOGY AND PATHOLOGY

Ufuk DEMİRCİ^{1*}, Busem BİNBÖĞA KURT², Tuğcan Alp KIRKIZLAR¹, Hakkı Onur KIRKIZLAR¹, Elif Gülsüm ÜMİT¹, Fulya ÖZ PUYAN², Ahmet Muzaffer DEMİR²

¹Department of Hematology, Faculty of Medicine, Trakya University, Edirne, TURKIYE

²Department of Pathology, Faculty of Medicine, Trakya University, Edirne, TURKIYE

*Correspondence: ufukdemirci3232@gmail.com

ABSTRACT

Objective: Hematological malignancies frequently affect the gastrointestinal (GI) tract, either by secondary extranodal or extramedullary extension to the GI tract or as the primary process, developing in the GI tract. Compared to other solid organ tumors of the GI tract, gastrointestinal non-Hodgkin's lymphomas (gNHL) are less common. Therefore, in the absence of nodal or extranodal involvement in imaging methods, difficulties may be encountered in diagnosis.

Materials and Methods: We retrospectively screened all B-cell lymphoma patients. Then, patients, who had been diagnosed without gastrointestinal system biopsy, were excluded from the study. Demographic data for these patients was obtained from the hospital information system and outpatient clinic files. Slides of these patients were obtained from pathology archive and re-evaluated under light microscope by two pathologists.

Results: Fifty-five patients were diagnosed with B-cell lymphoma via endoscopic or colonoscopic biopsies. Forty of these patients were diagnosed with Diffuse Large B-Cell Lymphoma (DLBCL), ten with Marginal Zone Lymphoma (MZL), two with Mantle Cell Lymphoma (MCL), two with Burkitt Lymphoma (BL) and one patient with Lymphoplasmacytic Lymphoma (LPL).

Conclusion: In line with the literature, in our study, the patients with GI tract diagnosis had the highest frequency of DLBCL. The second most common B-cell lymphoma was MALToma. Although the frequency of GI involvement is high in MCL, the number of patients, diagnosed with GI involvement was small. The reason for this was that the patients had been diagnosed on the basis of nodal involvement rather than GI biopsy.

Keywords: non-Hodgkin's lymphomas; B-cell neoplasm; Gastrointestinal lymphomas; Pathology

Received: 02 February 2025

Revised: 17 March 2025

Accepted: 24 March 2025

Published: 23 June 2025



Copyright: © 2025 by the authors. Published by Aydın Adnan Menderes University, Faculty of Medicine and Faculty of Dentistry. This article is openly accessible under the Creative Commons Attribution-NonCommercial 4.0 International (CC BY-NC 4.0) License.

INTRODUCTION

Hematological malignancies consist of a wide range of disorders and comprise lymphoproliferative and myeloproliferative malignancies. In lymphoproliferative diseases, gastrointestinal (GI) system involvement is more common. Lesions in the GI system may be of direct GI origin or may be accompanied by extramedullary or extranodal involvement. In addition, it is observed as extranodal involvement, which is frequently seen in patients with Non-Hodgkin's Lymphoma (NHL) and is difficult to manage. Although primary GI NHL are rare, compared to other GI malignancies (1-4%), it accounts for about 10-15% of all NHL and 30-40% of extranodal involvement (1,2). However, GI involvement is detected in around 50% of autopsy cases (3).

Gastrointestinal non-Hodgkin's lymphomas (gNHL) are less prevalent compared to other solid organ tumours of the GI tract. Therefore, in the absence of nodal or extranodal involvement in imaging methods, there may be difficulties in diagnosis. In terms of diagnosis, hematologists receive a more important support from pathologists compared to from imaging methods. Therefore, providing detailed information to the pathologists about the patient's clinical findings and imaging results is of great importance for diagnosis. The clinician must properly establish this information network.

For pathologists, it is important to evaluate GI biopsies in combination with clinical, endoscopic and radiological findings (Computed tomography (CT), Endoscopy-Colonoscopy, Endoscopic Ultrasonography (EUS), etc.). If B symptoms (fever, night sweats and weight loss) are present, possibility of lymphoma must be considered. However, typical site-related gastrointestinal symptoms, such as dyspepsia, abdominal pain, nausea and vomiting, may be the only manifestation. In some patients, GI lymphoma may be incidentally present. Symptomatic patients may not have typical corresponding endoscopic features (4). Although exophytic, ulcerative or hypertrophic lesions are common, the only endoscopic findings may consist of inflammation-like patterns such as petechia or normal/hyperaemic mucosa (5,6). After gathering the information, distinguishing-especially low grade-lymphomas from inflammatory lesions, is the initial approach of a pathologist to avoid any delays in diagnosis. Dense lymphoid infiltrates with numerous lymphoepithelial lesions, moderate cytological atypia or Dutcher bodies, alongside with features such as muscularis mucosae invasion or ulceration, are considered as alarming for lymphoma diagnosis (7). After the initial

diagnosis, subtyping is essential for determination of treatment decision and prognosis (8).

Under the light of our experiences in our clinic, we aimed to examine our B-cell gNHL patients and to share the approaches by hematologists and pathologists to these patients. In addition, we intended to discuss the management process of these patients from diagnosis to treatment under the light of current literature.

MATERIALS AND METHODS

We retrospectively screened all B-cell lymphoma patients, who had been diagnosed in our clinic between 01.01.2015 and 01.01.2021. Subsequently, patients, who had not been diagnosed via gastrointestinal system biopsy, were excluded from the study. Demographic data for these patients was obtained from the hospital information system and outpatient clinic files. Also, we examined the response rates of the patients to treatment and their follow-up progress with respect to the gastrointestinal system.

Slides of these patients were obtained from pathology archive and re-evaluated under light microscope by two pathologists. All cases were diagnosed in line with revised World Health Organization (WHO) 2017 classification. Immunohistochemical results were obtained from the pathology reports and verified through examination of previously stained slides. Cell of origin (COO) was assessed according to the Hans criteria. According to the Hans criteria, cases were considered positive if 30% or more of the tumor cells were stained by the antibody. The Hans algorithm consisted of three markers (CD10 antibody for Germinal Center (GC) origin, BCL6 antibody for GC and non-GC origin, MUM1 antibody for post-GC origin). Based on combination of these three markers, DLBCL could be classified under two subtypes using the Hans algorithm, namely GC and non-GC.

The Helsinki Declaration of Ethical Principles of Medical Research was followed. Patients signed informed consent. Study approved by Trakya University ethics committee (TÜTF-BAEK 2021/234). Statistical analyses were performed using SPSS PC Ver.26 (IBM © SPSS Inc. USA). Descriptive statistics were given as number, percentage, and arithmetic mean \pm standard deviation. A two-sided p value, smaller than 0.05, was considered significant. Overall survival (OS) was defined as time from diagnosis of lymphoma until death. To evaluate OS, Kaplan-Meier estimates were calculated. Log-rank test

and Cox regression analysis were performed to estimate hazard ratios (HR) and 95% Confidence Intervals (CI).

RESULTS

Fifty-five patients were diagnosed with B-cell lymphoma via endoscopic or colonoscopic biopsies. Forty patients had been diagnosed with Diffuse Large B-Cell Lymphoma (DLBCL), ten patients with Marginal Zone Lymphoma (MZL), two patients with Mantle Cell Lymphoma (MCL), two patients with Burkitt Lymphoma (BL) and one patient with Lymphoplasmacytic Lymphoma (LPL) (Figure 1) / (Table 1).

Table 1: Demographic characteristics of GI Non-Hodgkin lymphoma patients

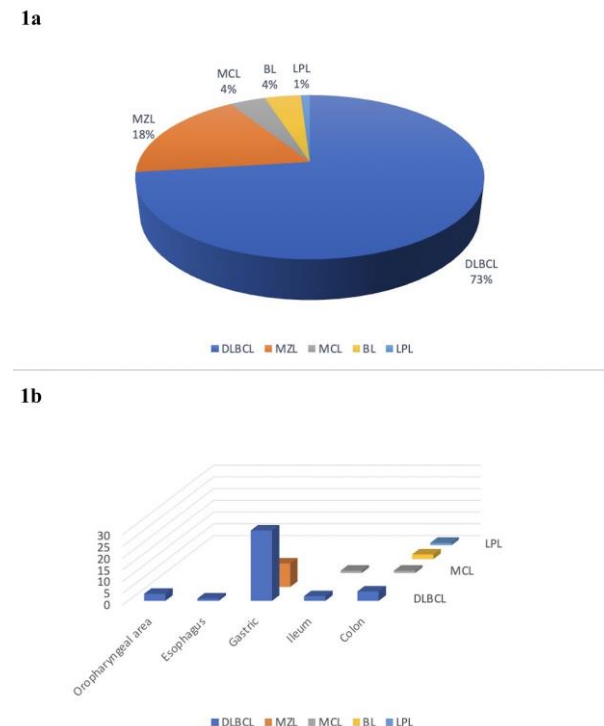
Demographic characteristics of GI Non-Hodgkin lymphoma patients	No. of cases N: 55 (%)
Gender Male/Female	37 / 18 (67/33)
Age	64 years (21-92)
Localization	
Oropharyngeal Area	3 (5,4)
Esophagus	1 (1,8)
Gastric	40 (72,7)
Ileum	3 (5,4)
Colon	8 (14,5)
Histological Type	
DLBCL	40 (72,7)
MZL	10 (18)
MCL	2 (3,6)
BL	2 (3,6)
LPL	1 (1,8)
Isolated GI Involvement	
DLBCL	20/55 (36,3)
MZL	15/40 (37,5)
MCL	5/10 (50)
BL	-
LPL	-
Clinical Symptoms or Signs of Patients Before Diagnosis	
Abdominal Pain	24 (43,6)
Weight loss	19 (34,5)
Vomiting	11 (20)
Dysphagia	2 (3,6)
Perforation	1 (1,8)
Asymptomatic	12 (21,8)

DLBCL: Diffuse large B-cell lymphoma, MCL: Mantle cell lymphoma, MZL: Marginal zone lymphoma, BL: Burkitt lymphoma, LPL: Lymphoplasmacytic lymphoma

Forty out of 55 patients, who had been diagnosed with B Cell NHL with gastrointestinal system involvement, had a diagnosis of Diffuse Large B-Cell Lymphoma. The mean age of DLBCL patients was 65 and 18 patients were female.

The majority of DLBCL patients had been diagnosed on the basis stomach biopsy (75%).

Figure 1. Diagnosis and involvement distribution of B Lymphoma



patients. 1a: Distribution of Patients with gastrointestinal (GI) involvement, 1b: Distribution of involvement regions

Four patients had been diagnosed on the basis of colon biopsy, three on the basis of biopsy of the oropharyngeal area, two on the basis of biopsy of the ileum and one on the basis of esophagus biopsy. Nine of the patients were asymptomatic at diagnosis, 19 patients had abdominal pain, 17 patients had weight loss, 11 patients had vomiting and two patients had dysphagia. One patient presented with perforation. Eighteen patients expressed CD10, BCL6 immunoreactivity and were diagnosed as germinal centre origin immunophenotype in line with the Hans algorithm. Eleven patients were double/triple expressor (c-MYC and BCL2 or c-MYC, BCL2 and BCL6 immunoexpression). When evaluated in terms of prognostic factors, we found that 21 patients had B symptom and 31 patients were diagnosed with high Lactate Dehydrogenase (LDH), 20 patients had R-IPI score > 2 and 26 patients had NCCN-IPI > 3. It was observed that 17 patients had died and seven of the deceased patients could not receive or did not want to receive treatment. Furthermore, ten patients had died in the first month. R-CHOP chemotherapy had been given to all treated patients. Mean survival of patients, who had received treatment, was 39.5 months. It was seen that only ten patients had undergone GI endoscopy after treatment.

Involvement of a different area of the ileum was observed in one patient. GI involvement was not detected in any other patients in the post-treatment setting. Radiological involvement was not detected in other living patients.

Ten patients had been diagnosed with MZL (MALTOMA) and six of these patients were male. Mean age was 67.4 years. Five patients had received treatment for H. Pylori. Also, five patients had received systemic therapy (R-CHOP for four patients, Rituximab for one patient) in line with their stages. Control endoscopy had been performed for all patients during their follow-up. It was observed that 2 patients had relapsed following systemic therapy. Mean follow-up duration of all patients was 47.9 months. No relapsed cases had been found among patients, who had received treatment for H. Pylori. All patients are currently followed-up.

Two patients had been diagnosed with MCL. One patient had been diagnosed on the basis of colon biopsy while another patient on the basis of biopsy of ileum. Both patients were male. Mean age of the patients was 63.5 years old. One of the patients had undergone autologous stem cell transplant (ASCT) following high dose treatment. Relapse disease had been detected in the patient during the first control after ASCT in the same location. Endoscopic control had not been performed in the other patient, instead, patient had been examined using PET / CT. No relapse had been detected. Both patients are currently alive, and the median survival was 21.5 months.

Two patients had been diagnosed with Burkitt's Lymphoma. All of them had been diagnosed on the basis of the colon biopsy. Mean age was 46 years and both patients were male. High-dose treatment had been administered and one patient had died after the first cycle due to sepsis and the other patient had been referred to ASCT due to complete response in control PET/CT. In one patient, LPL diagnosis had been made on the basis of colonoscopy. The 74-year-old male patient had been followed-up for 24 months..

DISCUSSION

Gastric NHLs, which constitute 1-4% of all GI malignancies, are seen most frequently in the stomach (60–75% of all cases) and less frequently in the small intestine and ileocecal area. Histopathological findings in GI tract reveal indolent as well as aggressive lymphomas, which may consist of mature B, T or NK cells. Intestinal B-cell lymphomas are more frequent (6:1) compared to T-cell

lymphomas (3,9). DLBCL and MZL are the most frequently encountered subtypes by the clinician.

On observation of GI tract conditions with a top to bottom approach, it is seen that a wide range of symptoms are observed in these patients. In upper GI tract involvement, patients may present with symptoms such as dysphagia and hoarseness. Symptoms such as abdominal pain, weight loss, nausea and vomiting may be observed in gastric involvement, which is seen in 60-75% of patients with gNHL. Patients with small intestine (%20) and colon (%6-12) involvements may present with clinical symptoms secondary to obstruction, weight loss and bleeding (3,9).

CT and MRI are important in demonstrating not only GI involvement but also other accompanying involvement. Endoscopic ultrasonography is more valuable in GI tract, in particular in case of mucosal involvement. It may also be used in the follow-up of patients following treatment. 18F-fluorodeoxyglucose positron emission tomography (FDG-PET) is frequently used in diagnosis and follow-up. However, histopathological evaluation is recommended for mucosal evaluation after treatment, in particular in patients diagnosed on the basis of stomach biopsy (9).

Main histopathologic groups of gastrointestinal lymphomas consist of mature B-cell lymphomas, T cell lymphomas and NK/T cell lymphomas. Since the most common group is mature B-cell, MALT lymphoma and DLBCL substitutes most of the cases. Other B-cell lymphomas are follicular lymphoma, BL, MCL and rarely lymphomatoid granulomatosis, LPL, EBV-positive DLBCL, high-grade B-cell lymphoma, small lymphocytic lymphoma, ALK-positive large B-cell lymphoma, plasmablastic lymphoma and extramedullary plasmacytoma (10).

Diffuse Large B-Cell Lymphoma is the most common subtype of gNHL. It accounts for 38-57% of gNHL patients. When all GI lymphoma subtypes are considered, it is seen that 40-78% of cases are DLBCL. DLBCL presents as a mass-forming lesion or, less commonly, as an infiltrative lesion (11). There is a tendency to invade nearby structures, which may cause mucosal ulceration and perforation. GI obstruction is less common. However, in case of muscularis propria invasion in small intestine involvement, aneurysmal dilatation may be seen as a result of the destruction of the intramural autonomic nerve plexus. Accompanying intraabdominal lymph node involvement is frequently seen. In treatment, classical R-CHOP regimen has been being used for a long time (9-12).

Consistent with the literature, most of our patients had been diagnosed with (73%) and with the diagnosis had been based on gastric biopsy. Most of the patients (77.5%) had had gastrointestinal system-related symptoms at the time of diagnosis, only nine patients had been asymptomatic. In the follow-ups, 42% of the patients had died. since a significant portion of these patients (58.8%) die within the first month after diagnosis, it must be emphasized that rapid and careful management is required after diagnosis.

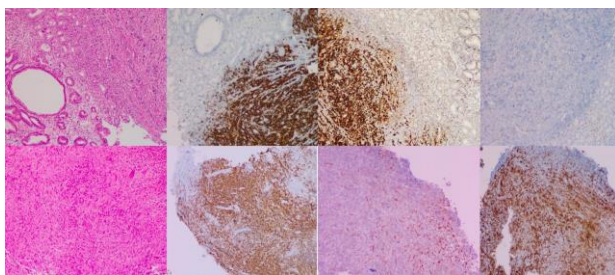


Figure 2. Diffuse large B cell lymphoma microphotographs (x100); Germinal center B cell. Atypical lymphocyte infiltration involving the lamina propria and submucosa of the stomach antrum, with dense crush artifact progressing between glands (A, H&E), CD20 (B) and bcl-6 positive (C), MUM1 negative (D). Activated B cell: Atypical lymphocytes with intense crush artifact infiltrated the submucosa of the antrum (E, H&E), CD20 diffuse positive (F), while CD10 is only positive in stromal cells (G) and MUM1 is strongly positive in atypical lymphocytes (H).

Pathologist perspective (PP); Diffuse large B-cell lymphoma consists of three main morphological variants: centroblastic, immunoblastic and anaplastic. Centroblasts are medium to large-sized cells with vesicular chromatin and 2-4 nucleoli, based on nuclear membrane, whereas immunoblasts have centrally located nucleolus (10). Anaplastic morphology must be distinguished from poorly differentiated carcinoma or melanoma. Neoplastic cells express pan-B cell markers such as CD20, CD19, CD79a and PAX5. Ki67 proliferation index is commonly >40% (13). COO is another important consideration in terms of treatment decision. Germinal center B-cell subtype (GC) is originated from germinal cells, whereas activated B-cell subtype (ABC) is derived from germinal center exit/post germinal center. Hans, et al, have developed an immunohistochemistry-based algorithm, which had high concordance with gene expression profiling, in order to classify cell of origin (14). Accordingly, CD10, BCL6 and IRF/MUM1 are considered positive if $\geq 30\%$ cells are stained. CD10+ or BCL6+ MUM1- refers to GC subtype, whereas BCL6- or BCL6+ MUM1+ refers to ABC subtype. Meyer, et al. (15), have included GCET1 and LMO2 as GC markers and FOXP1 as

ABC marker. HGAL/GCET2 has also been considered as a GC marker (16). CD30 positivity has been observed in 10-20% patients with DLBCL (17). DLBCL lymphoma could also express MYC and BCL2 by immunohistochemistry, in which case, it is called double expressor (18) (Figure 2).

Marginal zone lymphoma is the second most common gNHL, with a frequency of 23-48%. Half of the patients had gastric involvement. H. pylori is an important risk factor and 90% of the patients with MALT lymphoma were positive and antibacterial therapy was sufficient in the majority of cases. Immunoproliferative small intestinal disease (IPSID) is seen in young patients with duodenum involvement and is common in the Middle East. This disease, also called Mediterranean lymphoma, is caused by C. jejuni. FDG-PET or CT may prove inadequate in MZL patients with an indolent lymphoma. Endoscopic methods with histopathological diagnosis are more valuable. In addition to wait and see approach, regimens such as Rituximab single, R-CVP, R-CHOP are used in treatment for patients in need of treatment (1,9, 11, 19).

In line with literature, MALT lymphoma (18%) was the second most common B lymphoma group in our patients. Our patients were also followed-up endoscopically due to the ability of diagnostic biopsy in MALT lymphoma patients with indolent course and since endoscopic methods were better for post-treatment evaluation. Relapse was detected in 20% of the patients at endoscopic follow-up.

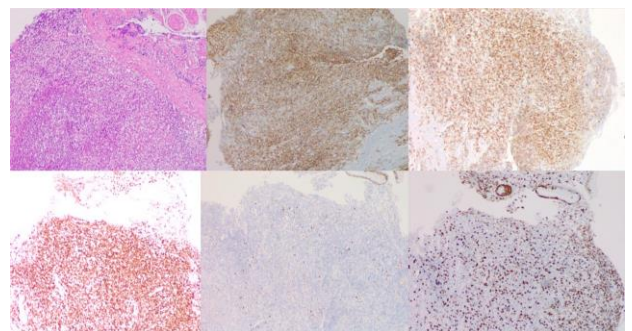


Figure 3. Extranodal marginal zone lymphoma of mucosa, associated lymphoid tissue (MALT lymphoma) microphotographs (x100). Lymphoid proliferation with gland destruction, passing through the muscularis mucosa and spreading to the submucosal area. Secondary follicles accompany this proliferation (A, H&E), atypical lymphocytes are CD20 positive (B), CD5 (C) and CD3 negative (D), CyclinD1 is also negative (E) while Ki67 proliferation index (F) is %20-30.

PP; MALT lymphoma which most frequently exhibits t[11;18] [q21;q21] (20), consists of small lymphoid cells

with irregular and hyperchromatic nucleus. Since there is no specific immunohistochemical profile and diagnosis is generally made by exclusion of other conditions, caution must be exercised to distinguish this tumor from benign reactive lymphoid tissue. Lymphoma cells proliferate in a marginal zone pattern and around reactive follicles, which then form confluent dense areas, leading to follicle replacement [10]. Lymphoepithelial lesions (aggregates of ≥ 3 marginal zone cells with distortion or destruction of the epithelium) and deeper infiltration should be examined carefully. CD20-positive cells may have plasmacytic differentiation, which can be highlighted by kappa and lambda immunostaining (21). CD21 and CD23 may be helpful to highlight the dispersed dendritic cell network. CD5-positivity may be observed in rare cases (22) (Figure 3).

Mantle Cell Lymphoma accounts for 5-13% of gNHL cases. It is known that extranodal involvement is common in MCL and approximately 90% of patients have GI involvement. However, routine screening is not recommended (23). Most patients did not have GI tract involvement at the time of diagnosis. It is detected as small mucosal polyps, often in the small intestine or colon. We think that the number of patients, diagnosed with gastrointestinal biopsy is low, since we do not routinely take endoscopic samples from all MCL patients at the time of diagnosis.

PP; Mantle cell lymphoma consists of small to medium sized monomorphic cell population with different patterns, which may cause diagnostic difficulties: nodular, diffuse, mantle zone and follicular (10). Lymphoma may occur as multiple mucosal polyps, called multiple lymphomatous polyposis (24). MCL is characterized by the translocation t[11;14] [q13;q32] and leads to Cyclin D1 overexpression (25). Main immunohistochemical features are CD5 positivity and BCL6, CD10 and CD23 negativity (may be weakly positive). Cyclin D1 is expressed in most of the cases (including CD5-negative cases) and SOX 11 is highly sensitive even in Cyclin D1-negative cases (26). DLBCL cases, especially those who show CD5 positivity, must be distinguished from blastoid variant of MCL. Cyclin D1 and SOX11 are useful in this aspect (Figure 4). Follicular Lymphoma (FL) is the most common lymphoma among indolent lymphomas. Among nodal lymphomas, FL is the second most common following DLBCL. Extranodal involvement is not common in patients. GI involvement is seen in 5-12% (11,18).

PP; Follicular lymphoma is a relatively rare extranodal lymphoma with gastrointestinal tract involvement, which

generally affects duodenum as primary (27) and which presents as multiple small polyps and subtyped as duodenal type FL with a good prognosis (10). The translocation (14;18) which involves BCL2 locus is observed in most of these cases (28). Follicular lymphoma subtypes, including in situ follicular neoplasia, is characterized by CD10 and BCL2 positivity of the effected germinal centers. This panel is important to distinguish it from reactive follicles. Ki67 proliferation index is usually low and restricted peripheral dendritic cells of the follicle may be highlighted by CD21 (29).

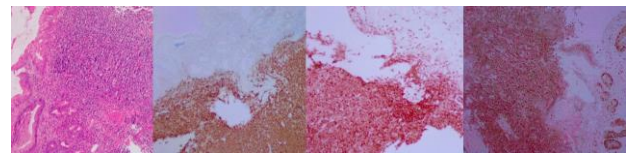


Figure 4. Mantle cell lymphoma microphotographs (x100). Infiltration of medium-sized monotone lymphocytes showing infiltration between antral mucosal glands and towards the submucosal area (A, H&E), CD20 (B) and CD5 (C) diffuse positive, strong immunoreaction of Cyclin D1 (D).

Burkitt's Lymphoma is an aggressive B lymphoma that is less common in adult lymphomas and constitutes 5% of gNHL cases. GI involvement is more common in this sporadic subtype. It is frequently encountered with bulky intraabdominal involvement. High lactate dehydrogenase and tumor lysis are the laboratory indicators, which may be encountered in diagnosis. The c-MYC rearrangement is non-specific, but is often found (11,30).

PP; Burkitt lymphoma is an aggressive tumor, mostly seen in terminal ileum of the gastrointestinal tract (31). Cells of Burkitt lymphoma are usually basophilic and medium-sized with angular borders. Chromatin is usually clumped with multiple nuclei. Tumors are highly proliferative with numerous mitotic figures and apoptosis. Starry sky appearance is due to tingible body macrophages (10). CD20, CD19 and CD79a are positive as well as germinal center markers such as CD10 and BCL6. Ki67 proliferation index is nearly %100 and there is MYC overexpression. Aberrant BCL2 expression may be observed, however, high expressions should be distinguished from high grade B cell lymphomas (32). DLBCL is another differential diagnosis, in particular if it is characterized by medium sized cells. However, BL cells are more monomorphic and Ki67 proliferation index is higher than DLBCL while latter is approximately %40-60 (Figure 5). Radiological

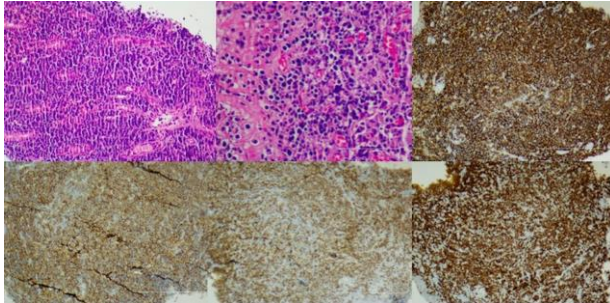


Figure 5. Burkitt lymphoma microphotographs: Dense atypical lymphoid proliferation in lamina propria of the stomach antrum (A, H&E, x100). Cells are monomorphic with coarse chromatin and mitotically active (B, H&E, x400). CD20 (C) and CD10 (D) are diffuse positive, c-myc %90 (E), ki67 proliferation index is %100 (F).

imaging also plays an important role in the diagnosis process. We are routinely using 18FDG PET/CT method for pre- and post-treatment evaluation in malignancies such as DLBCL, BL, MCL, which may show a progressive course and have a high proliferation index. However, similar benefit in indolent malignancies may not be achieved due to slow proliferation of the malignant tissues. Endoscopic methods and CT are more frequently used in the follow-up of these patients. In our study, relapses had been observed by endoscopic method in four patients during follow-up. Two of these patients had indolent disease. However, no relapses had been detected during follow-up by PET/CT and endoscopic imaging was not required for these patients. We think that follow-up can be done by PET/CT. Although we frequently use 18FDG PET/CT for follow-up, it is important to use endoscopic methods, as they can be used for diagnostic purposes as well as imaging.

CONCLUSION

Clinician and pathologist communication is the most important factor in the diagnostic process in gastrointestinal manifestations of mature B-cell neoplasms. Due to its prevalence, clinicians often consider solid malignancies as the initial differential diagnosis for masses in GI tract. In order to clarify the diagnosis and the stage of the disease, the clinical information of the patients must be fully described and transferred by the clinician to the pathologist. The presence of B symptoms, splenomegaly and lymph adenomegaly are important indicators in terms of differential diagnosis. If cytopenias are accompanied by laboratory findings, they must be emphasized and shared with pathologists for accurate diagnosis and clinical management.

Acknowledgments

None

Authorship contributions

UD and BBK planned and designed the study, gathered the data, and performed the statistics. UD and BBK wrote the paper. BBK and FÖP took the pathological pictures. EGU, TAK, HOK supervised. FÖP and AMD reviewed the paper and statistics.

Data availability statement

The authors state that the data supporting the study's results can be found in the article. Additionally, the raw data can be obtained from the corresponding author upon a reasonable request.

Declaration of competing interest

Authors state that they have no conflict of interest.

Ethics

The study was conducted following the Declaration of Helsinki, Ethical Principles for Medical Research, and was approved by the Trakya University Faculty of Medicine Ethical Committee (TÜTF-BAEK2021/234). Consent forms were obtained from the patients for the study. No artificial intelligence-supported technology was used in our study.

Funding

This study was not funded by any financial or governmental authority.



REFERENCES

- 1) Bautista-Quach MA, Ake CD, Chen M, Wang J. Gastrointestinal lymphomas: Morphology, immunophenotype and molecular features. *J Gastrointest Oncol*. 2012 Sep;3(3):209-25.
- 2) Chin CK, Tsang E, Mediawake H, Khair W, Bickler J, Hapgood G, et al. Frequency of bowel perforation and impact of bowel rest in aggressive non-Hodgkin lymphoma with gastrointestinal involvement. *Br J Haematol*. 2019 Mar;184(5):826-828.
- 3) Herrmann R, Panahon AM, Barcos MP, Walsh D, Stutzman L. Gastrointestinal involvement in non-Hodgkin's lymphoma. *Cancer*. 1980 Jul 1;46(1):215-22.
- 4) Small S, Barnea Slonim L, Williams C, Karmali R. B Cell Lymphomas of the GI Tract. *Curr Gastroenterol Rep*. 2021 May 8;23(7):9.
- 5) Tran QT, Nguyen Duy T, Nguyen-Tran BS, Nguyen-Thanh T, Ngo QT, Tran Thi NP, et al. Endoscopic and Histopathological Characteristics of Gastrointestinal Lymphoma: A Multicentric Study. *Diagnostics (Basel)*. 2023 Aug 26;13(17):2767.

- 6) Kanno T, Katano T, Shimura T, Nishigaki R, Kojima Y, Sasaki M, et al. Characteristic endoscopic findings of gastrointestinal malignant lymphomas other than mucosa-associated lymphoid tissue lymphoma. *Acta Gastroenterol Belg*. 2022 Jul-Sep;85(3):477-483.
- 7) Alvarez-Lesmes J, Chapman J.R, Cassidy D, Zhou Y, Garcia-Buitrago M, Montgomery E.A, et al. Gastrointestinal Tract Lymphomas: A Review of the Most Commonly Encountered Lymphomas. *Arch Pathol Lab Med* 1 December 2021; 145 (12): 1585–1596.
- 8) Vetro C, Romano A, Amico I, Conticello C, Motta G, Figuera A, et al. Endoscopic features of gastro-intestinal lymphomas: from diagnosis to follow-up. *World J Gastroenterol*. 2014 Sep 28;20(36):12993-3005.
- 9) Olszewska-Szopa M, Wróbel T. Gastrointestinal non-Hodgkin lymphomas. *Adv Clin Exp Med*. 2019 Aug;28(8):1119-1124.
- 10) Swerdlow SH CE, Harris NL, Jaffe ES, Pileri SA, Stein H. WHO classification of tumours of haematopoietic and lymphoid tissues- Revised 4th edition. World Health Organization Classification of Tumours. 2017.
- 11) Hanafy AK, Morani AC, Menias CO, Pickhardt PJ, Shaaban AM, Mujtaba B, et al. Hematologic malignancies of the gastrointestinal luminal tract. *Abdom Radiol (NY)*. 2020 Oct;45(10):3007-3027.
- 12) Pizzi M, Sabattini E, Parente P, Bellan A, Doglioni C, Lazzi S. Gastrointestinal lymphoproliferative lesions: a practical diagnostic approach. *Pathologica*. 2020 Sep;112(3):227-247.
- 13) Harlendea NJ, Harlendo K. Ki-67 as a Marker to Differentiate Burkitt Lymphoma and Diffuse Large B-cell Lymphoma: A Literature Review. *Cureus*. 2024 Oct 23;16(10):e72190.
- 14) Hans CP, Weisenburger DD, Greiner TC, Gascoyne RD, Delabie J, Ott G, et al. Confirmation of the molecular classification of diffuse large B-cell lymphoma by immunohistochemistry using a tissue microarray. *Blood*. 2004 Jan 1;103(1):275-82.
- 15) Meyer PN, Fu K, Greiner TC, Smith LM, Delabie J, Gascoyne RD, et al. Immunohistochemical methods for predicting cell of origin and survival in patients with diffuse large B-cell lymphoma treated with rituximab. *J Clin Oncol*. 2011 Jan 10;29(2):200-7.
- 16) Gualco G, Bacchi LM, Domeny-Duarte P, Natkunam Y, Bacchi CE. The contribution of HGAL/GCET2 in immunohistological algorithms: a comparative study in 424 cases of nodal diffuse large B-cell lymphoma. *Mod Pathol*. 2012 Nov;25(11):1439-45.
- 17) Hu S, Xu-Monette ZY, Balasubramanyam A, Manyam GC, Visco C, Tzankov A, et al. CD30 expression defines a novel subgroup of diffuse large B-cell lymphoma with favorable prognosis and distinct gene expression signature: a report from the International DLBCL Rituximab-CHOP Consortium Program Study. *Blood*. 2013 Apr 4;121(14):2715-24.
- 18) Peña C, Villegas P, Cabrera ME. Double or triple-expressor lymphomas: prognostic impact of immunohistochemistry in patients with diffuse large B-cell lymphoma. *Hematol Transfus Cell Ther*. 2020 Apr-Jun;42(2):192-193.
- 19) Shirwaikar Thomas A, Schwartz M, Quigley E. Gastrointestinal lymphoma: the new mimic. *BMJ Open Gastroenterol*. 2019 Sep 13;6(1):e000320.
- 20) Matysiak-Budnik T, Priadko K, Bossard C, Chapelle N, Ruskoné-Fourmestraux A. Clinical Management of Patients with Gastric MALT Lymphoma: A Gastroenterologist's Point of View. *Cancers (Basel)*. 2023 Jul 27;15(15):3811.
- 21) Cheah CY, Seymour JF. Marginal zone lymphoma: 2023 update on diagnosis and management. *Am J Hematol*. 2023 Oct;98(10):1645-1657.
- 22) Xia Y, Ge J, Sun Z, Nan F, Wan W, Xu D, et al. CD5-positive marginal zone lymphoma: Clinicopathological features and survival outcomes. *Leuk Res*. 2022 Jun;117:106840.
- 23) Jain P, Wang M. Mantle cell lymphoma: 2019 update on the diagnosis, pathogenesis, prognostication, and management. *Am J Hematol*. 2019 Jun;94(6):710-725.
- 24) Nguyen V, Nguyen B, Petris GD, Nguyen C. Education and imaging. *Gastrointestinal: gastrointestinal involvement of mantle cell lymphoma*. *J Gastroenterol Hepatol*. 2012 Mar;27(3):617.
- 25) Li S, Xu J, You MJ. The pathologic diagnosis of mantle cell lymphoma. *Histol Histopathol*. 2021 Oct;36(10):1037-1051.
- 26) Al-Mansour M. Treatment Landscape of Relapsed/Refractory Mantle Cell Lymphoma: An Updated Review. *Clin Lymphoma Myeloma Leuk*. 2022 Nov;22(11):e1019-e1031.
- 27) Iwamuro M, Tanaka T, Okada H. Review of lymphoma in the duodenum: An update of diagnosis and management. *World J Gastroenterol*. 2023 Mar 28;29(12):1852-1862.
- 28) Fischer L, Dreyling M. Follicular lymphoma: an update on biology and optimal therapy. *Leuk Lymphoma*. 2023 Apr;64(4):761-775.
- 29) Takata K, Sato Y, Nakamura N, Tokunaka M, Miki Y, Yukie Kikuti Y, et al. Duodenal follicular lymphoma lacks AID but expresses BACH2 and has memory B-cell characteristics. *Mod Pathol*. 2013;26(1):22-31.
- 30) Roschewski M, Staudt LM, Wilson WH. Burkitt's Lymphoma. *N Engl J Med*. 2022 Sep 22;387(12):1111-1122.
- 31) López C, Burkhardt B, Chan JKC, Leoncini L, Mbulaiteye SM, Ogwang MD, et al. Burkitt lymphoma. *Nat Rev Dis Primers*. 2022 Dec 15;8(1):78.
- 32) Chong Y, Kim TE, Cho U, Jin MS, Yim K, Thakur N, et al. Comparison of Ki-67 Labeling Index Patterns of Diffuse Large B-Cell Lymphomas and Burkitt Lymphomas Using Image Analysis: A Multicenter Study. *Diagnostics (Basel)*. 2021 Feb 19;11(2):343.

Research Article

ARM AND LEG DOMINANCE DOES NOT AFFECT FUNCTIONAL BALANCE TESTS

 Emre SÖYLEMEZ ¹,  Mehmet CAN ^{2*}

¹ Department of Audiology, Karabuk University, Vocational School of Health Services, Karabuk, TURKIYE

² Department of Audiology, Karamanoğlu Mehmet Bey University, Vocational School of Health Services, Karaman, TURKIYE

*Correspondence: mehmtcan027@gmail.com

ABSTRACT

Objective: Functional balance tests are frequently used to evaluate individuals' balance, monitor rehabilitation outcomes, and determine fall risk. Motor tasks requiring strength and accuracy are performed with the dominant extremities. Therefore, there is a possibility that limb dominance may affect functional balance tests. The literature has no consensus on whether the dominant leg affects balance tests. To our knowledge, there is no study for the dominant arm. The purpose of this study is to investigate whether the dominant leg affects the one-leg standing test (OLST) and tandem stance test (TST), while the dominant arm affects the functional reach test (FRT).

Materials and Methods: One hundred healthy young adults were included in this prospective cross-sectional study. Participants' age, height, and weight were noted, and their body mass index (BMI) was calculated. Participants underwent OLST and TST on the dominant and non-dominant legs. FRT was applied with the dominant and non-dominant arms.

Results: While 93 (93.0%) of the participants were right extremity dominant, 7 (7.0%) were left extremity dominant. There was no difference in terms of OLST, and TST performed with the dominant and non-dominant leg ($p>0.05$). There was no difference in terms of FRT applied with the dominant and non-dominant arms ($p>0.05$).

Conclusion: Our study revealed that leg dominance did not affect OLST and TST, and arm dominance did not affect FRT. The extremity for applying OLST, TST, and FRT can be left to participant preference or applied based on the dominant/non-dominant extremity as appropriate to the situation.

Keywords: Balance, motor dominance, postural control, functional balance, arm

Received: 20 November 2024

Revised: 02 April 2025

Accepted: 06 May 2025

Published: 23 June 2025



Copyright: © 2025 by the authors. Published by Aydın Adnan Menderes University, Faculty of Medicine and Faculty of Dentistry. This article is openly accessible under the Creative Commons Attribution-NonCommercial 4.0 International (CC BY-NC 4.0) License.

INTRODUCTION

Balance and coordination facilitate maintaining posture, performing daily activities such as walking and running, and executing fine motor movements. Sensor and motor functions must work optimally to ensure balance and coordination (1). While sensory functions refer to vestibular, proprioceptive and visual inputs, motor function refers to corrective neuromuscular responses to maintain the centre of gravity vertically on the base of support (2). Impairments in one or more of these functions or impaired coordination between them reduce the quality of life and increase the risk of falls and hospitalization.

Sensory balance systems function in an organized and coordinated manner. The vestibulo-ocular reflex (VOR), which connects the vestibular and visual systems, stabilizes retinal images during head movements (3). For normal VOR gain, eye velocity should be equal to or closely matched with head velocity during head movements. The vestibulo-spinal reflex (VSR), on the other hand, connects the vestibular and proprioceptive systems (4). VSR plays a crucial role in maintaining posture against gravity and regulating muscle activity. In cases of abnormal VSR input, postural control weakens, balance disorders emerge, and coordination impairments may be observed.

Many complex systems, such as computerized dynamic posturography and biodex balance systems, are used to evaluate balance (5). However, accessing these systems is quite difficult and using these devices requires expertise. Balance and falls are interdisciplinary conditions that concern many branches, such as otorhinolaryngology, emergency medicine, neurosurgery and physical therapy. Therefore, functional balance tests are still frequently used to evaluate individuals' balance, monitor rehabilitation outcomes, and determine fall risk. Another advantage of these tests is that static, semi-static and dynamic balance can be quickly evaluated, and the tests can be modified. One-leg standing test (OLST), one of the static tests in which proprioceptive input is reduced, can be applied with eyes open and closed or on hard and soft ground, depending on the appropriate condition. Functional reach test (FRT), one of the semi-static tests, can be applied sitting or standing in the frontal and lateral planes (6). A timed up and go test is frequently preferred to evaluate dynamic balance in single and dual-task conditions.

Functional balance tests, while primarily assessing the coordination between balance systems and postural control, also provide valuable insights into the vestibular system through the VSR. On a firm and stable support

surface in a well-lit environment, healthy individuals rely on the somatosensory system (70%), the visual system (10%), and the vestibular system (20%) (7). However, when the support surface becomes unstable or visual input is obstructed, reliance on vestibular information increases (7). Therefore, modified balance tests conducted with eyes closed or on a soft surface are crucial for evaluating vestibular system function.

Although the human body is anatomically symmetrical, one of the bilateral organs tends to be dominant. This phenomenon is explained by the concept of cerebral lateralization, which refers to the asymmetric distribution of specific functions between the two hemispheres of the brain. Accordingly, morphological and functional differences in the brain hemispheres determine which side of the body exhibits dominance. Studies have suggested that environmental factors such as birth stress, maternal age at delivery, the season of birth, fetal testosterone levels, and fetal position in the womb play a significant role in shaping cerebral lateralization (8-12). On the other hand, some studies indicate that cerebral lateralization is already present by the 15th week of intrauterine development (11). Therefore, genetic factors are thought to play a predominant role in the formation of cerebral lateralization (12).

Motor tasks requiring strength and accuracy are performed with the dominant (or preferred) extremities. Dominant extremities are often used when conducting tests in case leg or arm dominance affects functional balance tests. However, some individuals may have orthopaedic disorders in their dominant extremities and can perform the tests with the non-dominant extremities. Therefore, knowing how dominant and non-dominant extremities affect functional balance scores is important. However, in the studies in the literature, there is no consensus on whether the dominant leg affects balance tests (13). To our knowledge, there is no study for the dominant arm.

The purpose of this study is to investigate whether the dominant leg affects the OLST and tandem stance test (TST), while the dominant arm affects the FRT.

MATERIALS AND METHODS

GPower 3.1 software was used to calculate the sample size. With an effect size of 1.046431, a power of 95%, and a significance level of 0.05, a minimum total sample size of 42 was required for the study (14).

One hundred healthy young adults were included in this prospective cross-sectional study. Written and verbal consent was obtained from the participants. In addition, permission was received from the ethics committee of Karabük University (Decision no: 2023/5). To determine the dominant extremity, individuals were asked which hand they preferred when writing and which foot they used when kicking the ball. In addition, height and weight information were noted, and body mass index (BMI) was calculated. Participants underwent OLST and TST on dominant and non-dominant legs. FRT was applied with dominant and non-dominant arms. Considering the possibility of getting tired, participants were given a one-minute rest period between each test. In addition, since participants' motivation/attention may affect the tests, the testing of 50 individuals was started with the dominant extremity and the testing of 50 individuals was started with the non-dominant extremity. A simple randomization method determined which individual would start the test with the dominant and which with the non-dominant limb. The study did not include individuals with systemic, neurological, or orthopaedic disorders, symptoms such as dizziness/vertigo, and individuals who do professional sports.

One leg standing test

Participants were asked to take off their shoes, fold their arms across their bodies, and lift one leg (dominant or non-dominant). Individuals were asked to stand in this position for 30 seconds, and the time they could stand was recorded with a stopwatch. The test was repeated on hard and soft ground, with eyes open and closed, and with the other leg. The stopwatch was stopped when the individual lost balance, raised his arms, moved his foot to maintain his balance, or opened his eyes.

Tandem stance test

Participants were asked to take off their shoes and place the toe of one foot touching the heel of the other. Like OLST, the time individuals could stand in the desired position was noted. The test was repeated with both the dominant and non-dominant legs, respectively.

Functional reaching test

A tape measure was placed on the wall, and a line was drawn at the start and end points of the tape measure. Participants were asked to stand parallel to the wall and flex the arm on the wall side to 90 degrees (parallel to the tape measure). The participant was asked to lie forward. The distance the individual could reach forward was calculated. The test was repeated with both dominant and non-dominant arms respectively.

Statistical analysis

IBM SPSS 21 software was used for statistical analysis. The significance level was accepted as 0.05. Balance scores between dominant and non-dominant extremities were evaluated with the T-test when the data were normally distributed and with the Mann Whitney-U test when the data were not normally distributed. The relationship between age, height, weight, and balance tests was evaluated using the Spearman correlation test.

RESULTS

Eighty-four (84%) of the participants were female, 16 (16%) were male, and the average age was 20.32 ± 3.40 (18-44). While 93 (93%) participants were right extremity dominant, 7 (7%) were left extremity dominant.

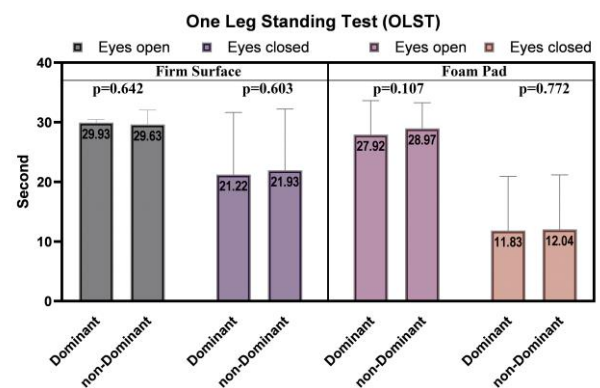


Figure 1. One Leg Standing Test for dominant and non-dominant legs.

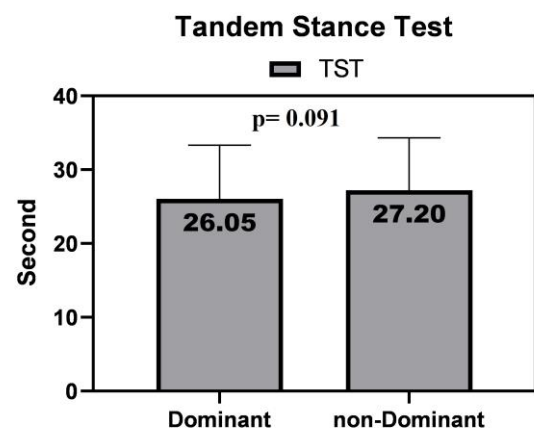


Figure 2. Tandem Stance Test for dominant and non-dominant legs.

There was no difference in terms of OLST performed with the dominant and non-dominant leg ($p>0.05$, Figure 1). There was no difference in terms of TST performed with the dominant and non-dominant leg ($p>0.05$, Figure 2). There was no difference in terms of FRT applied with the dominant and non-dominant arms ($p>0.05$, Figure 3).

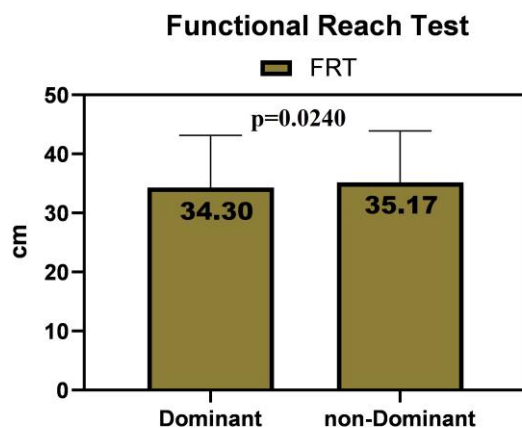


Figure 3. Functional Reach Test according to dominant and non-dominant leg.

There was a relationship between BMI and firm surface eyes closed OLST (Figure 4A), height and FRT and TST (Figure 4B), weight and FRT (Figure 4C), and age and firm surface eyes closed OLST (Figure 4D) ($p<0.05$).

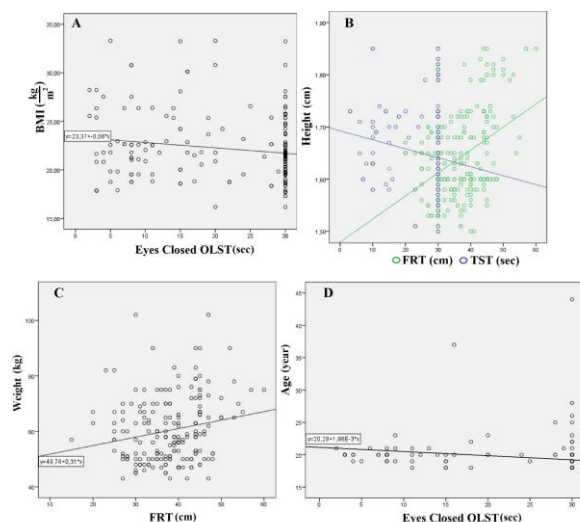


Figure 4. A: Relationship between BMI and firm surface eyes closed OLST. B: Relationship between height and FRT and TST. C: Relationship between weight and FRT. D: Relationship between age and firm surface eyes closed OLST.

The relationship between age, height, weight, BMI and functional balance tests is presented in Table 1.

Table 1. Relationship between age, height, weight, BMI and functional balance tests (N=200).

	Age	Weight	Height	BMI
	20.32±3.40	60.38±11.61	164.69±8.16	22.18±3.46
	Correlation coefficient (p value)			
OLST, Firm Surface, second				
Eyes Open	29.93±0.49	-0.11 (.271)	-0.08 (.256)	-0.02 (.732)
Eyes Closed	21.22±10.42	-0.25 (.011)	-0.08 (.240)	-0.07 (.274)
OLST, Foam Pad, second				
Eyes Open	27.92±5.70	-0.00 (.927)	-0.06 (.387)	0.07 (.315)
Eyes Closed	11.83±9.09	-0.12 (.263)	-0.02 (.769)	0.09 (.200)
TST, second	26.05±7.26	-0.10 (.294)	-0.04 (.521)	-0.18 (.009)
FRT, cm	37.34±7.94	-0.04 (.689)	0.19 (.005)	0.35 (<.001)

Spearman Correlation test, OLST: One Leg Standing Test, TST: Tandem Stance Test, FRT: Functional Reach Test

DISCUSSION

This study aimed to determine whether arm and leg dominance affects OLST, TST and FRT. Our study determined that leg dominance did not affect OLST and TST, and arm dominance did not affect FRT.

The VSR is connected to the upper cervical region (medial tract) and lower extremities (lateral tract). Functional balance tests, in which we investigate arm and leg dominance, mainly evaluate the ipsilateral VSR. The lateral VSR primarily extends to the ipsilateral spinal cord and modulates the α and γ motor neurons of the intraspinal pathways and lower extremity muscles (15). It stimulates lower extensor motor neurons and suppresses flexor motor neurons. In other words, it ensures an upright posture against gravity and plays an important role in maintaining balance by controlling muscle activity. OLST and TST are similar in terms of application. In both, surface area and proprioceptive input are reduced. Thus, confidence in the vestibular system increases. When performed with eyes closed, the visual system is also disabled, and the test becomes even more difficult. However, the main difference between the OLST and TST tests is the force exerted on the muscle and skeletal system. In TST, the body weight is shared on each leg, while in OLST, all the force is on one leg. For this reason, OLST is

more susceptible to being affected by muscle strength. It has been reported in the literature that there are differences between dominant and non-dominant leg muscle strength (hamstring and quadriceps) (16). The main difference is that the flexor muscles are weak in the dominant leg while the extensor muscles are strong. Considering that the functional balance tests we applied constitute knee extension, it is expected that there may be a performance difference between the dominant and non-dominant legs due to the difference in strength. However, the findings of studies in the literature vary (14,17,18) Mala et al. (17) categorized football players according to age groups and investigated the effect of leg dominance on postural stability (PS). The authors reported that leg dominance did not affect PS. Muehlbauer et al. (18) performed OLST on 30 healthy young adults with dominant and non-dominant legs in 3 different situations (eyes open/firm ground, eyes open/foam ground and eyes closed/firm ground). The authors stated that leg dominance does not affect OLST and that both legs can be used during OLST. Another study (14) evaluated the stabilometric analysis of leg dominance using the OLST in athletes (football (n = 20), basketball (n = 20), windsurfing (n = 20)) and sedentary individuals (n = 20). The authors reported that football players exhibited better balance on the non-dominant leg. However, they found no significant difference in OLST performance between legs in the other athletes. This situation was explained by the fact that football players did a lot of training and that this training improved their non-dominant leg balance. The findings in the literature generally show no difference between balance tests performed on the dominant and non-dominant legs. The better performance of football players on the non-dominant leg during the OLST test is likely due to intense exercise, which leads the non-dominant leg to surpass the dominant leg. In other words, while there is no impact of leg dominance on balance performance in individuals with normal daily activities, training the non-dominant leg in football players gives it an advantage in terms of balance. We included young adults in our study, which was similar to Muehlbauer's study. The participants were not doing professional sports but performing daily activities. In our study, there was no difference in terms of OLST and TST between dominant and non-dominant legs. In other words, dominant and non-dominant legs can be used interchangeably in standard OLST and TST tests.

On the other hand, maintaining posture, balance, and activities such as walking in daily life requires continuity. Therefore, muscle fatigue can affect these functional abilities. Simoneau et al. (19) reported that muscle fatigue negatively impacts balance skills and that individuals

compensate for this balance loss by allocating a greater proportion of cognitive resources to the active control of the balance task. Muscle fatigue also affects the dominant and non-dominant legs differently. Increased reliance on the dominant leg and prolonged exposure to high forces lead to excessive loading of the muscle-tendon components in this leg compared to the non-dominant leg (20). In our study, we did not assess participants' baseline fatigue levels. Additionally, we provided a one-minute rest period between tests and legs. Therefore, our findings do not simulate daily life but rather reflect results obtained in a laboratory setting. Future studies could investigate how muscle fatigue influences balance tests performed with the dominant and non-dominant legs. Moreover, the impact of limb dominance on motor performance in dual-task scenarios that simulate daily life would be crucial in understanding the real-world effects of leg dominance.

Our study also detected a negative relationship between BMI and eyes closed-firm surface OLST. Individuals with higher BMI spend more effort maintaining their balance in OLST. Therefore, leg muscles get tired faster. Thus, the negative relationship between BMI and eyes closed-firm surface OLST shows that fatigue can affect balance and investigating leg dominance in tired muscles will clarify the results. The lack of a relationship between BMI and other foam surface OLST can be explained by the emergence of different factors (such as vestibular abilities) that disrupt balance in the foam surface.

Ageing affects muscle mass. Muscle mass decreases by approximately 3-8% per decade after age 30 (21,22). The age range of the participants in our study was between 18-44. Although all participants were young adults, there was a negative relationship between age and eyes closed-firm surface OLST. This shows that the loss of muscle mass after the age of 30 affects OLST. For this reason, age should be considered when preparing normative data for OLST, and if possible, OLST results should be interpreted in decades.

FRT is designed to measure the maximum distance a person's arm length can reach forward while maintaining a stable base of support in the foot, that is, to evaluate the individual's anteroposterior stability (23). The test can be easily administered with a simple tape measure, and individuals' semi-dynamic balance skills can be evaluated validly and accurately. Studies in the literature generally state that FRT should be applied with the dominant arm (24). Although there are studies investigating different modifications of FRT in the literature (25), to the best of our knowledge, there is no study investigating the effect

of arm dominance on FRT. Karabulut et al. (25) applied FRT on the firm and foam surface with the dominant and double arms. The authors reported that the most appropriate version to evaluate postural control is the firm surface of both arms FRT. Differently, we investigated the effect of arm dominance on FRT. Our study showed that arm dominance does not affect FRT. That is, in cases such as inappropriate room conditions or unilateral upper limb amputation, FRT can be applied validly, reliably and accurately with the dominant or non-dominant arm.

By its nature, FRT is affected by upper body length. Therefore, height and FRT have a positive relationship (26). On the contrary, fat [excess weight] in the belly area will make it challenging to maintain the centre of gravity when reaching forward and negatively affect FRT performance. We detected a positive relationship between FRT and height, which is consistent with the literature. However, a positive relationship also existed between FRT and weight. This can be explained by the fact that weight increases as height increases. Similarly, the lack of a relationship between FRT and BMI confirms our hypothesis.

This study has some limitations. First, we included only healthy adult participants, with the majority of the sample consisting of females (84%). Therefore, these findings are specifically applicable to healthy adults, and the uneven gender distribution may not fully reflect potential differences between sexes. Another limitation is that we did not assess participants' baseline fatigue before testing. Additionally, participants were given a one-minute rest period between tests. Future studies could consider the effects of fatigue or implement longer rest intervals between tests to explore the impact of the dominant extremity on balance performance in different populations, such as individuals with various medical conditions, athletes, children, or older adults.

CONCLUSION

In addition to the afferent information coming from the sensory organs, the contribution of the musculoskeletal system is also of great importance in maintaining posture and balance. Our study revealed that leg dominance did not affect OLST and TST, and arm dominance did not affect FRT. The extremity for applying OLST, TST, and FRT can be left to participant preference or applied based on the dominant/non-dominant extremity as appropriate to the situation.

Acknowledgments

There is no acknowledgement.

Authorship contributions

Conception: ES - Design: ES, MC - Supervision: ES, MS- Data Collection and/or Processing: MC - Analysis and/or Interpretation: ES - Literature Review: ES, MC - Writing: ES,MC- Critical Review: ES.

Data availability statement

Data available upon request

Declaration of competing interest

The authors declare that there is no conflict of interest.

Ethics

Ethical approval was obtained for the study from the university's ethics commission (Decision no: 2023/5).

Funding

No source of funding

REFERENCES

1. Cug M, Özdemir R, Ak E. Influence of Leg Dominance on Single-Leg Stance Performance During Dynamic Conditions: An Investigation into the Validity of Symmetry Hypothesis for Dynamic Postural Control in Healthy Individuals. *Turk J Physiother Rehabil*. 2014; 60(1): 22-26. <https://doi.org/10.5152/tftrd.2014.59354>
2. Forth KE, Metter EJ, Paloski WH. Age associated differences in postural equilibrium control: A comparison between EQscore and minimum time to contact (TTCmin). *Gait Posture*. 2007; 5:56-62. <https://doi.org/10.1016/j.gaitpost.2005.12.008>
3. Fetter M. Vestibulo-ocular reflex. *Dev Ophthalmol*. 2007;40:35-51. doi: 10.1159/000100348. PMID: 17314478.
4. (MacKinnon CD. Sensorimotor anatomy of gait, balance, and falls. *Handb Clin Neurol*. 2018;159:3-26. <https://doi.org/10.1016/B978-0-444-63916-5.00001-X>.
5. Vanicek N, King SA, Gohil R, Chetter IC, Coughlin PA. Computerized dynamic posturography for postural control assessment in patients with intermittent claudication. *J Vis Exp*. 2013; (82):e51077. <https://doi.org/10.3791/51077>.
6. Scena S, Steindler R, Ceci M, Zuccaro SM, Carmeli E. Computerized Functional Reach Test to Measure Balance Stability in Elderly Patients With Neurological Disorders. *J Clin Med Res*. 2016; 8(10):715-20. <https://doi.org/10.14740/jocmr2652w>
7. Peterka RJ. Sensorimotor integration in human postural control. *J Neurophys*. 2002; 88: 1097-118. <https://doi.org/10.1152/jn.2002.88.3.1097>
8. Badian NA. Birth order, maternal age, season of birth, and handedness. *Cortex*. 1983 Dec;19(4):451-63. [https://doi.org/10.1016/s0010-9452\(83\)80027-6](https://doi.org/10.1016/s0010-9452(83)80027-6).
9. Geschwind N, Behan P. Left-handedness: association with immune disease, migraine, and developmental learning disorder.

- Proc Natl Acad Sci USA. 1982;79(16):5097-100. <https://doi.org/10.1073/pnas.79.16.5097>.
10. Coren S, Porac C. Birth factors and laterality: effects of birth order, parental age, and birth stress on four indices of lateral preference. *Behav Genet.* 1980;10(2):123-38. <https://doi.org/10.1007/BF01066263>.
11. Hepper PG, Shahidullah S, White R. Handedness in the human fetus. *Neuropsychologia.* 1991;29(11):1107-11. [https://doi.org/10.1016/0028-3932\(91\)90080-r](https://doi.org/10.1016/0028-3932(91)90080-r).
12. Annett M. Left, right, hand and brain: The right shift theory. LEA, Hillsdale, NJ, 1985.
13. Paillard T, Noé F. Does monopodal postural balance differ between the dominant leg and the non-dominant leg? A review. *Hum Mov Sci.* 2020; 74:102686. doi: 10.1016/j.humov.2020.102686. <https://doi.org/10.1016/j.humov.2020.102686>.
14. MacKinnon CD. Sensorimotor anatomy of gait, balance, and falls. *Handb Clin Neurol.* 2018; 159:3-26. <https://doi.org/10.1016/B978-0-444-63916-5.00001-X>.
15. Lanshammar K, Ribom EL. Differences in muscle strength in dominant and non-dominant leg in females aged 20-39 years--a population-based study. *Phys Ther Sport.* 2011; 12(2):76-9. <https://doi.org/10.1016/j.ptsp.2010.10.004>.
16. Mala L, Maly T, Zahalkab F. Postural performance in the bipedal and unipedal stance of elite soccer players in different age categories. *Acta Kinesiológica.* 2017; 11:101-105.
17. Muehlbauer T, Mettler C, Roth R, Granacher U. One-leg standing performance and muscle activity: are there limb differences? *J Appl Biomech.* 2014; 30(3):407-14. <https://doi.org/10.1123/jab.2013-0230>
18. Barone R, Macaluso F, Traina M, Leonardi V, Farina F, Di Felice V. Soccer players have a better standing balance in nondominant one-legged stance. *Open Access J Sports Med.* 2010 Dec 16;2:1-6. <https://doi.org/10.2147/OAJSM.S12593>.
19. Simoneau M, Bégin F, Teasdale N. The effects of moderate fatigue on dynamic balance control and attentional demands. *J Neuroeng Rehabil.* 2006;28;3:22. <https://doi.org/10.1186/1743-0003-3-22>.
20. Ford KR, Myer GD, Hewett TE. Valgus knee motion during landing in high school female and male basketball players. *Med Sci Sports Exerc.* 2003;35(10):1745-50. <https://doi.org/10.1249/01.MSS.0000089346.85744.D9>.
21. Melton LJ, Khosla S, Crowson CS, O'Connor MK, O'Fallon WM, Riggs BL. Epidemiology of sarcopenia. *J Am Geriatr Soc.* 2000; 48(6):625-30.
22. Volpi E, Nazemi R, Fujita S. Muscle tissue changes with aging. *Curr Opin Clin Nutr Metab Care.* 2004; 7(4):405-10. <https://doi.org/10.1097/01.mco.0000134362.76653.b2>
23. Weiner DK, Bongiorno DR, Studenski SA, Duncan PW, Kochersberger GG. Does functional reach improve with rehabilitation? *Arch Phys Med Rehab.* 1993; 74:796-800. [https://doi.org/10.1016/0003-9993\(93\)90003-s](https://doi.org/10.1016/0003-9993(93)90003-s).
24. Scena S, Steindler R, Ceci M, Zuccaro SM, Carmeli E. Computerized Functional Reach Test to Measure Balance Stability in Elderly Patients With Neurological Disorders. *J Clin Med Res.* 2016; 8(10):715-20. <https://doi.org/10.14740/jocmr2652w>
25. Karabulut M, Gürses R, Aksoy S. An alternative postural control test: Correlation of modified functional reach with limits of stability. *JETR.* 2023; 10(2):122-31. <https://doi.org/10.15437/jetr.992084>
26. Nakhostin-Ansari A, Naghshtabrizi N, Naghdi S, Ghafouri M, Khalifelloo M, Mohammadzadeh M, Vezvaei P, Nakhostin Ansari N. Normative values of functional reach test, single-leg stance test, and timed "UP and GO" with and without dual-task in healthy Iranian adults: A cross-sectional study. *Ann Med Surg (Lond).* 2022; 80:104053. <https://doi.org/10.1016/j.amsu.2022.104053>

Research Article

THE IMPACT OF INCREASED PLATELET COUNT ON ERYTHROCYTE AGGREGATION IN OBESE INDIVIDUALS WITHOUT CARDIOVASCULAR DISEASE

 Serpil ÇEÇEN¹,  Zozan GÜLEKEN^{2*}

¹ Faculty of Hamidiye Medicine, Department of Physiology, Health Sciences University, Istanbul, TURKIYE

² Faculty of Medicine, Department of Physiology, Gaziantep Islam Science and Technology University, Gaziantep, TURKIYE

*Correspondence: zozanguleken@gmail.com/zozan.guleken@gibtu.edu.tr

ABSTRACT

Introduction: Although obesity raises the risk of cardiovascular illnesses, it is an important issue for public health. Platelets play important role in thrombosis and inflammation, and elevated number of platelets has been noted in obese individuals. The erythrocyte aggregation process involves the clumping of red blood cells, is influenced factors, including platelet activation. This study aimed to investigate the relationship amongst platelet levels and erythrocyte aggregation in obese individuals without cardiovascular disease.

Methods: Anthropometric measurements of obese individuals (n=101) and non-obese controls (n=37) were recorded. Erythrocyte aggregation parameters, such as aggregation index (AI%), aggregation half-time (t1/2), and aggregation amplitude (AMP), were measured using a laser-based aggregometer. Platelet counts were determined by automated hematology analyzer. We examined the relationship between anthropometric parameters, platelet counts, and erythrocyte aggregation measures.

Results: Obese individuals had significantly higher BMI, fat percentage, fat mass, and fat-free mass versus non-obese controls. In the obese group, Fat mass, increasing fat percentage and BMI, were associated with decreased AMP and t1/2 values, and increased AI% values. Platelet counts were also significantly elevated in the obese group and were inversely correlated with AMP and t1/2 values. No significant associations were observed between anthropometric parameters, platelet counts, and erythrocyte aggregation measures in the non-obese group.

Conclusion: There was strong association between elevated platelet levels and altered erythrocyte aggregation in obese individuals. Findings suggest that obesity-induced increases in platelet count may contribute to increased erythrocyte aggregation, potentially leading to an elevated risk of thrombotic events. Targeting platelet-related pathways may be a promising therapeutic strategy to mitigate cardiovascular complications in obese individuals.

Keywords: Obesity; Anthropometric Measurements; Platelets; Erythrocyte Aggregation

Received: 26 December 2024

Revised: 09 May 2025

Accepted: 15 May 2025

Published: 23 June 2025



Copyright: © 2025 by the authors. Published by Aydın Adnan Menderes University, Faculty of Medicine and Faculty of Dentistry. This article is openly accessible under the Creative Commons Attribution-NonCommercial 4.0 International (CC BY-NC 4.0) License.

INTRODUCTION

Obesity is a long-term, multisystem illness that is becoming more widespread across the globe (1). Obesity is recognized by the increase of the of the adipose tissue and the presence of a persistent inflammatory response (2). The increase in adipose tissue activates inflammatory mechanisms, resulting persistent inflammation (1). Considering obesity is a long-term illness, the possibility of developing complications is elevated. Cerebrovascular and cardiovascular complications are frequently observed and affect quality of life (3). Studies on obesity have shown that the emergence of complications is linked to persistent inflammation, hyperlipidemia, hypertension, diabetes, and increased whole blood and plasma viscosity (4-8). It is conceivable that any condition disrupting blood flow affects tissue perfusion. Changes in blood cells also influence flow properties. An increase in the aggregation of erythrocytes, the most abundant cells in circulating blood, can reduce tissue perfusion and oxygen delivery to tissues, leading to ischemia (9). Investigations has indicated that enhanced erythrocyte aggregation plays a role in vascular complications in obesity (10). Identifying factors that enhance aggregation becomes crucial. While various studies have been conducted in this area, research is increasingly focusing on how inflammation in obesity contributes to increased aggregation (11). In obesity, there is also an increase in platelet count along with increased adipose tissue (12), and it has been shown that inflammation in obesity enhances prothrombotic events, leading to arterial and venous thrombosis (13). It is believed that platelets can trigger inflammation, with platelet activation increasing in inflammatory diseases and contributing to atherothrombotic events (14). While previous researches have established a link between obesity, inflammation, and increased erythrocyte aggregation, the specific role of platelets in this process remains relatively unexplored. Furthermore, studies have investigated the connection between obesity, inflammation, and platelet activation, the direct impact of increased platelet count on erythrocyte aggregation in obese individuals has not been comprehensively examined.

To address this gap, we investigated the connection amongst anthropometric measurements, erythrocyte aggregation, and platelet counts in obese and non-obese individuals. By exploring this connection, we seek to enhance understanding of the mechanisms underlying vascular complications in obesity and potentially identify novel therapeutic targets.

Despite, previous studies have shown that inflammation and platelet count increase in obesity, but our study is one of the few to directly correlate platelet count with erythrocyte aggregation parameters. Understanding the interplay between obesity, platelets, and erythrocyte aggregation can provide valuable insights into the pathophysiology of obesity-related cardiovascular complications and inform the progression of the targeted interventions.

This study aims to investigate whether increased platelets in obesity affect erythrocyte aggregation, Figure 1.

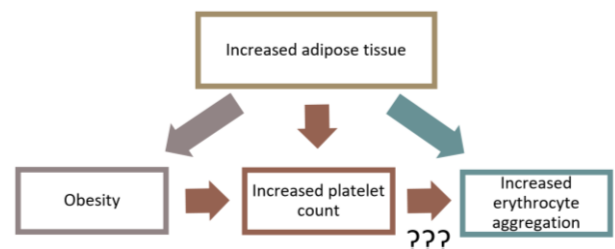


Figure 1. The central research question addressed in the study, focusing on the relationship between anthropometric measurements, erythrocyte aggregation, and platelet counts in obese and non-obese groups.

MATERIALS AND METHODS

Ethical Approval

This study was approved by the Clinical Research Ethics Committee of Haydarpasa Numune Research and Training Hospital (Number: HNEAH-KEAK2022/136).

Participants

Individuals between the ages of 18 to 65 with body mass index (BMI) of 25 were recruited from the Endocrinology outpatient clinic at Haydarpasa Numune Training and Research Hospital. Participants with a history of malignancy, infection, pregnancy, drug use, or any other significant medical conditions were excluded. Height was recorded in centimeters with participants standing barefoot on a flat surface using a stadiometer. Body composition analysis was conducted via a Tanita-BC418 (bioimpedance device) which assessed BMI, weight, mass body fat percentage, fat-free mass and fat mass. Pregnant participants those with certain conditions were omitted from the study by the conditions that elevate blood viscosity. Also, the healthy individuals in the control group had no previous diagnosis of blood or heart disorders. Hematological and biochemical parameters, electrocardiogram, transthoracic echocardiography, carotid and vertebral artery color Doppler ultrasonography were evaluated by an expert physician to

make election of participants in the clinics of the university hospital.

Blood Sample Collection

Samples were taken from participants in a 10 mL purple-capped tube. Routine blood biochemistry tests were performed on a separate blood sample. Samples of blood were drawn from the antecubital vein and stored in K₂-EDTA purple tubes (1.8 mg/dl K₂EDTA, BD Vacutainer) and analyzed in the Hemorheology Laboratory of our Faculty, within a maximum of 4 hours. All measurements related to hemorheology were performed at 37 °C.

Aggregation Measurement of Erythrocytes

The aggregation of erythrocyte (EA) was assessed in the Hamidiye Medical Faculty. The erythrocyte aggregation properties of the samples were also evaluated with a laser echocytometer (RR Mechatronics, Hoorn, Netherlands; Laser-assisted Optical Rotational Cell Analyzer LORCA). The aggregation measurement principle is as mentioned previously (15), (16). Undiluted whole blood is used for this measurement. Since the amount of HbO₂ (oxyhemoglobin) in the blood, Since it could affect aggregation parameters, oxygenation is routinely applied to all samples before measurement (15). For oxygenation, the whole blood sample is kept in a tube with a volume at least 10 times its volume for 10 minutes (for contact with oxygen in the air). During this time, the sample is gently turned upside down to bring it into contact with oxygen. Aggregation index (AI) (aggregation index in percentage, %): Percentage of erythrocyte aggregation in stasis, Aggregation amplitude (AMP) (aggregation magnitude parameter in arbitrary units, au): The total alteration in the signal of aggregation, Half-time of aggregation ($t_{1/2}$) (half-time of aggregation in seconds, sec): Taken as the duration needed for the aggregation signal to reduce to half of the maximum change, Figure 2.

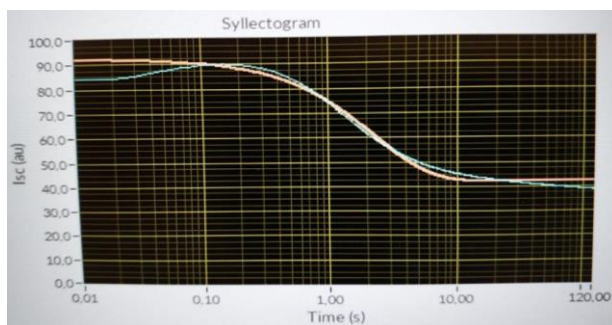


Figure 2. Syllactogram of obese subjects

The parameters AMP, AI, and $t_{1/2}$, which are examined when evaluating erythrocyte aggregation, are obtained

from the sedimentation curve. Accordingly, AMP, representing the aggregation amplitude, is the distance between the peak point of the shape correction phase and the point where the formation of three-dimensional aggregates ends. AI (aggregation index) is obtained by dividing the area A indicated on the graph by the sum of areas A and B. It expresses both the aggregation amplitude and the kinetics of aggregation. The $t_{1/2}$ parameter determines the required time for the amplitude to diminish half of the peak point ($I_{1/2}$), Figure 3.

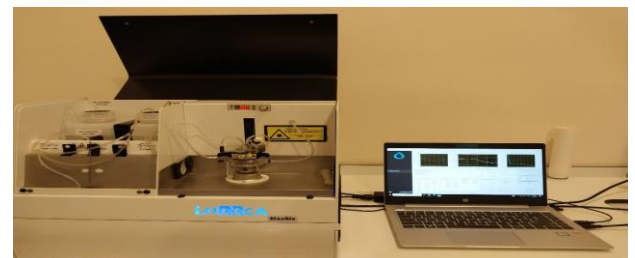


Figure 3. Data was collected using LORCA, a laser-based ektacytometer. Basic instrument (left) computer screen (right) presents disaggregation curve, syllectogram, iteration curve, measurement parameters etc. The laser ektacytometer images were obtained at the Hemorheology Research Laboratory, University of Health Sciences, Hamidiye Faculty of Medicine.

Statistics

To summarize characteristics of the patient's descriptive statistics as the mean and standard deviation were performed using software (GraphPad Prism 6). All continuous variables were tested for normality using the Shapiro-Wilk test. For normally distributed data, Student's t-test and Pearson's correlation were used; otherwise, non-parametric equivalents Mann-Whitney U, were applied. Equality of variances was tested using Levene's test. Age differences between groups were significant ($p < 0.001$), and age was included as a covariate in multivariate analyses where appropriate. ANOVA (Analysis of Variance) was utilized to compare means across more than two grouped data groups in order to determine if there were statistically significant differences. To determine the direction and strength of the linear link between two or more continuous variables, correlation analysis was performed using the Pearson correlation coefficient. $p < 0.05$ is noted for statistical significance.

RESULTS

The statistical analysis of the demographic and anthropometric data showed that the obese group exhibited substantially higher values (mean \pm SD) than the non-obese group (Table 1).

Table 1. The comparison of demographic and anthropometric data between the obese (n=101) and the non-obese group (n=37). The values are reported as mean \pm SD (Standard deviation). All comparisons show statistically significant differences amongst the groups, with p-values less than 0.001.

Variables	Obese Group (n=101)		Non-obese Group (n=37)		p value
	Mean	SD	Mean	SD	
Age (year)	45.3	1.2	33.7	2	0.001
Height (cm)	160	0.8	167.4	1.2	0.001
Weight (kg)	90.9	2.1	61.4	1.3	0.001
BMI (kg/m ²)	35.2	0.6	21.8	0.3	0.001
Fat (%)	37.9	0.6	23.1	1	0.001
Fat mass (kg)	34.9	1.1	14.2	0.7	0.001
Fat free mass (kg)	56	1.3	47.2	1.2	0.001

In the obese group, AMP value decreased with BMI and fat mass, and AI (%) value increased statistically significantly with weight, BMI, fat percentage, fat mass. t1/2 value decreased statistically significantly with BMI, fat percentage, fat mass (Table 2).

Table 2. The correlations between erythrocyte aggregation parameters and anthropometric measurements in the obese group. The parameters analyzed include AMP (aggregation magnitude parameter in arbitrary units, au), AI (aggregation index in percentage, %), and t1/2 (half-time of aggregation in seconds, sec). The correlation coefficients (r) and their corresponding p-values (p) are provided for each anthropometric measurement. (* noted as p<0.05).

Obese Group Variables	AMP (au)		AI (%)		t 1/2 (sec)	
	r	p	r	p	r	p
Age (year)	0.04	0.62	0.07	0.46	-0.12	0.21
Height (cm)	0.03	0.75	-0.15	0.11	0.12	0.19
Weight (kg)	-0.15	0.22	0.1	0.039*	-0.16	0.09
BMI (kg/m ²)	-0.19	0.041*	0.36	0.0001*	-0.29	0.001*
Fat (%)	-0.18	0.05	0.43	<0.0001*	-0.39	<0.0001*
Fat mass (kg)	-0.21	0.025*	0.38	<0.0001*	-0.32	0.0007*
Fat free mass(kg)	-0.04	0.61	0.06	0.48	-0.06	0.53

In the obese group, the platelet value positively correlated with BMI, % fat, fat mass and T1/2, while AMP values negatively correlated with platelet and platelet A (%) values (Table 3). In the non-obese group, AMP value decreased statistically significantly with fat percentage, fat mass, AI (%) and t1/2 values were not affected by anthropometric parameters (Table 4). In the non-obese group, platelet value was not affected by anthropometric parameters and erythrocyte aggregation parameters. (Table 5).

Table 3. The correlations between platelet count and various anthropometric measurements, as well as erythrocyte aggregation parameters in the obese group. The correlation coefficients (r) and their corresponding p-values (p) are provided for each variable (* noted as p<0.05, ** noted as p<0.01, ***p<0.001).

Obese Group Variables	Platelet	
	r	p
Weight (kg)	0.18	0.068
BMI (kg/m ²)	0.228	0.021*
Fat (%)	0.202	0.041*
Fat mass (kg)	0.246	0.012*
Fat free mass (kg)	0.015	0.879
aggregation half-time (t 1/2)	-0.348	<0.001**
Aggregation index (AI (%))	0.416	<0.0001***
Aggregation amplitude (AMP; arbitrary units, au)	-0.431	<0.001**

Table 4. The correlations between erythrocyte aggregation parameters and anthropometric measurements in the non-obese group. The parameters analyzed include AMP (aggregation magnitude parameter in arbitrary units, au), AI (aggregation index in percentage, %), and t1/2 (half-time of aggregation in seconds, sec). The correlation coefficients (r) and their corresponding p-values (p) are provided for each anthropometric measurement. (* noted as p<0.05).

Non-obese group Variables	AMP (au)		AI (%)		t 1/2 (sec)	
	r	p	r	p	r	p
Age (year)	0.04	0.81	0.21	0.20	-0.17	0.30
Height (cm)	0.16	0.32	-0.09	0.57	0.08	0.62
Weight(kg)	0.02	0.88	0.04	0.78	-0.04	0.79
BMI (kg/m2)	-0.14	0.40	0.1	0.35	-0.13	0.41
Fat percentage (%)	-0.36	0.025*	0.15	0.34	-0.11	0.48
Fat mass (kg)	-0.33	0.042*	0.4	0.38	-0.10	0.51
Fat free mass(kg)	0.22	0.17	-0.02	0.86	0.01	0.94

Table 5. The correlations between platelet count and various anthropometric measurements, as well as erythrocyte aggregation parameters in the non-obese group. The correlation coefficients (r) and their corresponding p-values (p) are listed for each variable. None of the correlations were statistically significant, as indicated by p-values greater than 0.05.

Non-obese Group Variables	Platelet	
	r	p
Weight (kg)	0.032	0.848
BMI (kg/m2)	0.08	0.634
%Fat	0.121	0.163
Fat mass	0.116	0.482
Fat free mass (kg)	-0.038	0.819
t 1/2	-0.027	0.873
AI (%)	0.014	0.933
AMP	0.093	0.579

DISCUSSION

In this study, our hypothesis was that increased platelet levels in obesity could enhance erythrocyte aggregation. Our findings support this hypothesis, revealing that elevated platelet levels in obesity indeed increase erythrocyte aggregation.

What could be the mechanism by which platelets enhance erythrocyte aggregation?

Secretion of Adhesion Molecules by Platelets

Adhesion molecules from the selectin family, such as P-selectin secreted by platelets, facilitate the developing of platelets cumulation on endothelial cells and their aggregation with leukocytes. This rolling interaction initiates the effect of platelets on target cells (17) and promotes leukocyte rolling on the endothelium (18). Subsequently, the secretion of intercellular adhesion molecules results in a tighter adhesion process among leukocytes. P-selectin primarily initiates interactions with monocytes (19), and the resulting monocyte-platelet complex has pro-inflammatory properties, contributing to atherosclerosis (20). The leukocytes adhesion to the endothelium, triggers the inflammatory process, increasing vascular reactivity (21), and the development of the platelet-monocyte complex leads to further endothelial disruption, which can enhance erythrocyte adhesion and accelerate aggregation processes. Our study indicates that in the obese group, increased platelet and erythrocyte aggregation parameters are proportional to fat tissue, a change not observed in the non-obese group. This suggests the importance of understanding the implications of increased platelets in obesity and potential secondary complications.

Secretion of Aggregation Factors by Platelets

Platelets form the first line of defense in maintaining vascular endothelial integrity and play a role in inflammation and atherogenesis (22). Platelet glycoprotein receptors interact with aggregation factors, coagulation factors, other platelets, and the endothelial layer (23). In chronic conditions such as diabetes, hypertension, obesity, and in the diseases of cardiovascular, the role of platelets in atherosclerosis is significant (24 -27). The progress of lesion in atherosclerosis and increased platelet binding in these areas activate platelets, and cause the release of granules containing adenosine diphosphate, factor Va, thrombospondin, von Willebrand factor, fibronectin, fibrinogen, heparinase, and thromboxane A₂ (TXA₂), which stimulate the aggregation process (28). Fibrinogen, in particular, is a significant factor in increasing of the aggregation of erythrocytes (29), and it is expected that an

increase in platelets will also enhance erythrocyte aggregation. Additionally, the disturbance in hemodynamics of vascular system might be the reason of improved erythrocyte aggregation.

Pro-inflammatory Effects of Platelets

Platelets has a role in the formation of inflammation (30). The chemokines (e.g., CXCL7, CXCL1, CXCL4, CXCL5) and cytokines (e.g., TNF-alpha, leukotrienes, thromboxane A₂, interleukin-1) secreted by platelets can stimulate both inflammation and atherosclerotic plaque development (25, 31). Platelets act as receptors for bioactive molecules and proteins involved in inflammation and immunity, such as those contained in δ -granules, α -granules, and lysosomes (14). They also encompass Toll-like receptors that can detect pathogens like bacteria and viruses (32, 30), and they can activate neutrophils (33), which may trigger inflammation and subsequently increase erythrocyte aggregation. The increase in platelet count and platelet-neutrophil interactions in systemic inflammation process such as ulcerative colitis (34) and systemic lupus erythematosus (SLE) (35) underscores the importance of platelets in inflammatory processes. The observed increase in the number of platelets in obesity, which was proportional to fat tissue increase, further supports the connection between platelets and inflammation.

Effects of Platelets on Vascular Circulation

The relationships between endothelial cells and platelet or immune cells (36), such as platelet-monocyte interactions, facilitate in the formation of atherosclerotic processes (14). Increased atherosclerotic plaque formation due to platelets can cause stasis in vascular structures, reducing blood circulation (37) and indirectly leading to increased erythrocyte aggregation through rouleaux formation. Additionally, a rise in count of platelets could also slow circulation in the vascular bed and, in turn, increase erythrocyte aggregation. Hydrodynamic forces in blood vessels push platelets toward the vessel walls while erythrocytes remain in the central flow. An increase in platelet count enhances this pushing effect and increases the area occupied by platelets, leading to slower erythrocyte circulation and increased aggregation.

Limitations

Our findings highlight the potential role of platelets in obesity-related hemorheological changes. While several plausible biological mechanisms have been proposed—such as platelet-driven secretion of adhesion molecules, inflammatory mediators, and aggregation factors—our study is cross-sectional in nature. Thus, although

significant correlations were observed, causality cannot be established. It remains unclear whether increased platelet count directly drives erythrocyte aggregation or whether both arise in parallel due to shared underlying processes like chronic inflammation or endothelial dysfunction in obesity. If future studies confirm a causal relationship, targeting platelet activity or count (e.g., via antiplatelet or anti-inflammatory therapies) may offer a novel approach to mitigating vascular complications in obese individuals—even those not yet diagnosed with cardiovascular disease. Furthermore, potential pathways should be explored. Future longitudinal or interventional studies will be needed to determine whether modulating platelet activity can alter erythrocyte aggregation profiles and reduce cardiovascular risk.

CONCLUSION

Despite their lower numbers compared to other blood cells, platelets are complex functional cells that influence hemodynamics through mechanisms such as the secretion of adhesion molecules, stimulation of aggregation, promotion of inflammation, and effects on vascular blood flow. These findings underscore the importance of recognizing platelets not only as markers of inflammation but also as active contributors to vascular risk in obesity. While causality cannot be confirmed due to the cross-sectional design, the consistent associations observed point to platelet-related pathways as promising therapeutic targets. Interventions aimed at modulating platelet activity may offer a novel strategy to mitigate the early vascular complications of obesity—even in the absence of overt cardiovascular disease. These findings highlight the importance of addressing obesity can potentially improve cardiovascular health.

Acknowledgments

None

Authorship contributions

Serpil Cecen: Writing– review & editing, Writing– original draft, Visualization, Validation, Resources, Methodology, Investigation, Resources, Data curation, Conceptualization. Zozan Guleken: Writing– review & editing, Validation, Methodology, Investigation, Formal analysis, Data curation, Conceptualization, Supervision.

Data availability statement

Data will be made available on reasonable request from the corresponding author.

Declaration of competing interest

The authors declare that they have no known competing financial interests or personal relationships that could have appeared to influence the work reported in this article.

Ethics

Ethical approval for this study was obtained from the Haydarpaşa Numune Training and Research Hospital Clinical Research Ethics Committee (HNEAH-KEAK2022/136).

Funding

The present study was not funded by any institutional, private or corporate financial support.

REFERENCES

1. Kawai T, Autieri M V., and Scalia R. Adipose tissue inflammation and metabolic dysfunction in obesity. *Am J Physiol - Cell Physiol* 2021; 320:C375–C391.
2. Purdy JC and Shatzel JJ. The hematologic consequences of obesity. *Eur J Haematol* 2021; 106:306–319.
3. Piché ME, Tchernof A, and Després JP. Obesity Phenotypes, Diabetes, and Cardiovascular Diseases. *Circ Res* 2020; 126:1477–1500.
4. Kojta I, Chacińska M, and Błachnio-Zabielska A. Obesity, bioactive lipids, and adipose tissue inflammation in insulin resistance. *Nutrients* 2020; 12:1305.
5. Sun H, Meng S, Chen J, and Wan Q. Effects of Hyperlipidemia on Osseointegration of Dental Implants and Its Strategies. *J Funct Biomater* 2023; 14:194.
6. Litwin M and Kułaga Z. Obesity, metabolic syndrome, and primary hypertension. *Pediatr Nephrol* 2021; 36:825–837.
7. Glatz JFC, Dyck JRB, and Des Rosiers C. Cardiac adaptations to obesity, diabetes and insulin resistance. *Biochim Biophys Acta - Mol Basis Dis* 2018; 1864:1905–1907.
8. Zeng NF, Mancuso JE, Zivkovic AM, Smilowitz JT, and Ristenpart WD. Red blood cells from individuals with abdominal obesity or metabolic abnormalities exhibit less deformability upon entering a constriction. *PLoS One* 2016; 11.
9. Baskurt OK and Meiselman HJ. Erythrocyte aggregation: Basic aspects and clinical importance. *Clin Hemorheol Microcirc* 2013; 53:23–37.
10. Solá E, Vayá A, Corella D, Santaolalia ML, España F, Estellés A, et al. Erythrocyte hyperaggregation in obesity: Determining factors and weight loss influence. *Obesity* 2007; 15:2128–2134.
11. Samocha-Bonet D, Lichtenberg D, Tomer A, Deutsch V, Mardi T, Goldin Y, et al. Enhanced erythrocyte adhesiveness/aggregation in obesity corresponds to low-grade inflammation. *Obes Res* 2003; 11:403–407.
12. Çeçen S. Platelet activation is a risk factor for obesity. *Turkish J Endocrinol Metab* 2020; 24:132–137.

13. Samad F and Ruf W. Inflammation, obesity, and thrombosis. *Blood* 2013; 122:3415–3422.
14. Mandel J, Casari M, Stepanyan M, Martyanov A, and Deppermann C. Beyond Hemostasis: Platelet Innate Immune Interactions and Thromboinflammation. *Int J Mol Sci* 2022; 23.
15. Hardeman MR, Goedhart PT, Dobbe JGG, and Lettinga KP. Laser-assisted optical rotational cell analyser (L.O.R.C.A.); I. A new instrument for measurement of various structural hemorheological parameters. *Clin Hemorheol Microcirc* 1994; 14:605–618.
16. Dobbe JGG, Streekstra GJ, Strackee J, Rutten MCM, Stijnen JMA, and Grimbergen CA. Sylllectometry: The effect of aggregometer geometry in the assessment of red blood cell shape recovery and aggregation. *IEEE Trans Biomed Eng* 2003; 50:97–106.
17. Ludwig RJ, Schön MP, and Boehncke WH. P-selectin: A common therapeutic target for cardiovascular disorders, inflammation and tumour metastasis. *Expert Opin Ther Targets* 2007; 11:1103–1117.
18. Hamadi N, Beegam S, Zaaba NE, Elzaki O, Ali BH, and Nemmar A. Comparative Study on the Chronic Vascular Responses Induced by Regular Versus Occasional Waterpipe Smoke Inhalation in Mice. *Cell Physiol Biochem* 2022; 56:13–27.
19. Ramirez GA, Manfredi AA, and Maugeri N. Misunderstandings between platelets and neutrophils build in chronic inflammation. *Front Immunol* 2019; 10:2491.
20. Gawaz M, Langer H, and May AE. Platelets in inflammation and atherogenesis. *J Clin Invest* 2005; 115:3378–3384.
21. Milstone DS, O'Donnell PE, Stavrakis G, Mortensen RM, and Davis VM. E-selectin expression and stimulation by inflammatory mediators are developmentally regulated during embryogenesis. *Lab Invest* 2000; 80:943–954.
22. Pasquarelli-do-Nascimento G, Braz-de-Melo HA, Faria SS, Santos I de O, Kobinger GP, and Magalhães KG. Hypercoagulopathy and Adipose Tissue Exacerbated Inflammation May Explain Higher Mortality in COVID-19 Patients With Obesity. *Front Endocrinol (Lausanne)* 2020; 11:530.
23. Lefrançois E and Looney MR. Platelet biogenesis in the lung circulation. *Physiology* 2019; 34:392–401.
24. Colwell JA and Nesto RW. The platelet in diabetes: focus on prevention of ischemic events. *Diabetes Care* 2003; 26:2181–2188.
25. Huilcaman R, Venturini W, Fuenzalida L, Cayo A, Segovia R, Valenzuela C, et al. Platelets, a Key Cell in Inflammation and Atherosclerosis Progression. *Cells* 2022; 11.
26. Randriamboavonjy V. Mechanisms Involved in Diabetes-Associated Platelet Hyperactivation. *Non-Thrombotic Role Platelets Heal Dis* 2015.
27. Ezzaty Mirhashemi M, Shah R V., Kitchen RR, Rong J, Spahillari A, Pico AR, et al. The Dynamic Platelet Transcriptome in Obesity and Weight Loss. *Arterioscler Thromb Vasc Biol* 2021; 41:854–864.
28. Choi JL, Li S, and Han JY. Platelet function tests: A review of progresses in clinical application. *Biomed Res Int* 2014; 2014.
29. Lominadze D and Dean WL. Involvement of fibrinogen specific binding in erythrocyte aggregation. *FEBS Lett* 2002; 517:41–44.
30. Mantovani A and Garlanda C. Platelet-macrophage partnership in innate immunity and inflammation. *Nat Immunol* 2013; 14:768–770.
31. Gear ARL and Camerini D. Platelet chemokines and chemokine receptors: Linking hemostasis, inflammation, and host defense. *Microcirculation* 2003; 10:335–350.
32. Marín Oyarzún CP, Glembofsky AC, Goette NP, Lev PR, De Luca G, Baroni Pietto MC, et al. Platelet Toll-Like Receptors Mediate Thromboinflammatory Responses in Patients With Essential Thrombocythemia. *Front Immunol* 2020; 11.
33. Roque M, Kim WJH, Gazdoin M, Malik A, Reis ED, Fallon JT, et al. CCR2 deficiency decreases intimal hyperplasia after arterial injury. *Arterioscler Thromb Vasc Biol* 2002; 22:554–559.
34. Pamuk GE, Vural Ö, Turgut B, Demir M, Ümit H, and Tezel A. Increased circulating platelet-neutrophil, platelet-monocyte complexes, and platelet activation in patients with ulcerative colitis: A comparative study. *Am J Hematol* 2006; 81:753–759.
35. Ceccarelli F, Perricone C, Cipriano E, Massaro L, Natalucci F, Spinelli FR, et al. Usefulness of composite indices in the assessment of joint involvement in systemic lupus erythematosus patients: correlation with ultrasonographic score. *Lupus* 2019; 28:383–388.
36. Ribeiro LS, Branco LM, and Franklin BS. Regulation of innate immune responses by platelets. *Front Immunol* 2019; 10:460217.
37. Duttaroy AK. Role of gut microbiota and their metabolites on atherosclerosis, hypertension and human blood platelet function: A review. *Nutrients* 2021; 13:1–17.

Research Article

OBJECTIVE LENS DENSITOMETRY EVALUATION USING SCHEIMPFLUG TOPOGRAPHY IN CHILDREN AFTER COVID-19 INFECTION

Onur KALAY¹, Ayşe İpek AKYÜZ ÜNSAL^{2*}, Erol ERKAN², Sayime AYDIN EROĞLU³, Sinan BEKMEZ⁴, Esin TUNCA KIRIKKAYA⁵, İmran KURT ÖMÜRLÜ⁶

¹Yalova State Hospital, Department of Ophthalmology, Yalova, TURKIYE

²Aydın Adnan Menderes University, Department of Ophthalmology, Aydın, TURKIYE

³İzmir Çiğli Research and Training Hospital, Department of Ophthalmology, İzmir, TURKIYE

⁴İzmir S.B.U Dr. Behcet Uz Child Diseases and Surgery Research and Training Hospital, Department of Ophthalmology, İzmir, TURKIYE

⁵İzmir Tepecik Research and Training Hospital, Department of Ophthalmology, İzmir, TURKIYE

⁶Aydın Adnan Menderes Üniversitesi, Biyoistatistik Ana Bilim Dalı, Aydın, TURKIYE

*Correspondence: ipekunsal@yahoo.com

ABSTRACT

Objective: To explore the effects of COVID-19 on lens structure in children using Pentacam HR Scheimpflug corneal topography and lens densitometry (LD).

Materials and Methods: This prospective case-control study involved patients aged 7 to 18 who were scheduled for ophthalmologic examination. Pentacam densitometry zones (PDZ 1, 2, and 3) were evaluated in children who had recovered from COVID-19 within the past 6 months and had no systemic diseases, with comparisons made to control subjects.

Results: A total of 114 eyes from 57 patients were evaluated, including 29 (50.9%) children in the patient group and 28 (49.1%) in the control group. PDZ 1 values for ages 7-10, all PDZ values for ages 11-14, and PDZ 3 values for ages 15-18 were significantly higher after COVID-19 compared to those in the control group ($P < 0.05$). Positive correlations were found between PDZ 1-3 values and the time since recovery from COVID-19 in patients aged 11-14 ($r = 0.639, 0.628, \text{ and } 0.590$, respectively; $P = 0.014, 0.016, \text{ and } 0.027$).

Conclusion: Vision quality is influenced not only by visual acuity but also by factors such as contrast sensitivity, higher-order optical irregularities, and the clarity of the visual axis. Our study reveals significant differences in lens density, particularly among children aged 11 to 14, highlighting the potential impact of COVID-19 on their visual quality and underscoring the need for more comprehensive studies on this topic.

Keywords: Children; COVID-19; Lens Densitometry; Pediatric; Scheimpflug Topography

Received: 10 March 2025

Revised: 25 March 2025

Accepted: 22 May 2025

Published: 23 June 2025



Copyright: © 2025 by the authors. Published by Aydın Adnan Menderes University, Faculty of Medicine and Faculty of Dentistry. This article is openly accessible under the Creative Commons Attribution-NonCommercial 4.0 International (CC BY-NC 4.0) License.

INTRODUCTION

COVID-19, a severe acute respiratory infection caused by the SARS-CoV-2 virus, was first declared a pandemic in China by the World Health Organization in late 2019 (1). Although COVID-19 is mainly associated with respiratory symptoms, its effects on the eyes and potential ocular complications merit investigation due to the established possibility of ocular transmission and involvement (2,3). Reported ocular symptoms of COVID-19 include dry eye, a foreign body sensation, itching, blurred vision, conjunctivitis, chemosis, and photophobia (4). Several studies have demonstrated the presence of the virus on the ocular surface, in tears, and in conjunctival swab samples (5).

In cases of COVID-19, virus-induced inflammation and subsequent cytokine storms can disrupt the dynamics of the eye, impacting the anterior segment, including anterior uveitis and changes to the overall lens structure (6,7). Aydemir et al. compared the lens structures of adult COVID-19 patients using the Pentacam HR Scheimpflug topography camera (Oculus Inc., Arlington, WA, USA), which captures detailed images of the entire anterior segment, from the anterior corneal surface to the posterior lens surface (7).

In light of the current literature search, we did not come across a study evaluating the effect of COVID-19 on lens density among pediatric patient groups. Thus, we have designed a prospective observational case-control study to compare objective lens densitometry (LD) measurements with a Scheimpflug topography device among children aged 7-18 who have recovered from COVID-19 with those of healthy children who have no documented history of SARS-CoV-2 infection.

MATERIALS AND METHODS

This prospective cross-sectional comparative study was conducted at the Ophthalmology Department, following the provision of specific information regarding parental consent and child assent, and approval from the local ethics committee (No:2022/31, Date:10.02.2022), in accordance with the tenets of the Declaration of Helsinki.

The patient group of this study included children aged 7-18 years at the time of inclusion who applied to our outpatient clinic for eye examinations between February 2022 and December 2022 and had a history of COVID-19 disease confirmed by at least one positive PCR test with more than 6 months having passed since their recovery.

All included patients had no additional chronic diseases and voluntarily participated in the research. The control group consisted of children of the same age range who applied to our outpatient clinic for eye examinations and had no confirmed history of COVID-19 (i.e., no positive COVID-19 PCR tests), reported no COVID-19 symptoms, had no chronic diseases, and volunteered to participate in the research. The exclusion criteria for both groups were age greater than 18 years, diabetes mellitus, glaucoma, diseases of the corneal surface, corneal edema, cataracts, and previous intraocular surgery.

Thorough ophthalmological examinations included best-corrected visual acuity with a Snellen chart, intraocular pressure with a non-contact tonometer device, and anterior segment examination with slit-lamp biomicroscopy. 2.5% phenylephrine, 1% cyclopentolate, and 0.5% tropicamide drops were instilled into both eyes at 5-minute intervals for fundus examination. This comprehensive approach ensured that all potential factors influencing lens clarity were taken into account, thereby enhancing the accuracy of our data.

After the dilated fundus exam, LD measurements were performed for all patients by the same practitioner (O.K.) under standard dim lighting conditions using the Scheimpflug topography imaging system (Pentacam HR, Oculus Inc., Wetzlar, Germany). The Pentacam HR was chosen for this study due to its ability to provide objective, noninvasive, and reproducible measurements of lens density using Scheimpflug imaging. This imaging technique has been previously validated for assessing subtle changes in lens opacity and has been widely utilized in corneal and lens densitometry research (7). Images that were difficult to evaluate due to poor quality or high levels of reflection were excluded from the study. Mean LD values were calculated at 2 mm in diameter for Zone 1, 4 mm for Zone 2, and 6 mm for Zone 3, using the middle of the pupil as the reference point. These values were recorded as Pentacam densitometry zones PDZ 1, PDZ 2, and PDZ 3, respectively (Figure 1). The average, standard deviation and maximum values of LD measurements were calculated.

The study included both eyes to enhance the robustness of the dataset and increase statistical power. Since systemic diseases commonly affect both eyes symmetrically, incorporating bilateral measurements allowed for a more comprehensive evaluation of potential alterations in lens density.

Statistical analysis

R software, version 4.1.0 (R Foundation for Statistical Computing, Vienna, Austria) was used for statistical analyses. To facilitate the statistical analysis of the obtained data and enable reliable comparisons, one-to-one matching was performed between the patient and control groups based on age and gender. Descriptive statistics are given as number (n), percentage (%), mean \pm standard deviation (SD), median (M), first quartile (Q1), and third quartile (Q3). The normality of numerical variables was evaluated using the Shapiro-Wilk normality test. Comparisons of numerical variables between the patient and control groups were performed using the independent two-sample t-test and the Mann-Whitney U test. Relationships between age and numerical variables were evaluated with Spearman correlation analysis. Values of $p < 0.05$ were accepted as statistically significant.

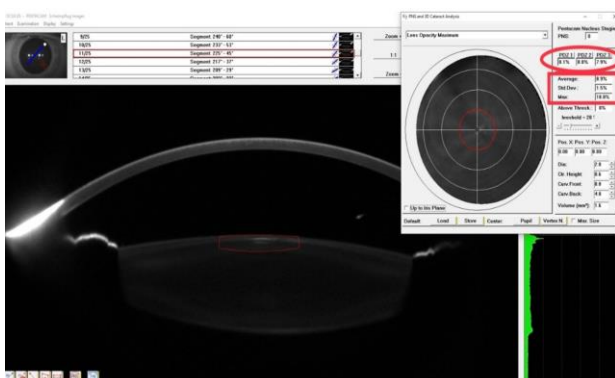


Figure 1. Screenshot of the Lens Densitometry Analysis using the Pentacam HR Scheimpflug Topography System.

RESULTS

Descriptive characteristics of the participants

Within the scope of this study, 114 eyes from a total of 57 children aged 7 to 18 were evaluated. The gender balance was carefully maintained, with 29 participants (17 boys and 12 girls) in the patient group and 28 participants (15 boys and 13 girls) in the control group. The study included 32 (56.1%) male participants and 25 (43.9%) female participants. This balanced representation ensures that our findings apply to a diverse pediatric population. The mean age was 12.92 ± 3.27 years in the patient group and 12.79 ± 3.43 years in the control group ($P = 0.880$). In the patient group, a mean of 15.95 ± 4.97 months had passed since COVID-19 infection.

There were no significant differences in PDZ values, average LD values, or maximum LD values measured for

the 58 eyes of the patient group and the 56 eyes of the control group ($p > 0.05$). The LD values obtained with the Pentacam HR imaging system are presented in Table 1 for comparison.

Table 1. Comparison of lens densitometry measurements by groups.

	Patient Group N = 58	Control Group N = 56	
Variables	M [Q1-Q3]		p*
PDZ 1 (%)	7.90 [7.80-8.10]	7.90 [7.80-8.17]	0.447
PDZ 2 (%)	7.90 [7.77-8.10]	7.90 [7.80-8.30]	0.396
PDZ 3 (%)	7.90 [7.80-8.10]	7.90 [7.80-8.20]	0.614
AVERAGE LD	8.70 [8.20-8.90]	8.60 [8.30-8.87]	0.472
STD DEV LD	1.50 [1.17-1.70]	1.40 [1.10-1.77]	0.776
DENSMAX	18.00 [16.00-	17.80 [15.80-	0.792
LD	22.10]	23.0]	

N: Number of eyes, PDZ: Pentacam densitometry zone, LD: Lens densitometry, STD DEV: Standard deviation, DENSMAX: Maximum densitometry, M: Median, Q1: First quartile, Q3: Third quartile. * Group comparisons were made using the Mann-Whitney U test.

No significant differences were observed in the PDZ values, average LD values, or maximum LD values measured for the 24 eyes of the girls in the patient group and the 26 eyes of the girls in the control group ($P > 0.05$). Similarly, no significant differences were observed in the PDZ values, average LD values, or maximum LD values measured for the eyes of the boys in the patient and control groups ($P > 0.05$).

Table 2. Comparison of lens densitometry measurements by groups for children aged 7-10.

	PATIENT GROUP N = 20	CONTROL GROUP N = 18	
Variables	M [Q1-Q3]		p*
PDZ 1 (%)	7.90 [7.80-8.10]	8.10 [7.87-8.42]	0.028
PDZ 2 (%)	7.90 [7.72-8.07]	8.20 [7.87-8.32]	0.063
PDZ 3 (%)	8.00 [7.72-8.10]	8.15 [7.95-8.22]	0.105
AVERAGE LD	8.55 [8.10-8.80]	8.60 [8.40-9.00]	0.141
STD DEV LD	1.55 [1.40-1.80]	1.80 [1.32-2.05]	0.217
DENSMAX	16.90 [15.40-	19.60 [17.52-	0.228
LD	21.90]	25.00]	

N: Number of eyes, PDZ: Pentacam densitometry zone, LD: Lens densitometry, STD DEV: Standard deviation, DENSMAX: Maximum densitometry, M: Median, Q1: First quartile, Q3: Third quartile. * Group comparisons were made using the Mann-Whitney U test.

For participants aged 7-10 years, the median PDZ 1 value in the patient group was 7.90, based on 20 eyes, while for the 18 eyes in the same age range as the control group, it was 8.10 ($p = 0.028$). However, the PDZ 2, PDZ 3, average LD, and maximum LD values did not differ significantly among participants aged 7-10 years ($p > 0.05$). The LD values of children from this age group are presented comparatively in Table 2.

For participants aged 11-14 years, the mean values of PDZ 1, PDZ 2, and PDZ 3 are presented in Table 3. A statistically significant difference was found between the groups for all these parameters. LD values also differed significantly between the groups among children aged 11-14 ($p < 0.05$).

Table 3. Comparison of lens densitometry measurements by groups for children aged 11-14.

	Patient Group	Control Group	
	N = 14	N = 18	
Variables	M [Q1-Q3]		p*
PDZ 1 (%)	8.05 [7.87-8.35]	7.80 [7.72-7.90]	0.010
PDZ 2 (%)	8.05 [7.87-8.12]	7.80 [7.72-7.90]	0.009
PDZ 3 (%)	8.10 [8.00-8.12]	7.80 [7.72-7.90]	0.001
AVERAGE LD	8.85 [8.50-9.22]	8.20 [8.00-8.60]	0.002
STD DEV LD	1.65 [1.47-1.85]	1.20 [1.02-2.47]	0.001
DENS MAX	21.20 [18.60-	16.10 [14.50-	<0.001
LD	24.30]	18.80]	

N: Number of eyes, PDZ: Pentacam densitometry zone, LD: Lens densitometry, STD DEV: Standard deviation, DENS MAX: Maximum densitometry, M: Median, Q1: First quartile, Q3: Third quartile. * Group comparisons were made using the Mann-Whitney U test.

Among children aged 15-18 years, only the median PDZ 3 value differed significantly between the groups ($p = 0.034$). There were no significant differences in the other LD values between the groups for this age range (Table 4).

Table 4. Comparison of lens densitometry measurements by groups for children aged 15-18.

	Patient Group	Control Group	
	N = 24	N = 22	
Variables	M [Q1-Q3]		p*
PDZ 1 (%)	7.90 [7.72-8.07]	7.90 [7.80-8.22]	0.147
PDZ 2 (%)	7.85 [7.70-8.00]	7.90 [7.80-8.30]	0.078
PDZ 3 (%)	7.90 [7.80-7.90]	7.95 [7.90-8.22]	0.034
AVERAGE LD	8.70 [8.12-8.87]	8.60 [8.30-8.95]	0.991
STD DEV LD	1.15 [0.90-1.47]	1.30 [1.10-1.50]	0.107
DENS MAX	16.50 [14.10-	17.65 [16.50-	0.172
LD	21.40]	23.40]	

N: Number of eyes, PDZ: Pentacam densitometry zone, LD: Lens densitometry, STD DEV: Standard deviation, DENS MAX: Maximum densitometry, M: Median, Q1: First quartile, Q3: Third quartile. * Group comparisons were made using the Mann-Whitney U test.

Correlation analysis results

Table 5 shows correlation analysis results for age and LD measurements. For the patient group, a significant weak negative correlation was detected between LD SD values and age ($r = -0.381$, $p = 0.003$). When the patient and control groups were examined, a significant weak negative relationship was again determined between LD SD and age ($r = -0.325$, $p < 0.001$).

The results of the correlation analysis were performed between LD findings and the number of months since COVID-19 diagnosis, according to the age of the patients. A significant moderate positive correlation was observed between the maximum LD values of children aged 7-10 in

the patient group and the time elapsed since COVID-19 infection ($r = 0.585$, $p = 0.006$). Similarly, a moderate positive correlation existed between LD SD and time since COVID-19 ($r = 0.521$, $p = 0.019$). Significant high-level positive correlations were detected between the PDZ 1, PDZ 2, and PDZ 3 values of patients aged 11-14 and time since COVID-19 ($r = 0.639$, 0.628 , and 0.590 and $p = 0.014$, 0.016 , and 0.027 , respectively).

Table 5. Correlation analysis of age and lens densitometry measurements.

Groups	PDZ 1	PDZ 2	PDZ 3	DENS MAX LD	AVERAGE LD	STD DEV LD
Patient Group (N = 58)	r 0.010	-0.035	-	-0.052	0.151	-0.381
	p* 0.938	0.793	0.546	0.700	0.257	0.003
Control Group (N = 56)	r -0.190	-0.192	-	-0.033	-0.009	-0.206
	p* 0.160	0.157	0.555	0.808	0.949	0.128
Total (N = 114)	r -0.082	-0.118	-	-0.044	0.085	-0.325
	p* 0.383	0.211	0.086	0.642	0.370	<0.001

N: Number of eyes, PDZ: Pentacam densitometry zone, DENS MAX: maximum densitometry, LD: Lens densitometry, STD DEV: Standard deviation. *Spearman's correlation test was applied

DISCUSSION

The COVID-19 pandemic has impacted the world in every aspect of life, and SARS-CoV-2 affects various parts of the body. However, data on the impact of COVID-19 on the structures of the anterior segment of the eye are still insufficient (8). Recently published studies have shown the presence of ACE2 receptors in the conjunctival, limbal, and corneal structures (9,10), and together with those findings, reported changes in both corneal and LD values in adult COVID-19 patients prompted us to investigate the effects of the virus on the cornea and other structures of the anterior segment in pediatric patients, who have a long life expectancy ahead of them. With this aim, we compared objective LD measurements in children between the ages of 7 and 18 years who had been serologically proven to have had COVID-19 with the LD values of age-matched children with no history of COVID-19 infection, using the Pentacam HR Scheimpflug topography system.

Children are estimated to account for only 1% of COVID-19 cases and have a significantly lower risk of severe illness or death (11). There are limited publications on the ocular findings of COVID-19 in the pediatric population. The most common ocular finding reported in non-ophthalmological studies is the congestion of conjunctival vessels (12).

Although the primary route for the transmission and spread of the SARS-CoV-2 virus is the upper respiratory tract, conjunctivitis in COVID-19 patients suggests that the ocular surface may serve as a reservoir for COVID-19 or a route for its transmission (13). After discovering that ACE2 is the primary binding receptor of the virus, the presence of this receptor in ocular structures was investigated (14). In recent studies, the ACE2 receptor, which is known to facilitate viral entry into cells after the virus binds to the receptor, and the transmembrane protease serine 2 (TMPRSS2) enzyme, which provides a path of entry for the virus, have been detected in the cornea, conjunctiva, and limbal regions (9,15,16). The eyes of human cadavers were examined to clarify the expression patterns of ACE2 and TMPRSS2, and it was determined that ACE2 expression was mainly present in the corneal epithelium, the conjunctival surface, and the limbus (17). Furthermore, ACE2 and TMPRSS2 expressions were detected in human corneal epithelial samples taken during refractive surgery (17,18). It has been reported that ACE2 and TMPRSS2 are co-expressed in the retinal pigment epithelium and cornea. The cornea is likely to be a non-respiratory entry point for SARS-CoV-2. In a study comparing the corneal densitometry parameters of patients with COVID-19 and a control group, Aydemir et al. identified effects of COVID-19 on the cornea, and especially the top layer and central zones (7). Corneal involvement in SARS-CoV-2 has been established in studies like those presented here, but knowledge about lens involvement in COVID-19 remains limited. While the development of episcleritis and uveitis due to virus-induced inflammation and subsequent cytokine storms has been demonstrated, it seems possible that the structures and transparency of the cornea or lens are also affected (19). The presence of the virus is also possible in various parts of the eye, such as the lens, as ACE2 receptors have been demonstrated in the aqueous humor (20). Although direct viral involvement of the structures of the lens could not be demonstrated in our study, the LD values of children who had recovered from COVID-19 infection at least 6 months previously were objectively evaluated by Scheimpflug topography and compared with the values of a control group, and the short-term effects of the disease were investigated.

To date, only one study in the literature has evaluated LD parameters in adult patients with a history of COVID-19. In that study, the mean, standard deviation (SD), and maximum LD values for zones 2 and 3 were significantly higher in patients compared to the control group (7). In the present study, following the COVID-19 pandemic, we observed that PDZ 1 values in children aged 7-10, all PDZ values in children aged 11-14, and PDZ 3 values in

children aged 15-18 were significantly higher compared to the control group. These findings suggest that COVID-19 affects lens clarity not only in adults but also in children. Although the presence of ACE2 receptors in the lens has not been demonstrated, infiltration of the aqueous humor by SARS-CoV-2 or disruption of the metabolic balance during the inflammatory process may negatively affect the nourishment of the lens (10).

The significant difference in LD values in the 11-14 age group may be attributed to heightened metabolic activity in the crystalline lens during this critical developmental phase, rendering it more vulnerable to external stressors such as systemic inflammation and oxidative damage. As the primary nutrient source for the avascular lens, the aqueous humor may mediate these effects, with potential alterations resulting from the presence of SARS-CoV-2 that could affect lens metabolism. Anatomical and physiological differences between pediatric and adult lenses further suggest that children in this age range may be more susceptible to metabolic imbalances triggered by systemic infections. Additionally, pubertal hormonal changes may play a role in modulating lens transparency and metabolism, potentially interacting with COVID-19-induced inflammatory processes (10).

In recent studies, the authors state that the intraocular effects of COVID-19 may depend on direct virus attachment to the ACE2 and TMPRSS2 receptors on the ocular surfaces, as well as indirectly through the inflammatory process it causes, such as anterior uveitis and multisystem inflammatory syndrome (21-25). Ishigooka et al. demonstrated that increased levels of ACE in the lens lead to cataract formation in an experimental rat model of diabetes. They showed that ACE blockade with candesartan prevents cataract development (26). Given these findings, we believe COVID-19 could raise ACE levels in the lens, resulting in increased oxidative damage, protein aggregation, and lens opacity.

The only previous study on this subject was conducted with adults, so the different results obtained in the present study may be due to differences in developmental processes between adult patients and children (7). Just as ACE levels may vary across different childhood stages, the sensitivity of lens clarity may also fluctuate after a COVID-19 infection. This could explain the varying LD levels in our study groups.

Our study has several limitations. First, the groups consisted of relatively small numbers of children. This was because relatively few pediatric patients experience COVID-19 infections, some are asymptomatic, and not all

patients have serological confirmation. In selecting the control group, any history of COVID-19-related symptoms in the participants or their household members was established as an exclusion criterion. Accordingly, only individuals with no history of symptoms suggestive of COVID-19 were included in the study. However, since this study involved a pediatric population, obtaining serological or PCR tests from children was not feasible due to ethical and practical constraints. Given that COVID-19-related ocular changes have been reported to be more pronounced in symptomatic cases, the likelihood of significant confounding effects from undiagnosed asymptomatic infections in the control group remains limited. Second, although our research employed a prospective design, LD measurements had not been performed for the patient group before the onset of COVID-19 infection; therefore, a causal relationship between COVID-19 and changes in the lens could not be fully established. Research conducted with larger cohorts of pediatric COVID-19 patients from multiple centers is needed to confirm our findings. Furthermore, this study investigated ocular changes in the early post-recovery period. As a result, it is currently not possible to determine whether the differences in LD values of the patients will persist over time or be reversed. On the other hand, this study also has its strengths. To our knowledge, this is the first case-control study in the literature involving LD measurements in children with a history of COVID-19. In addition, since no relevant treatments were given to the children during their COVID-19 infections, possible drug side effects on the lens were excluded.

CONCLUSION

Our study has revealed significant changes in the LD values of children who applied to our clinic for various reasons and did not have diabetes, glaucoma, corneal diseases, cataracts, or a history of trauma or intraocular surgery, but did have a history of COVID-19, compared to children who did not have a history of COVID-19. Although the pandemic appears to be waning, the effects of COVID-19 continue to affect many people. The measurement of LD values using the Pentacam HR device, a reliable, easy-to-use, and non-invasive method, enables the objective evaluation and clinical monitoring of lens health in children who have had COVID-19. In this study, although no differences were observed in the LD values between the groups, a significant difference was found for patients aged 11-14. It should be remembered that lens transparency may deteriorate at any stage among these patients, even if there is no immediate visible loss in lens clarity. Visual quality depends not only on visual acuity

but also on contrast sensitivity, high-order aberrations, and visual axis clarity. Our results, particularly those obtained for the 11-14 age group, may reflect long-term impacts on visual quality in children after COVID-19. Long-term studies are needed with larger patient groups, and ophthalmologists should consider the potential effects of COVID-19 when performing eye examinations on pediatric patients.

Acknowledgments

None

Authorship contributions

Concept and design: A.İ.A.Ü., O.K., İ.K.Ö.; Data Collection and Processing: A.İ.A.Ü., O.K.; Analysis or Interpretation: A.İ.A.Ü., O.K., S.A.E., E.E., S.B., E.K., İ.K.Ö. ; Literature Search: and Writing: A.İ.A.Ü., O.K., S.A.E., E.E., S.B., E.K., İ.K.Ö.

Data availability statement

The data that support the findings of this study are available from the corresponding author upon reasonable request.

Declaration of competing interest

None.

Ethics

Aydin Adnan Menderes University Ethics Committee and Review Board (code and decision number: 2022/31; 22.12.2022-287204-13).

Funding

None.

REFERENCES

1. Veritti D, Sarao V, Bandello F, Lanzetta P. Infection control measures in ophthalmology during the COVID-19 outbreak: a narrative review from an early experience in Italy. *Eur J Ophthalmol* 2020;30:621-628.
2. Seah I, Agrawal R. Can the coronavirus disease 2019 (COVID-19) affect the eyes? A review of coronaviruses and ocular implications in humans and animals. *Ocul Immunol Inflamm* 2020;28:391-395.
3. Ho D, Low R, Tong L, Gupta V, Veeraghavan A, Agrawal R. COVID-19 and the ocular surface: a review of transmission and manifestations. *Ocul Immunol Inflamm* 2020;28:726-734.
4. Mahayana IT, Angsana NC, Alya Kamila A, Fatiha NN, Sunjaya DZ, Andajana W et al. Literature review of conjunctivitis, conjunctival swab and chloroquine effect in the eyes: a current

updates on COVID-19 and ophthalmology. *Berkala Ilmu Kedokteran* 2020;52:21-28.

5. Nasiri N, Sharifi H, Bazrafshan A, Noori A, Karamouzian M, Sharifi A. Ocular manifestations of COVID-19: a systematic review and meta-analysis. *J Ophthalmic Vis Res* 2021;16:103-112.

6. Sanjay S, Mutalik D, Gowda S, Mahendradas P, Kawali A, Shetty R. Post coronavirus disease (COVID-19) reactivation of a quiescent unilateral anterior uveitis. *SN Compr Clin Med* 2021;3:1843-1847.

7. Aydemir E, Aksoy Aydemir G, Atesoglu H, Goker YS, Kiziltoprak H, Ozcelik KC. Objective assessment of corneal and lens clarity in patients with COVID-19. *Optom Vis Sci* 2021;98:1348-1354.

8. Hu K, Patel J, Swiston C, Patel BC. Ophthalmic Manifestations of Coronavirus (COVID-19). *StatPearls Publishing LLC*; 2022. Accessed February 16, 2024. <https://www.ncbi.nlm.nih.gov/books/NBK556093/>.

9. Collin J, Queen R, Zerti D, Dorgau B, Georgiou M, Djidrovski I et al. Co-expression of SARS-CoV-2 entry genes in the superficial adult human conjunctival, limbal and corneal epithelium suggests an additional route of entry via the ocular surface. *Ocul Surf* 2021;19:190-200.

10. Ma D, Chen CB, Jhanji V, Xu C, Yuan XL, Liang JJ et al. Expression of SARS-CoV-2 receptor ACE2 and TMPRSS2 in human primary conjunctival and pterygium cell lines and in mouse cornea. *Eye (Lond)* 2020;34:1212-1219.

11. She J, Liu L, Liu W. COVID-19 epidemic: Disease characteristics in children. *J Med Virol* 2020;92:747-754.

12. Li LQ, Huang T, Wang YQ, Wang ZP, Liang Y, Huang TB et al. COVID-19 patients' clinical characteristics, discharge rate, and fatality rate of meta-analysis. *J Med Virol* 2020;92:577-583.

13. Wu P, Duan F, Luo C, Liu Q, Qu X, Liang L et al. Characteristics of ocular findings of patients with coronavirus disease 2019 (COVID-19) in Hubei Province, China. *JAMA Ophthalmol* 2020;138:575-578.

14. Wan Y, Shang J, Graham R, Baric RS, Li F. Receptor recognition by the novel coronavirus from Wuhan: an analysis based on decade-long structural studies of SARS coronavirus. *J Virol* 2020;94:e00127-20.

15. Ma N, Li P, Wang X, Yu Y, Tan X, Chen P et al. Ocular manifestations and clinical characteristics of children with laboratory-confirmed COVID-19 in Wuhan, China. *JAMA Ophthalmol* 2020;138:1079-1086.

16. Zhou L, Xu Z, Castiglione GM, Soiberman US, Eberhart CG, Duh EJ. ACE2 and TMPRSS2 are expressed on the human ocular surface, suggesting susceptibility to SARS-CoV-2 infection. *Ocul Surf* 2020;18:537-544.

17. Yuan J, Fan D, Xue Z, Qu J, Su J. Co-expression of mitochondrial genes and ACE2 in cornea involved in COVID-19. *Invest Ophthalmol Vis Sci* 2020;61:13.

18. Cheema M, Aghazadeh H, Nazarali S, Ting A, Hodges J, McFarlane A et al. Solarte C. Keratoconjunctivitis as the initial

medical presentation of the novel coronavirus disease 2019 (COVID-19). *Can J Ophthalmol* 2020;55:e125-e129.

19. Roshanshad A, Ashraf MA, Roshanshad R, Kharmandar A, Zomorodian SA, Ashraf H. Ocular manifestations of patients with coronavirus disease 2019: a comprehensive review. *J Ophthalmic Vis Res* 2021;16:234-247.

20. Holappa M, Valjakka J, Vaajanen A. Angiotensin(1-7) and ACE2, "the hot spots" of renin-angiotensin system, detected in the human aqueous humor. *Open Ophthalmol J* 2015;9:28-32.

21. Oren B, Kocabas, DO. Assessment of corneal endothelial cell morphology and anterior segment parameters in COVID-19. *Therapeutic advances in ophthalmology*. 2022; 14, 25158414221096057.

22. Soysal GG, Seyyar SA, Kimyon S, Mete A, Güngör K. Examination of the Corneal Endothelium in Pediatric Patients With COVID-19. *Eye & Contact Lens*. 2023; 49(11), 508-510.

23. SeyedAlinaghi S, Mehraeen E, Afzalian A, Dashti M, Ghasemzadeh A, Pashaei A, et al Dadras O. (2024). Ocular manifestations of COVID-19: A systematic review of current evidence. *Preventive Medicine Reports*. 2024;38, 102608.

24. Kaya-Guner E, Sahin A, Ekemen-Keles Y, Karadag-Oncel E, Kara-Aksay A, Yilmaz D. A prospective long-term evaluation of the ocular findings of children followed with the diagnosis of multisystem inflammatory syndrome (long-term evaluation of ocular findings following MIS-C). *Eye*, 2023; 37(16), 3442-3445.

25. Alnahdi, M. A., & Alkharashi, M. (2023). Ocular manifestations of COVID-19 in the pediatric age group. *European Journal of Ophthalmology*, 33(1), 21-28.

26. Ishigooka, G., Mizuno, H., Oosuka, S., Jin, D., Takai, S., & Kida, T. (2023). Effects of angiotensin receptor blockers on streptozotocin-induced diabetic cataracts. *Journal of Clinical Medicine*, 12(20), 6627.

Research Article

EFFECT OF EXTENDED POLYMERIZATION TIMES ON THE DEGREE OF CONVERSION AND MICROHARDNESS OF RESIN COMPOSITES

 Tuğçe ERDEM^{1*},  Sezer DEMİRBUĞA¹,  Hacer BALKAYA¹

¹Department of Restorative Dentistry, Faculty of Dentistry, Erciyes University, Kayseri, TURKIYE

*Correspondence: tugce.aydin.94@gmail.com

ABSTRACT

Objective: This study is of significant importance as it evaluates the polymerization properties of bulk-fill and conventional resin composites regarding the degree of conversion (DC) and microhardness (MH) at different polymerization times. The findings of this research can potentially influence the future of restorative dentistry.

Materials and Methods: In this study three different polymerization times (20 s, 60 s, and 100 s) were applied to disc-shaped samples (6 mm wide; and 2 mm high) prepared from two bulk-fill resin composites (Filtek One Bulk Fill Restorative, X-tra Fil) and two traditional resin composites (Filtek Z550, Charisma Smart). The DC of the polymerized samples was measured with a Fourier Transform Infrared/ Attenuated Total (FT-IR/ATR) device, and the MH values were measured with a Vickers hardness device. The collected data were subjected to statistical analysis.

Results: The FT-IR analysis and Vickers microhardness test results demonstrated that the DC and MH values of the groups exposed to 100 s of light curing were significantly higher than those of the other groups ($p<0.05$).

Conclusions: The extended polymerization time applied to the resin composites in this study significantly increased the materials' DC and MH.

Keywords: Bulk fill composite, Degree of conversion, Microhardness, Resin composite

Received: 21 October 2024

Revised: 21 December 2024

Accepted: 21 April 2025

Published: 23 June 2025

This study was presented as an oral presentation at the FDI international dentistry congress on September 12, 2024.



Copyright: © 2025 by the authors. Published by Aydın Adnan Menderes University, Faculty of Medicine and Faculty of Dentistry. This article is openly accessible under the Creative Commons Attribution-NonCommercial 4.0 International (CC BY-NC 4.0) License.

INTRODUCTION

At present, resin composites represent the most widely utilized restorative materials in dental practice for treating dental hard tissue defects (caused by caries, trauma, systemic disease, congenital factors, etc.) to restore the aesthetic and functional functions of teeth by ensuring the integrity and continuity of the dental tissue with correct diagnosis and appropriate treatment of the defects (1). The maximum thickness that can be applied to ensure adequate polymerization in traditional resin composites is 2 mm (2). For this reason, conventional resin composites are applied incrementally in deep cavities. In addition to requiring technical precision, incremental application is time consuming and there is a risk of contamination and gaps between layers (3). To overcome these limitations, manufacturers have developed bulk-fill resin composites that can be applied in 4-5 mm increments by incorporating modifications such as the use of alternative photoinitiators, adjustments in the size of inorganic fillers, and alterations in the monomer composition (4).

Adequate polymerization of resin composites is essential for the success of restorations (5). The physicomechanical properties of resin composites depend on the degree of polymerization; and, thus, on certain variables such as the color, content, and thickness of the composite, light polymerization unit, light intensity, wavelength and polymerization time (6, 7). Ideally, all the monomers in resin composites should be converted to polymers during the polymerization reaction. However, dimethacrylate monomers cannot polymerize completely and residual monomers (double carbon bonds) may remain, which can cause irreversible damage to the pulp through the dentinal tubules (8).

As the degree of polymerization increases, the amount of residual monomer that does not participate in the reaction in the organic matrix decreases, which enhances the physical properties of the material, such as the elastic modulus, color stability, biocompatibility, solubility and monomer release (9, 10). As the DC increases and the material's residual monomer content decreases, the resin composite's hardness increases (11). An indicator of the high DC of resin composites is that they reach sufficient hardness values. When the literature is scanned, microhardness tests are frequently used as an indirect method when determining DC (12).

While previous studies have compared the microhardness and monomer conversion rates of bulk-fill and conventional resin composites, the effect of extended light

exposure time has yet to be thoroughly investigated (13, 14). This study aimed to assess the impact of extended polymerization times on the DC and MH of two different bulk-fill and two conventional resin composites. The null hypothesis of our study is as follows:

1. The DC does not change as the light application time increases.
2. MH does not change as the light application time increases.

MATERIALS AND METHODS

In this study, one traditional nanohybrid resin composite (FZ550; Filtek™ Z550, 3M ESPE, St Paul, MN, USA), one traditional microhybrid resin composite (CS; Charisma Smart, Heraeus Kulzer GmbH, Hanau, Germany) and two bulk fill resin composites (FOBF; Filtek™ One Bulk Fill Restorative, 3M ESPE, St Paul, MN, USA) and (XF; X-tra Fil, Voco, Cuxhaven, Germany) were used.

A power analysis was conducted to determine the appropriate sample size. According to the power analysis results of the test performed in the G*Power 3.1 program with an alpha value of 0.05 and an 85% confidence interval, the minimum number of samples was 5. For this reason, the number of samples in our study was determined to be 6.

Specimen preparation

In our study, resin composites were applied to a Teflon mold (6 mm in diameter, 2 mm in height) placed on glass with the help of a handpiece. Then, another glass was placed under constant hand pressure to provide a flat form to the upper surface and prevent air bubbles from remaining. To achieve equal light distance standards for each resin composite sample, the tip of the light device was positioned in direct contact with the glass and perpendicularly. The prepared samples were polymerized with an LED light device (Valo / Cordless, Ultradent Products Inc, South Jordan, UT, USA) for 20 s (control group), 60 s and 100 s. After the samples were prepared, finishing and polishing procedures were performed in a dry condition the Sof-Lex Composite Finishing and Polishing Disc Set (3M ESPE, St Paul, MN, USA) sequentially from coarse to fine grit with a low-speed handpiece. Each disc was used for 30 seconds and every two samples were changed. The prepared samples were categorized according to their groups, placed in dry conditions within lightproof containers, and stored at room temperature for 24 hours. The DC of the composite samples was evaluated via FT-IR/ATR analysis, and the

MH values were evaluated via Vickers hardness measurements.

Vickers microhardness

The samples (12 groups n=6) were placed under the Vicker notch tip of the microhardness device (EMCO Test/DuroScan, Kellau, Kuchl, Austria). A load of 100 g (2,942 N) was applied to the samples for 15 s, and three measurements of each sample were made at three different points. The mean of the three measurements was calculated and recorded as the hardness value of each sample. Rectangular-shaped notches were made with a Vicker's notching tip positioned perpendicular to the surfaces of the samples. After the notch was opened, the diagonal lengths of the quadrangular notches formed in the samples placed under the x40 magnification lens of the microhardness device were manually determined with the help of the arms moving in the x-y-z plane of the hardness device, and the device automatically calculated the Vickers hardness value.

FT-IR/ATR analysis

The spectra of the polymerized samples (12 groups, n=6) for which the DC of the monomer was measurements were measured with an FT-IR/ATR device (Perkin Elmer/ 400 FT-IR/ATR Spectrometer Spotlight 400 Imaging System, Waltham, Massachusetts, USA) at 4000-400. In the cm^{-1} wavenumber range, 20 scan counts and 4 cm^{-1} wavenumber resolution were recorded. First, FT-IR/ATR spectra of non-polymerized composite samples were recorded. Subsequently, the polymerized composite samples were positioned against the ATR crystal, and the device's clamping arm was secured. In this way, spectral measurements of each sample were performed, and the absorbance values were measured. The DC was calculated by substituting the obtained data and the determined absorbance values of the double-bonded carbons into the formula below.

$$\text{DC (\%)} = \left(1 - \frac{\left(\frac{\text{aliphatic}}{\text{aromatic}} \right) \text{polymer}}{\left(\frac{\text{aliphatic}}{\text{aromatic}} \right) \text{monomer}} \right) * 100$$

Statistical analysis

While the findings obtained in the study, were being evaluated the SPSS 20 (SPSS Inc.; Chicago, IL, USA) program was used for statistical analysis. Statistical analyses of the data obtained from the samples studied with FT-IR/ATR and Vicker's Hardness devices were performed via one-way variance (One-Way ANOVA) to

evaluate the differences between groups, and two-way variance (Two-Way ANOVA) to assess the effects of various times and materials was performed. Multiple comparisons were performed using Bonferroni and Tukey HSD post-hoc analyses. A p-value of less than 0.05 was considered statistically significant for all analyses.

RESULTS

The mean values and standard deviations for the DC and MH of the resin composites evaluated in this study are presented in Table 1. Based on the calculated results, extending the polymerization time significantly enhanced the DC and MH values of the resin composites tested ($p < 0.05$). The MH values of the FOFB and CS resin composites increased as the polymerization time increased, but the difference was not statistically significant ($p > 0.05$). When the MH values of individual resin composites were examined during the polymerization period, FZ550 presented the highest value, and the CS resin composite presented the lowest value.

Table 2 displays the resin composites' DC and MH values and standard deviations, regardless of the light curing duration. When we looked at the DCs of the resin composites used regardless of the polymerization time, XF had the highest value, and the CS resin composite had the lowest value.

Table 1. Average degree of conversion (DC) and microhardness (MH) findings and standard deviations of resin composites according to light application time

Resin Composite	Time	N	Degree of Conversion		Microhardness	
			Mean DC±SD	Statistical Difference	Mean MH±SD	Statistical Difference
FZ550	20 s	6	50.7±0.7	A	74.6±8.3	A
	60 s	6	55.8±1.3	B	109.5±13.7	B, C
	100 s	6	68±1.5	C	112.4±14.4	B, C
CS	20 s	6	27.2±0.8	D	97.1±14.8	B
	60 s	6	35±1.5	E	103.5±16.8	B
	100 s	6	39.8±1.4	F	126.1±4.4	C
FOFB	20 s	6	30.4±1.1	G	59.1±13	A, D
	60 s	6	32.2±0.8	G	59.5±20.4	A, D
	100 s	6	49.6±1.1	A	75.6±16	A
XF	20 s	6	59.8±0.8	H	39.8±6.6	D
	60 s	6	65.2±0.5	I	54.3±15.4	A, D
	100 s	6	65.6±0.8	I	58.2±8.6	A, D

The DC and MH values and standard deviations of the resin composites used with different polymerization times regardless of the type of composite are shown in Table 3.

Table 2. Average degree of conversion (DC) findings and standard deviations of the resin composites used regardless of the light application time

Resin Composite	N	Degree of Conversion		Microhardness	
		Mean DC±SD	Statistical Difference	Mean MH±SD	Statistical Difference
FZ550	18	57.9±8.8	A	108.9±15.2	A
CS	18	34±6.3	B	50.8±9.6	B
FOBF	18	37.4±10.6	C	64.7±9.4	C
XF	18	63.5±3.2	D	98.8±21	D

Table 3. Average degree of conversion (DC) findings and standard deviations of resin composites due to light application, regardless of the resin composite type

Time	N	Degree of Conversion		Microhardness	
		Mean DC±SD	Statistical Difference	Mean MH±SD	Statistical Difference
20 s	24	42± 15.07	A	67.65± 24.2	A
60 s	24	47.1± 16.1	B	81.7± 28.8	B
100 s	24	55.6± 13.3	C	93± 31.5	C

DISCUSSION

In our study, increasing the polymerization time of bulk-fill and traditional resin composites from 20 s to 100 s significantly increased their DC. There was no statistically significant difference between the 20 and 60 s polymerization times of the FOBF samples and the 60 and 100 s polymerization times of the XF samples. Therefore, according to our findings, the first null hypothesis of the study, which was that the DC would not change as the light application time increased, was rejected.

It is hypothesized that the DC of resin composites is directly correlated with the duration of light-curing exposure (15). In our study, the impact of varying light curing durations on the DC across different resin composite materials was investigated, and it was observed that increasing the light application time from 20 seconds to 100 seconds resulted in increased DC in the samples. Lempel et al. (13) and Szalewski et al. (15) compared the DC of resin composite samples by polymerizing them for different periods; and a positive correlation existed between the duration of light curing and the DC. These data in the literature support the results of our study.

The literature has reported that DC is affected by the type of monomers in the organic matrix and their viscosity (16). Yıldırım et al. (17), and Szczesio-Włodarczyk et al. (18) in their study comparing the DC of methacrylate-based resins, reported that the highest DC in TEG-DMA and the lowest DC in Bis-GMA. They also found the DC order was Bis-GMA < Bis-EMA < UDMA < TEGDMA. Manufacturers

combine Bis-GMA with other monomers to increase the DC of resin composites by reducing viscosity. In particular, the presence of amine groups in the UDMA monomer increases the mobility of radical sites through characteristic chain transfer reactions that provide a second pathway for the continuation of polymerization. Thus, DC has increased (16).

Although both the FZ550 and CS groups used in our study are traditional resin composites, the reason different DCs may be due to the differences in the compositions of the materials. The manufacturer reported that the CS composite contains only Bis-GMA in its matrix. Its low DC can be explained by the high amount of this high-viscosity compound in its organic matrix. FZ550 contains UDMA, Bis-EMA and TEG-DMA in addition to Bis-GMA. Since these monomers decreased the viscosity of Bis-GMA and increased monomer mobility, they may have caused an increase in DC.

In our study, the FOBF groups generally presented low DC in all periods. A study evaluating the DC of different types of resin composites polymerized by applying light for a standard time, suggested that FOBF had the lowest DC, possibly due to its organic matrix content (14). FOBF contains different monomers such as high molecular weight AUDMA, AFM, and DDDMA, which can increase the stiffness of the polymer chain. High molecular weight monomers reduce the number of reactive groups on the organic matrix and inhibit their mobility during the polymerization reaction. This information supports the results of the monomer conversion degree obtained by looking at the monomer content of the resin composites we used in the study.

Since bulk-fill resin composites are applied at relatively high thicknesses, their opacity is reduced and their translucency is increased by reducing the amount of inorganic fillers in their structure for increased light transmission and sufficient polymerization (19). It is claimed in the literature that a high filler ratio negatively affects DC. It is thought that increasing the number of inorganic fillers causes the interaction of monomers, especially those with high viscosity, such as Bis-GMA, to weaken. As a result, it becomes difficult for the material to polymerize (5, 21). In contrast, in our study, the amount of inorganic fillers in the resin composites used was between 76% and 86%. According to our results, the percentage of DC in FZ550 (81.8%) was greater than that of the other samples. These results showed that the amount of inorganic fillers alone may not have much effect on DC, and may be due to the geometry of the inorganic fillers or differences in their components.

Microhardness testing is another commonly employed method to assess the DC in resin composites. In our study, as the duration of light application increased, it increased in MHs as in DCs. Therefore, our second null hypothesis was also rejected. MH is affected by the inorganic filler content of resin composites. Adding zirconium, barium and ytterbium particles to the inorganic filler structures of resin composites to increase their radiopacity also increases their light transmittance (22). Tekçe et al. (23) suggested that the high inorganic filler ratio and the presence of Zr/SiO₂ particles effectively increase the MH value of the FZ550 resin composite. In line with the data we obtained in parallel with this information, the significant superiority in the MS values of XF and FZ550 can be attributed to the high Zr/SiO₂ ratio in the inorganic filler.

Nagi et al. (24) compared the MH values of two bulk-fill resin composites polymerized at different thicknesses (2, 3 and 4 mm) and for various times (10, 20, 40 and 60 s). The XF group had higher hardness values than the other resin composites. It has been suggested that the XF bulk-fill resin composite shows high MH due to the large size and amount of inorganic filler particles. However, no statistically significant differences were detected in the MH values of the XF bulk fill resin composite across varying light curing durations. In our study, XF groups with a thickness of 2 mm to which light was applied for different periods, presented high MH values. In contrast, there was a statistically significant difference in the MH values at 20 s compared with those at 60 s and 100 s.

This study's limitations include its in vitro design, which does not account for the effects of temperature, humidity, and oral fluids. Additionally, the optical properties of dental tissues, such as their ability to reflect and transmit light were not considered. The impact of the type of light source used was not evaluated, and the effects of different light sources should be further investigated. Moreover, the study examined only specific polymerization durations, which constitutes another significant limitation..

CONCLUSION

Considering the limitations of the present study, it can be concluded that the resin composite XF exhibited the highest degree of conversion (DC) regardless of light exposure duration, while FZ550 showed the highest DC specifically at 100 seconds of light application. Furthermore, Vickers microhardness (MH) testing revealed that FZ550

had the highest MH values among the tested composites. Overall, both the degree of conversion and microhardness generally increased with extended light exposure up to 100 seconds.

Acknowledgments

We would like to thank the Proofreading & Editing Office of the Dean for Research at Erciyes University for copyediting and proofreading service for this manuscript.

Authorship contributions

Concept: SD, HB, Design: SD, HB Data collection or processing: TE Analysis and interpretation: HB, TE Literature search: TE Writing: HB, TE.

Data availability statement

The data supporting this study's findings are available from the corresponding author upon reasonable request.

Declaration of competing interest

There is no conflict of interest in this study.

Ethics

This study does not require ethical committee approval.

Funding

The study was supported by Erciyes University Scientific Research Projects Unit with the project number TDH-2021-11269.

REFERENCES

1. Fahad F, Majeed MA. Fracture resistance of weakened premolars restored with sonically-activated composite, bulk-filled and incrementally-filled composites (A comparative in vitro study). J Bagh Coll Dent 2014; 26, 22-27.
2. Alqudaihi FS, Cook NB, Diefenderfer KE, Bottino MC, Platt JA. Comparison of internal adaptation of bulk-fill and increment-fill resin composite materials. Oper Dent 2019; 44(1): E32-E44.
3. Karadas M, Hatipoğlu O, Er H, Akyüz Turumtay E. Influence of different light-curing units on monomer elution from bulk fill composites. JAST 2018; 32(23): 2631-2646.
4. Yu P, Yap A, Wang X. Degree of conversion and polymerization shrinkage of bulk-fill resin-based composites. Oper Dent 2017; 42(1), 82-89.
5. Obeid AT, Kojic DD, Felix C, Velo MM, Furuse AY, Bombonatti JF. Effects of radiant exposure and distance on resin-based composite polymerization. Am. J. Dent 2022; 35(4): 172-177.
6. Algamaiah H, Silikas N, Watts DC. Conversion kinetics of rapid photo-polymerized resin composites. Dent Mater J 2020; 36(10): 1266-1274.

7. Gonulol N, Ozer S, Tunc ES. Effect of a third - generation LED LCU on microhardness of tooth - colored restorative materials. *Int J Paediatr Dent* 2016; 26(5), 376-382.
8. Odabaşı D, Guler C, Kucukaslan D. Evaluation the amount of residual monomer released from different flowable composite resins. *BMC Oral Health* 2024; 24(1): 244.
9. Sarosi C, Moldovan M, Soanca A, Roman A, Gherman T, Trifoi et al. Effects of monomer composition of urethane methacrylate based resin on the C=C degree of conversion residual monomer content and mechanical properties. *Polymers* 2021; 13(24):
10. Moldovan M, Balazsi R, Soanca A, Roman A, Sarosi C, Prodan D et al. Evaluation of the degree of conversion, residual monomers and mechanical properties of some light-cured dental resin composites. *Materials* 2019; 12(13):
11. Hatipoğlu Ö, Par M, and Hatipoğlu FP. Comparison of degree of conversion performance of bulk-fill resin composites: A systematic review and network meta-analysis of in vitro studies. *J Dent* 2024; 105289.
12. El-Maksoud OA, Hamama HHH, Wafaie RA, El-Wasefy N, Mahmoud SH. Effect of shelf-storage temperature on degree of conversion and microhardness of composite restorative materials. *BMC Oral Health* 2023; 23(1):57.
13. Lempel E, Öri Z, Szalma J, Lovász BV, Kiss A, Tóth Á et al. Effect of exposure time and pre-heating on the conversion degree of conventional, bulk-fill, fiber reinforced and polyacid-modified resin composites. *Dent Mater* 2019; 35(2): 217-228.
14. Strini BS, Marques JFDL, Pereira R, Sobral-Souza DF, Pecorari VGA, Liporoni PCS et al. Comparative evaluation of bulk-fill composite resins; knoop microhardness, diametral tensile strength and degree of conversion. *Clin Cosmet Investig Dent* 2022; 225-233.
15. Szałewski L, Wójcik D, Sofińska-Chmiel W, Kuśmierz M, Różyło-Kalinowska I. How the duration and mode of photopolymerization affect the mechanical properties of a dental composite resin. *Materials* 2022; 16(1): 113
16. Deng H, Liu F, He J. The Effect of Inorganic Filler Content on the Properties of BPA-Free Bulk-Fill Dental Resin Composites. *Materials* 2024; 17(20): 5040.
17. Yıldırım ZS, Eyiler E, Kürklü ZGB. Effect of thickness on the degree of conversion, monomer elution, depth of cure and cytotoxicity of bulk-fill composites. *J. Oral Sci* 2023; 65(2): 121-126.
18. Szczesio-Włodarczyk A, Domarecka M, Kopacz K, Sokolowski J, Bociong K. An evaluation of the properties of urethane dimethacrylate-based dental resins. *Materials* 2021; 14(11): 2727.
19. Sampaio CS, Abreu JLBD, Kornfeld B, Silva EMD, Giannini M, Hirata R. Short curing time bulk fill composite systems: volumetric shrinkage, degree of conversion and Vickers hardness. *Braz. Oral Res* 2024; 38: e030.
20. Haugen HJ, Marovic D, Par M, Khai Le Thieu M, Reseland JE, Johnsen GF. Bulk fill composites have similar performance to conventional dental composites. *Int. J. Mol. Sci* 2020; 21(14): 5136.
21. Duman AN, Cevik P, Doğan A. The Effect of the Resin Type and Filling Placement Techniques on the Degree of Conversion of Various Resin-Based Composites. *Appl. Sci* 2024; 14(23): 11215.
22. Pedreira PR, Damasceno JE, Cerqueira GAD, Souza AF, Aguiar FHB, Marchi GM. Radiopacity and physical properties evaluation of infiltrants with Barium and Ytterbium addition. *Braz. Dent. J.* 2023; 34: 93-106.
23. Tekçe N, PALA K, Özel E, Tuncer S, Demirci M. Üç Farklı Kompozit Materyalinin Yüzey Sertliği Üzerinde Polimerizasyon Süresinin Etkisi. *Türkiye Klinikleri Journal of Dental Sciences* 2015; 21(2).
24. Nagi SM, Moharam LM, Zaazou MH. Effect of resin thickness, and curing time on the micro-hardness of bulk-fill resin composites. *J Clin Exp Dent* 2015; 7(5), e600.

Research Article

EVALUATION OF THE CONNECTIONS OF DIFFERENT TYPE OF ABUTMENTS TO THE IMPLANT BODY UNDER MASTICATION

 Yezdan Dilan ERKCAN¹,  Mehmet Ali KILIÇARSLAN^{2*},  Bora AKAT³,  Burak
BILECENOĞLU⁴,  Kaan ORHAN⁵

¹ Magusa Medical Center Hospital, Gazimağusa, TURKISH REPUBLIC OF NORTHERN CYPRUS

² Department of Prosthodontics, Faculty of Dentistry, Ankara University, Ankara, TURKIYE

³ Department of Prosthodontics, Faculty of Dentistry, Ankara University, Ankara, TURKIYE

⁴ Department of Basic Medical Sciences, Faculty of Medicine, Ankara Medipol University, Ankara, TURKIYE

⁵ Department of Oral and Maxillofacial Radiology, Faculty of Dentistry, Ankara University, Ankara, TURKIYE

*Correspondence: ufukdemirci3232@gmail.com

ABSTRACT

Objective: This study aims to compare the biomechanical behavior of the implant-abutment connection against in-vitro loading in the use of Straight and Angled standard fabricated abutments and CAD/CAM abutments in a locally designed and produced special connection.

Materials and Methods: Ti Grade5 Straight abutment was used in the first group, 25° Angled Ti Grade5 fabricated abutment was used in the 2nd Group, and TiBase abutment was used in the 3rd Group. The implant diameter was used as 4.8 mm, and each sample was fixed on the implant manually or using a torque wrench. The crowns were cemented or screwed to the superstructures, which were torqued or manually tightened to 30 Ncm twice a day apart, and the first images were taken with the Micro-CT device. Four-year use of each sample was simulated in 1000000 cycles in the chewing simulator application. Micro-CT was again used to measure implant-abutment contact areas after loading.

Results: There is a significant difference between all groups, except for the range in the tightening group with 30Ncm torque before simulation, only on one side and at the internal measurement point.

Conclusion: When we look at the compatibility of the connection screw with the abutment before and after the chewing simulation; In general, it has been noticed that the fabricated straight abutments and Universal Ti-Base abutments have a tighter connection gap, while the connection of Angled abutments is weaker. When looking at the compatibility of the abutment contact areas with the implant body before and after the chewing simulation; It has been observed that the tightest connection values are generally created by CAD/CAM and Straight abutments, to a greater extent than screw fit.

Keywords: Implant-abutment connection, Micro-gap, Micro-ct

Received: 11 December 2025

Revised: 06 April 2025

Accepted: 14 April 2025

Published: 23 June 2025



Copyright: © 2025 by the authors. Published by Aydın Adnan Menderes University, Faculty of Medicine and Faculty of Dentistry. This article is openly accessible under the Creative Commons Attribution-NonCommercial 4.0 International (CC BY-NC 4.0) License.

INTRODUCTION

Although implant-supported dentures are a successful treatment option, some failures may be encountered, as in every treatment. Abutment-related complications; Problems in the adaptation between the implant and the abutment material, abutment angulation, abutment screw loosening or screw fractures. Implant-abutment connection; It is very important for the long-term success and stability of the prosthesis. Incompatibility between these components is an issue that should be taken into consideration because, in addition to mechanical problems such as screw loosening and damage to the internal screw threads, it also causes biological complications due to microorganism colonization in the interior of the implant. As a result of these biological complications, inflammation occurs in the peri-implant tissues, followed by pain, marginal bone loss, and in the worst case scenario, deterioration of osseointegration may result (1).

The internal connection formed by the abutment and extends up to 4 to 6 mm into the implant bodies. This design increases the adaptation between the bodies and the abutments (2). In the internal connection, the first part of the implant in contact with the abutment resists most of the forces coming from the outside, thus eliminating the majority of the forces applied to the screw, significantly reducing the adaptation loss and ensuring the continuity of the stability of the implant abutment connection (3). The internal connection has superiority over the external connection in ensuring the adaptation of the implant and abutment connection, preventing torque loss and resisting screw loosening (4,5).

Ideally, implants should be placed parallel to axial forces. Due to improper interjaw relationships or improper bone structure, the long axis of the placed implant and the long axis of the planned prosthetic superstructure may be incompatible, and angled abutment is used in prosthetic restorations in order to provide ideal aesthetics and position by combining these two planes. Angled abutments are frequently preferred in all-on-four and all-on-six treatment concepts used in the treatment of edentulous patients, for aesthetic reasons, to ensure distance from anatomical formations, and to provide convenience for the patient and physician by reducing treatment costs and duration (6-8). When the implant is not placed parallel to axial forces, angled abutments are used. Although the use of angled abutments makes it easier to provide aesthetics by giving the final shape to prosthetic restorations, the use of angled abutments is more prone to creating transverse forces during the

applied loads compared to straight abutments and this leads to the formation of off-axis forces.

The aim of present study is that a comparison of the mechanical situation of the implant and abutment connection against chewing in the use of straight and angled prefabricated abutments in a "deep internal hexagonal" connection and customized abutments produced in Universal Ti-Base and CAD/CAM technique. The clinical importance of present study is that observe the effect of chewing for implant-abutment connection fit. The null hypothesis of present study is; 1) Since the geometry and clearance area of the connection part and internal structures of the implant body used in the study are the same, there are not any differences between the post-connection micro gaps of all abutment designs, 2) in terms of abutments, there are not any differences for the gap between the groups tightened by hand and tightened with a torque wrench. 3) after the chewing simulation, there are no differences either.

MATERIALS AND METHODS

In this study, NucleOSSTM T6 Bone level implants (Turkey) were used, with a diameter of 4.8 mm, a conical internal hex structure with a 140 degree connection and made of pure titanium (Grade 4) compatible with international standards. Ti Grade5 fabricated straight, fabricated 25° Angled and personal CAD/CAM supports were used to connect to the implant bodies. Each material was divided into subgroups, each of which was tightened manually and with a torque wrench, and a total of 6 groups, each with n = 9 samples, were included in the study (Table 1). All hand tightening operations were

Table 1. Test groups

Group	Abutment and Connected Implant Body Diameter (mm)	Tightening Type
1	T6 WD051 Straight - Ti Grade5 prefabricated abutment(Diameter: 4,8)	Manual
2	T6 WD141 25° Angled Ti - Grade5 prefabricated abutment (Diameter: 4,8)	Manual
3	T6 32804 CAD/CAM abutment (Diameter: 4,8)	Manual
4	T6 WD051 Straight - Ti Grade5 prefabricated abutment (Diameter: 4,8)	30 Ncm
5	T6 WD141 25° Angled Ti - Grade5 prefabricated abutment (Diameter: 4,8)	30 Ncm
6	T6 32804 CAD/CAM abutment (Diameter: 4,8)	30 Ncm

Table 2. Before and After Chewing Simulator Values of the Gap Between the Screw and the Abutment According to "Tightening Type – Abutment" Factors (μm)

		SVD1	SVD2	SVM1	SVM2
Tightening Type	Abutment	Mean \pm Standard Deviation	Mean \pm Standard Deviation	Mean \pm Standard Deviation	Mean \pm Standard Deviation
Before	T6 WD051 Straight	15.90 ^A \pm 0.109	15.46 ^A \pm 0.178	16.37 ^A \pm 0.178	16.59 ^A \pm 0.123
	Manual T6 WD141 25° Angled	18.59 ^B \pm 0.098	19.01 ^B \pm 0.217	18.94 ^B \pm 0.402	19.68 ^B \pm 0.183
	T6 32804 CAD/CAM	15.34 ^C \pm 0.162	15.36 ^A \pm 0.278	15.16 ^C \pm 0.339	16.34 ^A \pm 0.470
	30 Ncm T6 WD051 Straight	11.51 ^A \pm 0.149	11.47 ^A \pm 0.156	12.07 ^A \pm 0.114	12.42 ^A \pm 0.204
	T6 WD141 25° Angled	14.57 ^B \pm 0.180	14.43 ^B \pm 0.157	14.65 ^B \pm 0.341	14.67 ^B \pm 0.424
	T6 32804 CAD/CAM	11.55 ^A \pm 0.109	11.11 ^A \pm 0.178	11.90 ^A \pm 0.178	11.83 ^A \pm 0.123
After	T6 WD051 Straight	28.54 ^A \pm 0.109	28.45 ^A \pm 0.178	28.54 ^A \pm 0.109	30.28 ^A \pm 0.123
	Manual T6 WD141 25° Angled	34.86 ^B \pm 0.098	33.98 ^B \pm 0.217	34.86 ^B \pm 0.098	36.07 ^B \pm 0.183
	T6 32804 CAD/CAM	33.61 ^C \pm 0.162	32.33 ^C \pm 0.278	33.61 ^C \pm 0.162	34.73 ^C \pm 0.470
	30 Ncm T6 WD051 Straight	28.78 ^A \pm 0.149	27.44 ^A \pm 0.156	28.78 ^A \pm 0.149	29.80 ^A \pm 0.204
	T6 WD141 25° Angled	43.64 ^B \pm 0.180	46.30 ^B \pm 0.157	43.64 ^B \pm 0.180	44.21 ^B \pm 0.424
	T6 32804 CAD/CAM	37.45 ^C \pm 0.109	35.06 ^C \pm 0.178	37.45 ^C \pm 0.109	37.91 ^C \pm 0.123

* The difference between the average value shown with a different letter in each "Tightening Type" subgroup is statistically significant ($P < 0.05$).

performed by the thesis researcher with maximum personal force (Groups 1-3). All tightening with a torque wrench was performed by the same researcher at a value of 30 Ncm according to manufacturer's instructions (Groups 4-6).

Standard metal crowns with the same form as the prosthetic superstructure were used to load the created mechanisms with the chewing simulation. To avoid motion artifacts, all samples were stayed in a vertical position in a mold with an inner diameter of 18.53 mm with using a paralelometer. For this purpose, the implant in each sample was fixed using autopolymerizing acrylic (Vertex-Dental, Netherlands) and embedded in the block mold. Groups with abutment screws tightened by hand force were tightened by a single physician twice, 24 hours apart, and standardized by applying the same force value for each sample. Torque group samples were completed by the same physician twice, with an interval of 24 hours, by applying a torque value of 30 Ncm according to the manufacturer's instructions. As the final stage of sample preparations; Cementation of metal crowns was performed with tgitmplaCEM dual-cure resin cement (Technical&General, London, UK), which is specially produced for implant applications.

Micro-CT scanning of the samples, Bruker SkyScan 1275 (Bruker Skyscan, Kontich, Belgium) device with high resolution scanning capacity was used in the Micro-CT laboratory of Ankara University Faculty of Dentistry. For

scanning parameters, the rotation step was determined as 0.5 for 100 kVp, 100 mA and 10 μm pixel size. After the scans were completed, each scanned sample was individually reconstructed using NRecon (NRecon, Version 1.6.7.2, Skyscan, Kontich, Belgium, 2020) software. Using NRecon software (Skyscan, Kontich, Belgium, 2020), images were reconstructed to show cross-sections of the samples. Additionally, CTAn (v.1.17.7.2, Bruker micro-CT, Kontich, Belgium) and the DataViewer program (v1.5.6.2; Bruker Micro-CT) were used to analyze and segment the three-dimensional models. The number of sections could be standardized for all samples and the same section corresponding to the center of the implants in all directions could be analyzed for each implant. By transferring the projections of the three-dimensional reconstruction samples to the CTAn (CTAn, 2020) software, from these points twice, before and after the chewing simulator; A comparison of measurements taken at certain points from the sagittal and coronal directions was made. For volumetric measurements, the upper and lower borders of the gap were marked with the software, and the gap boundaries to be calculated were determined in each of the remaining sections separately using the function called regions of interest (ROI). Then, the ROI created for each section was automatically combined by the software to create the volume of interest required for three-dimensional analysis.

Table 3. Before and After Chewing Simulator Values of the Gap Between the Abutment and the Implant Body According to "Tightening Type – Abutment" Factors (µm)

			AVD1	AVD2	AVM1	AVM2
	Tightening Type	Abutment	Mean±Standard Deviation	Mean±Standard Deviation	Mean±Standard Deviation	Mean±Standard Deviation
Before	Manual	T6 WD051 Straight	18.13 ^A ±0.315	18.41 ^A ±0.335	16.59 ^A ±0.171	18.97 ^A ±0.337
		T6 WD141 25° Angled	20.76 ^B ±0.096	20.82 ^B ±0.103	19.38 ^B ±0.362	20.87 ^B ±0.291
		T6 32804 CAD/CAM	21.32 ^C ±0.339	21.44 ^C ±0.375	19.82 ^C ±0.092	21.52 ^C ±0.380
		T6 WD051 Straight	17.54 ^A ±0.120	17.45 ^A ±0.232	17.64 ^A ±0.258	18.39 ^A ±0.196
	30 Ncm	T6 WD141 25° Angled	18.12 ^B ±0.300	17.97 ^B ±0.308	17.29 ^B ±0.158	18.96 ^B ±0.437
		T6 32804 CAD/CAM	16.54 ^C ±0.604	15.94 ^C ±0.281	17.25 ^B ±0.281	16.63 ^C ±0.280
		T6 WD051 Straight	30.13 ^A ±0.315	30.76 ^A ±0.335	28.64 ^A ±0.171	31.84 ^A ±0.337
		T6 WD141 25° Angled	37.76 ^B ±0.096	44.51 ^B ±0.103	39.68 ^B ±0.362	43.62 ^B ±0.291
	Manual	T6 32804 CAD/CAM	38.33 ^C ±0.339	42.13 ^C ±0.375	39.11 ^C ±0.092	42.27 ^C ±0.380
		T6 WD051 Straight	31.54 ^A ±0.120	32.14 ^A ±0.232	34.93 ^A ±0.258	34.15 ^A ±0.196
		T6 WD141 25° Angled	42.14 ^B ±0.300	44.73 ^B ±0.308	22.49 ^B ±0.158	49.97 ^B ±0.437
		T6 32804 CAD/CAM	37.54 ^C ±0.604	37.98 ^C ±0.281	43.19 ^C ±0.281	40.25 ^C ±0.280

* The difference between the average value shown with a different letter in each "Tightening Type" subgroup is statistically significant (P<0.05).

The samples with the first Micro-CT scan were placed in the chewing simulator (Esetron, Turkey) device, and each sample was subjected to mechanical loading of 100 N with a frequency of 2 Hz at a speed of 45 mm per second from a distance of 5 mm vertically, and 1000 N with intraoral simulation at 37°C water temperature. Four years of use in 1000000 cycles is simulated (9). Following this process, the same samples were scanned again using the same parameters with the SkyScan 1275 device to evaluate the adaptation of the implant parts.

Data were evaluated using Analysis of Variance (ANOVA) for the size of the microvoid expressed as mean ± standard deviation. TUKEY HSD multiple comparison test was applied according to the distribution of the results. Statistical significance level was determined as P < 0.05. Homogeneity of variances was tested with Levene test.

RESULTS

In the part of this study where connection fit was evaluated using Micro-CT, sample measurement values were first divided into two groups: linear and volumetric (Figure 1). Linear measuring points; It is divided into subgroups to evaluate the gap between the connection

screw and the abutment (Screw Vertical Distal - SVD and Screw Vertical Mesial - SVM) and to evaluate the gap between the implant body (Abutment Vertical Distal - AVD and Abutment Vertical Mesial - AVM). By transferring the projections of the three-dimensional reconstruction samples to the CTAn (CTAn, 2020) software, the sagittal measurements taken from these

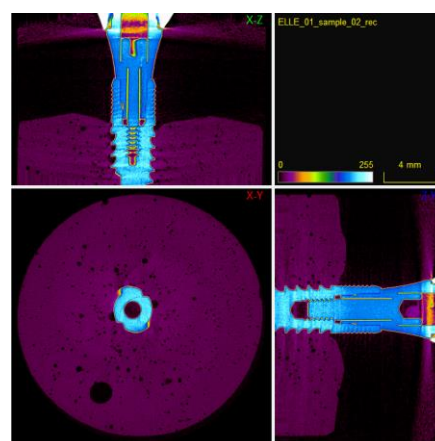


Figure 1. Micro-ct evaluation for screw and abutments.

points were compared twice, before and after the chewing simulator (Table 2).

When the abutment and the implant body were evaluated in terms of compatibility according to the results of the TUKEY HSD multiple comparison test conducted for the "Tightening Type - Abutment" factors before and after the chewing simulator; There is a significant difference between all groups, except for the range in the tightening group with 30Ncm torque before simulation, only on one side and at the internal measurement point (AVM1). At the AVM1 point, which differs from the general, the straight abutments showed a statistically significant difference compared to the other two abutments. According to the data obtained, the lowest range values are; It was determined in the measurements before the chewing simulation in straight and CAD/CAM abutments tightened with a torque of 30 Ncm (Table 3).

DISCUSSION

Gastric NHLs, which constitute 1-4% of all GI When the results of this study were critically evaluated, it was observed that although the parts sitting on the implant body had the same geometry, the abutment superstructure design especially affected the connection compatibility. Additionally, in almost all samples, notable differences were detected in the compliance values after the chewing simulation compared to before the simulation. Considering all these data, the null hypothesis of our study was partially accepted. 1) Although the geometry and gap area of the connection internal structures of the implant bodies used in the study are the same, contrary to our hypothesis, different abutment designs revealed different microgap values and our first hypothesis is invalid, 2) This hypothesis is rejected, as it is generally seen more in the groups compressed with a torque wrench before being exposed to the chewing simulation. 3) This hypothesis is rejected because the amount of gap in all groups after the chewing simulation is greater than the first measurements.

Although the popularity of implant-supported prostheses is increasing day by day, this increase; has brought about the frequency of encountering various complications. Frequently reported mechanical complications; Failures of prosthetic components, loss of retention, screw loosening and implant fracture. Screw-related complications in implant-supported restorations are frequently reported in the literature, and screws are known as the weakest link of these restorations. It has been observed that various complications occur as a result of screw loosening.

Additionally, loose screws are more prone to breakage under load, leading to long-term prosthesis complications (10, 11).

He et al. aimed to examine the microcavities at the implant and abutment interface and the change in the contact area for two different connection designs under angular cyclic loading. In the two-piece implant system consisting of a conical connection group and an external hexagonal connection group, the samples were subjected to cyclic loading by applying increasing loads up to 220 N. After loading, the samples were scanned using Micro-CT and the resulting level of leakage was evaluated using silver nitrate, a high-contrast penetrating agent. In this study, it was observed that the conical connection showed more resistance to the formation of microcavities at the implant and abutment interface compared to the external hexagonal connection (12).

Zipprich et al. aimed to examine the mechanical situation of different implants and abutment connections with X-ray imaging. 20 different implant systems, with different implant sizes and different implant abutment connections, were used in the study. The samples were subjected to static and dynamic force (200 N). The width and length of the gap between the implant-abutment interface and different implant-abutment connection types were compared. As a result of the study, it was observed that eight of the 20 implant systems with conical connections had no measurable microgaps under 200 N load, while all other systems with straight abutment connections had measurable gaps in static and dynamic loading. Using x-ray imaging, reduced microvoid formation and micromobility have been detected in systems with tapered implant-abutment connections compared to systems with straight connections (13).

Hamilton et al. compared the titanium, CAD/CAM abutments with prefabricated abutments of five different implant types (Brånemark System, NobelReplace RP, Astra Tech OssesoSpeed 4.0, Straumann Bone Level RC, Straumann Standard Plus RN). As a result of the study, the average difference of 1.86 μm between the CAD/CAM abutments on the gold synOcta and Straumann Standard Plus implant was found to be statistically significant. For the remaining implant types, less than 0.4 μm difference was found between prefabricated abutments and CAD/CAM abutments and no statistical difference was observed. A statistically significant mean difference of 34.4 μm (gold) and 44.7 μm (titanium) was found between CAD/CAM abutments and prefabricated abutments on Straumann Standard Plus implants. An average difference

of 15 μm was observed on the NobelReplace implant and the CAD/CAM abutment, and this value was found to be statistically significant. All other groups had differences of less than 4 μm and this value was not found to be statistically significant. In most systems evaluated, CAD/CAM abutments demonstrated compliance comparable to prefabricated abutments. In our study, when looking at the compliance with chewing simulation; In general, it has been noticed that the fabricated Straight implant abutments exhibit a tighter connection gap, while the connection of Angled abutments is weaker (14).

Focusing on implant abutments and taking into account the advantages, disadvantages and complications of CAD/CAM abutments, the study aims to discuss the use of custom abutments in the anterior region (CAD/CAM). It has been concluded that the use of CAD/CAM concepts in production provides advantages over both stock abutments and traditional cast custom abutments. CAD/CAM abutments are available in a variety of materials and different attachment platforms to the implant to meet aesthetic, functional and biological demands. CAD/CAM technology is a system that should be considered in the restoration of dental implants in the aesthetic zone (15).

The compatibility of the implant body - abutment - screw combination is not only the parameters related to the superstructure success of implant-supported prostheses, but also affects the survival time of the implant body in the bone. All in vitro studies in this field, including the Micro-CT analysis method used in this study, are efforts to collect data to increase the survival time of implant-supported prostheses in the mouth and thus to give ideas to both manufacturers and users. In addition, after prosthetic applications are completed and implant-supported prostheses are used, perhaps the most difficult prosthetic complication to compensate for is screw fractures. For this reason, choosing designs with the highest durability during the use process will increase the comfort and safety of use. For this reason, it is expected that the in vitro study, examining the most important parameters of implant systems related to oral survival and testing them in a large sample group, will also be predictive of clinical success.

CONCLUSION

Within the limitations of present study;
In general, screw has been noticed that the fabricated straight abutments exhibit a tighter connection gap, while the connection of Angled abutments is weaker. When evaluating the compatibility of the screw within the body,

the adaptable result among all groups was generally observed to be the most incompatible group, the CAD/CAM group. Another observed fact is that the screw connection under function decreases significantly over time. Implant body has been observed that the most strict adaptation values are generally created by CAD/CAM and straight abutments to a greater extent than the abutment compliance. It has been determined that aging negatively affects the connection values in terms of the fit of the abutment to the implant body.

Acknowledgments

The authors expressed gratitude to for their support thank Mr. Mustafa Yeşil for his support as a laboratory technician.

Authorship contributions

YDE and MAK planned and designed the study. YDE and BA collected and processed the data. YDE, MAK, BB, and KO contributed to the data analysis and interpretation. YDE conducted the literature search. YDE, MAK, BA, and BB drafted the manuscript.

Data availability statement

The data that support the findings of this study are available from the corresponding author upon reasonable request.

Declaration of competing interest

There is no conflict of interest in this study.

Ethics

Since resources obtained from humans or animals were not used in this study, ethics committee approval was not obtained.

Funding

No financial support was received from any institution or organisation for this study.

REFERENCES

1. Ramalho I, Witek L, Coelho PG, Bergamo E, Pegoraro LF, Bonfante EA. Influence of abutment fabrication method on 3D fit at the implant-abutment connection. *Int J Prosthodont* 2020; 33: 641-7.
2. Huang Y, Wang J. Mechanism of and factors associated with the loosening of the implant abutment screw: A review. *J Esthet Restor Dent* 2019; 31: 338-45.
3. Cibirka RM, Nelson SK, Lang BR, Rueggeberg FA. Examination of the implant-abutment interface after fatigue testing. *J Prosthet Dent* 2001; 85: 268-75.

- 4.Michalakakis KX, Calvani PL, Muftu S, Pissiotis A, Hirayama H. The effect of different implant-abutment connections on screw joint stability. *J Oral Implantol* 2014; 40: 146-52.
- 5.Sakamoto K, Homma S, Takanashi T, Takemoto S, Furuya Y, Masao Y, Yajima Y. Influence of eccentric cyclic loading on implant components: comparison between external joint system and internal joint system. *Dent Mater J* 2016; 35: 929-37.
- 6.Antoun H, Belmon P, Cherfane P, Sitbon JM. Immediate Loading of Four or Six Implants in Completely Edentulous Patients. *Int J Periodontics Restorative Dent* 2012; 32: e1-9.
- 7.Asvanund P, Cheepsathit L. Effect of different angulation angled abutment on screw loosening of implants under cyclic loading. *M Dent J* 2016; 36: 337-44.
- 8.Eger DE, Gunsolley JC, Feldman S. Comparison of angled and standard abutments and their effect on clinical outcomes: A preliminary report. *Int J Oral Maxillofac Implants* 2000; 15: 819-23.
9. Ferreira RM, Prado AM, Oliveira MS, Tonin RE, Mori AA, Ferruzzi F. Influence of Mechanical Cycling on Torque Values of Tapped-In and Screw-In Implant-Suppoorted Crowns. *Eur J Prosthodont Restor Dent* 2023; 31: 104-8.
- 10.Cho SC, Small PN, Elian N, Tarnow D. Screw loosening for standard and wide diameter implants in partially edentulous cases: 3- to 7-year longitudinal data. *Implant Dent* 2004; 13: 245-50.
11. Molinero-Mourelle P, Peter L, Gaviria AS, Fonseca M, Schimmel M, Katsoulis J. Tactile misfit detection ability at the implant-abutment interface of internal connection dental implants: an in-vitro study. *Acta Odontol Scand* 2023; 81: 591-6.
- 12.He Y, Fok A, Aparico C, Teng W. Contact analysis of gap formation at dental implant-abutment interface under oblique loading: A numerical-experimental study. *Clin Implant Dent Relat Res* 2019; 21: 741-52.
- 13.Zipprich HD, Weigl P, Ratka C, Lange B, Lauer HC. The micromechanical behavior of implant-abutment connections under a dynamic load protocol. *Clin Implant Dent Relat Res* 2018; 20: 814-23.
- 14.Hamilton A, Judge RB, Palamara JE, Evans C. Evaluation of the Fit of CAD/CAM abutments. *Int J Prosthodont* 2013; 26 :370-80.
- 15.De Kok IJ, Katz LH, Duqum IS. CAD/CAM Custom Abutments for Esthetic Anterior Implant-Supported Restoration: Materials and Design. *Curr Oral Health Rep* 2018; 5: 121-6.

Research Article

PSYCHOLOGICAL COMPARISON OF ADULTS WITH DIZZINESS: DEPRESSION, ANXIETY, AND SOMATIZATION IN TYPICAL vs. ABNORMAL VESTIBULAR TEST RESULTS

 Hanifi KORKMAZ^{1*},  Ahmet KUTLUHAN²,  Banu MÜJDECI³,  Erkan KARATAŞ⁴

¹ Department of Medical Health Services and Vocational School Malatya Turgut Özal University Battalgazi, Malatya, TURKIYE

² Ahmet Kutluhan Department of Ear, Nose, and Throat Faculty of Medicine Pamukkale University Ankara, TURKIYE

³ Banu Mujdeci Department of Audiology Faculty of Health Sciences Ankara Yıldırım Beyazıt University Ankara, TURKIYE

⁴ Erkan Karataş Department of Ear, Nose, and Throat Istanbul Atlas University Istanbul, TURKIYE

*Correspondence: hanifikorkmaz444@gmail.com

ABSTRACT

Objective: This study aimed to investigate the relationship between vestibular test results and levels of depression, anxiety, and somatization in patients with dizziness. It also examined the correlation between vestibulo-ocular reflex (VOR) findings and subjective assessment scales.

Materials and Methods: Sixty patients with complaints of dizziness were divided into two groups: Group I (n=30, abnormal vestibular test findings) and Group II (n=30, normal vestibular test results). All participants underwent audiological and vestibular evaluations [videonystagmography (VNG), video head impulse test (vHIT)] as well as psychological assessments using the Beck Depression Inventory (BDI), Beck Anxiety Inventory (BAI), and the Somatization subscale of the Symptom Checklist-90 (SCL-90). Data were analyzed using SPSS version 22.0, with statistical significance set at $p<0.05$.

Results: No significant differences were found between the groups in terms of BDI, BAI, or somatization scores ($p>0.05$). However, Group I had significantly higher total and emotional subscale scores on the Dizziness Handicap Inventory (DHI) ($p<0.05$). In this group, DHI scores showed a positive correlation with both BDI and BAI scores ($p<0.05$). No significant correlation was observed between vHIT results and psychological measures in either group.

Conclusion: Vestibular test results do not appear to significantly influence levels of depression, anxiety, or somatization. However, subjective tools such as the DHI may reflect the psychological impact of dizziness and can be useful in guiding appropriate clinical management.

Keywords: Dizziness, vestibular system, vHIT, anxiety, depression, somatization

Received: 29 December 2024

Revised: 06 January 2025

Accepted: 10 June 2025

Published: 23 June 2025



Copyright: © 2025 by the authors. Published by Aydın Adnan Menderes University, Faculty of Medicine and Faculty of Dentistry. This article is openly accessible under the Creative Commons Attribution-NonCommercial 4.0 International (CC BY-NC 4.0) License.

INTRODUCTION

Dizziness and imbalance are common medical complaints, affecting 20%–30% of the general population, leading to a reduced quality of life (1). These symptoms often can result from various causes, including organic, psychosomatic, and psychiatric factors (2). The vestibular system, which plays a critical role in oculomotor control, balance regulation, and self-motion, is vital in maintaining equilibrium. Consequently, any dysfunction in the vestibular system can manifest as dizziness, balance issues, and even perceptual, memory, and emotional disturbances (2, 3). While psychological issues like depression and anxiety are commonly observed in vestibular disorder patients, dizziness and imbalance are also seen in individuals with psychiatric disorders (4). Some patients present with medically unexplained symptoms, such as fatigue, pain, and numbness, which may further complicate diagnosis and treatment (5).

The difficulty in identifying the main etiology of dizziness is exacerbated by the variability in how patients describe their symptoms. Patients are often referred to multiple specialists, such as neurologists or psychiatrists, before identifying the cause or ruling out others. This diagnostic process is not only emotionally and financially taxing for patients but also exhausting for healthcare providers, who may experience frustration and burnout due to poor clinical outcomes and patient dissatisfaction (5, 6).

Vestibular disorders affect individuals differently in terms of functional outcomes and recovery. As objectively measured, Vestibular deficits show little correlation with the severity of symptoms or functional impairment, except in cases of acute complaints (7, 8). Longitudinal studies have demonstrated that vestibular testing alone cannot predict which patients will recover following acute illness (7, 9, 10).

Given that dizziness can originate from various sensory and motor systems (11), comprehensive diagnostic methods are essential for accurate diagnosis. Test results should be interpreted alongside patient-reported symptoms and subjective evaluations. Diagnosing dizziness remains challenging due to the broad range of potential causes (12). Despite physical, neurological, and otological examinations, 10%–40% of dizziness cases remain undiagnosed (12, 13). Existing studies have largely focused on the comorbidity between vestibular disorders and psychological conditions. However, to our knowledge, no research has compared the subjective and objective findings in patients who report dizziness but show normal

vestibular test results. According to a review by Hoffman et al. (14), 69% to 76% of dizziness diagnoses can be made based on patient history alone (15, 16). While self-reflection questionnaires provide valuable insights into the subjective experience of dizziness (17), factors such as anxiety and depression are consistently correlated with the severity of vestibular symptoms (18).

Vestibular tests are fundamental clinical tools for distinguishing between peripheral and central causes of dizziness. In particular, the video Head Impulse Test (vHIT) and Suppression Head Impulse Paradigm (SHIMP) have proven effective in detecting peripheral vestibular hypofunction, demonstrating high diagnostic accuracy even in pediatric populations (19). In acute dizziness cases, vHIT offers 100% sensitivity for the rapid detection of central pathologies such as stroke (20). When combined with audiological assessments, vestibular testing provides a comprehensive evaluation of inner ear function (Garrison et al., 2019). The inclusion of caloric and oculomotor tests further enhances diagnostic precision and supports appropriate clinical decision-making (21).

Patients often bear negative beliefs about the consequences of dizziness, which can lead to avoidance of physical and social activities, further exacerbating the condition. Longitudinal studies have shown that such negative beliefs predict handicap severity, even after controlling for symptom severity (22). The agreement between patients' and physicians' assessments of dizziness symptoms tends to be moderate. Moreover, anticipating future dizziness episodes may cause greater distress than symptoms (23). Therefore, a preliminary evaluation using subjective surveys may help identify the psychological impact of dizziness before referring patients for further vestibular testing or to psychiatric services.

This study aimed to assess depression, anxiety, and somatization in patients with dizziness using subjective inventories to answer the following questions: 1. Do objective vestibular test results influence psychological test outcomes in patients with dizziness? 2. Are there any correlations between vestibuloocular test findings measured by vHIT and subjective findings? 3. How effective are subjective test findings in directing patients to appropriate outpatient clinics?

MATERIALS AND METHODS

This prospective study was derived from the master's thesis of Hanifi Korkmaz, conducted under the supervision of Ahmet Kutluhan. The study was approved

by the University's Clinical Research Ethics Committee (January 17, 2018; Decision Number: 11) and conducted in accordance with the Declaration of Helsinki. Informed consent was obtained from all participants. The study was conducted in a tertiary medical center, with sample size calculations performed using G*Power 3.1 software. A total of 60 dizzy patients were divided into two groups: Group I (30 patients with positive vestibular test results) and Group II (30 patients with normal vestibular test results) (Faul et al., 2009). Exclusion criteria included central vestibular deficits, neurological disorders, musculoskeletal or visual disorders, tinnitus, hearing loss, chronic dizziness (\geq three months), and psychiatric disorders (24). The sample included 60 patients (18 men, 42 women), aged 18–65. Group I consisted of patients with abnormal vestibular test results, while Group II included those with normal results.

Patient histories indicated that 65% of patients ($n = 39$) experienced position-related dizziness, overlapping with Persistent Postural-Perceptual Dizziness (PPPD) criteria. However, since no triggering factors for PPPD (e.g., upright posture or complex visual stimuli exposure) were present, the differential diagnosis was made (24). Patients underwent detailed medical histories, audiological assessments, and vestibular testing (VNG and vHIT). In this study, all patients underwent detailed clinical interviews, audiological assessments, and vestibular evaluations, including videonystagmography (VNG) and the vHIT, as part of a comprehensive diagnostic protocol. These tests were selected to objectively determine whether the dizziness originated from a peripheral vestibular dysfunction or a central/non-vestibular source. vHIT, in particular, was chosen due to its high sensitivity in detecting central pathologies such as stroke, especially in emergency clinical contexts (20). The integration of vestibular and audiological evaluations aimed to provide a complete assessment of inner ear function, which is particularly important in patients with overlapping or complex otological symptoms (25). Following the vestibular work-up, psychological assessments were conducted using the Beck Depression Inventory (BDI), Beck Anxiety Inventory (BAI), the Somatization subscale of the SCL-90, and the Dizziness Handicap Inventory (DHI).

Audiological evaluation

Pure-tone audiometry (0.25–8 kHz), high-frequency audiometry (10–16 kHz), and speech tests were performed using Interacoustic AC 40 clinical audiometry and TDH 39 P supra-aural headphones. Tympanometric and acoustic reflex tests were conducted using a 226-Hz probe tone

(Interacoustics AZ 26, Denmark). Normal hearing was defined as a pure-tone threshold <25 dB HL at all frequencies (26).

Vestibulospinal tests and evaluation

Past pointing tests, static postural tests (Romberg and tandem Romberg), and gait evaluations were performed. Abnormal results indicated past pointing deviation, difficulty maintaining posture, or gait instability (Krager, 2018). Severe gait instability is often associated with neurological issues (27).

Videonystagmography (VNG)

The VNG included oculomotor tests, spontaneous nystagmus evaluation, head-shaking nystagmus, positional tests, and the Dix-Hallpike maneuver using the Micromedical Technologies INC device with VisualEyes software. Abnormal findings included gaze-evoked nystagmus and direction-changing nystagmus. The central vestibular disorder was considered present based on the results of the following tests: The Gaze-evoked nystagmus (horizontal or vertical axis) test, direction-changing nystagmus, and gaze-evoked nystagmus opposite to Alexander's law were considered as central vestibular findings (28).

Video head impulse test (vHIT)

The vHIT assessed all semicircular canals using the EyeSeeCam system (Interacoustics, Denmark). Abnormal results included gain scores outside the 0.76–1.18 range and corrective saccades (29).

Dizziness handicap inventory (DHI)

The DHI was used to assess patients' perceived disability due to dizziness, comprising emotional, physical, and functional domains. Higher scores indicate greater perceived disability (30). The Turkish version was utilized (31).

Beck depression inventory (BDI) and beck anxiety inventory (BAI)

The BDI and BAI were used to measure depression and anxiety severity, respectively (32, 33).

Symptom checklist 90 (SCL-90)

SCL-90 was employed to assess psychological symptoms across nine subscales, including somatization, anxiety, and depression (34).

Statistical analysis

Statistical analyses were performed using SPSS 22.0 (IBM Corp., Armonk, NY, USA). Descriptive statistics were

used to summarize patient characteristics, including frequencies, means, and standard deviations. To compare psychological scores (BDI, BAI, SCL-90, and DHI) between Group I and Group II, independent t-tests were used. The chi-square test was applied for categorical variables. For correlations between psychological measures and vestibular test results, Pearson correlation coefficients were calculated. A p-value < 0.05 was considered statistically significant.

RESULTS

In Group I, vestibulospinal abnormalities were identified in 12 patients (40%), head-shaking test abnormalities in 4 patients (13%), positional test abnormalities in 16 patients (53%), and vHIT abnormalities in 14 patients (47%). Vertigo was reported by 60% of patients (n=39), lightheadedness by 33% (n=20), and disequilibrium by 7% (n=1). In 65% of patients (n=39), dizziness was episodic and position-related. Fifteen patients (23%) reported dizziness without any identifiable trigger, while 9 patients (15%) experienced dizziness in specific situations (e.g., stress, trauma, seasonal changes, or life events). No statistically significant differences were observed between groups in terms of age (p = 0.951) or gender (p = 0.261). (See Table 1).

Table 1. Comparison of groups by gender and age

Variable	Group I (n=30)	Group II (n=30)	Total (n=60)	Test Value	P Value
Gender					
Female	17 (56.6 %)	20 (66.6%)	37 (61.6%)	-0.131	0.261
Male	13 (43.3%)	10 (33.3%)	23 (38.3%)		
Age					
Mean ± SD	39.26 ± 12.04	37.16 ± 12.11		Mann-Whitney	0.951
Median (M)	39	37			
Min-Max	20-61	19-61			

n: number of samples, %: percent, Test value: Chi-square test value (χ^2), p value: statistical significance (p<0.05 indicates a statistically significant difference between the groups). While the different letters in the lines show the difference between the groups, the same letters indicate no difference.

Comparison of subjective scales between the groups

No statistically significant differences were found between the groups in BDI (p = 0.116), BAI (p = 0.230), or SOM scores (p = 0.953). However, a significant difference was observed in the emotional subscale and total scores of the

DHI (p = 0.025), indicating a key finding. There were no significant differences in the physical and functional subscales of DHI (p = 0.727) (see Table 2).

Comparison of intra-intra-group vestibular test and subjective scale findings in group I

Table 2. Comparison of BDI, BAI, SOM, and DHI findings among the groups

Variable	Group I (n=30)	Group II (n=30)	P Value
Beck Depression Inventory	11.26±0.05 (2.00-37.00)	15.06±0.05 (0.00-39.00)	0.116
Beck Anxiety Inventory	15.06±0.05 (0.00-39.00)	16.56±0.05 (4.00-44.00)	0.230
Somatization	10.30±0.05 (0.50-2.41)	10.31±0.05 (0.20-2.50)	0.953
DHI-Physical	10.93±0.05 (2.00-20.00)	13.20±0.05 (2.00-22.00)	0.060
DHI - Emotional	10.03±0.05 (0.00-20.00)	12.86±0.05 (4.00-26.00)	0.025
DHI-Functional	11.13±0.05 (2.00-20.00)	11.56±0.05 (4.00-20.00)	0.727
DHI-Total	31.63±0.05 (12.00-54.00)	37.83±0.05 (10.00-54.00)	0.020

DHI: Dizziness Handicap Inventory, p value: statistical significance (p<0.05 indicates a statistically significant difference between the groups).

No statistically significant correlations were found between vHIT gain values and BDI, BAI, or somatization scores (p > 0.05) (see Table 3). In contrast, a statistically significant correlation was observed between DHI scores and both BDI (p = 0.004) and BAI (p = 0.034). Positive correlations were also identified between BDI, BAI, and the physical (p = 0.022; p = 0.012) and total (p = 0.004; p = 0.034) subscales of the DHI (see Table 3).

Comparison of intra-intra-group vestibular test and subjective scale findings in group II

No statistically significant correlations were observed between vHIT gain values and BDI, BAI, or somatization scores (p > 0.05) (see Table 4). However, a positive correlation was found between BAI and the functional subscale of the DHI (p = 0.023) (see Table 4).

DISCUSSION

The intricate relationship between dizziness and psychological distress is a complex phenomenon. While dizziness can lead to psychological distress in specific individuals, for others, the psychological distress they experience may manifest as dizziness or vertigo. The mechanism that connects psychological symptoms with dizziness symptoms has yet to be fully understood. However, some experts suggest it may be due to a significant overlap between neuroanatomical regions,

Table 3. Correlation between BDI, BAI, SOM findings and vHIT gain findings, and DHI scores in Group I

Variable	vHIT Gain (n=60)	Right LSCC	Left LSCC	Right ASCC	Left PSCC	Left ASCC	Right PSCC	DHI- Physical	DHI- Emotional	DHI- Functional	DHI- Total
BDI	r	0.121	-0.237	0.003	0.127	-0.280	0.007	0.416	0.332	0.303	0.496
	p	0.523	0.207	0.989	0.503	0.133	0.969	0.022	0.076	0.104	0.004
BAI	r	0.113	-0.262	0.094	0.346	-0.335	0.022	0.451	0.198	0.235	0.389
	p	0.551	0.162	0.621	0.061	0.070	0.907	0.012	0.295	0.211	0.034
SOM	r	-0.052	-0.181	0.278	0.299	-0.283	0.159	0.268	0.361	0.093	0.280
	p	0.784	0.338	0.137	0.108	0.129	0.402	0.153	0.050	0.624	0.134

L = Lateral, A = Anterior, P = Posterior, SSC = Semicircular Canal, BDI = Beck Depression Inventory, BAI = Beck Anxiety Inventory, DHI = Dizziness Handicap Inventory, SOM = Somatization Score. Pearson correlation is significant at the 0.05 level (2-tailed).

Table 4. Correlation between BDI, BAI, SOM findings and vHIT gain findings, and DHI scores in Group II

Variable	vHIT Gain (n=60)	Right LSCC	Left LSCC	Right ASCC	Left PSCC	Left ASCC	Right PSCC	DHI- Physical	DHI- Emotional	DHI- Functional	DHI- Total
BDI	r	0.307	0.099	-0.084	-0.009	-0.228	0.356	0.048	0.196	0.206	0.229
	p	0.099	0.602	0.658	0.964	0.226	0.054	0.803	0.298	0.275	0.223
BAI	r	0.102	0.146	-0.013	-0.185	-0.010	0.107	-0.451	0.218	0.415	0.238
	p	0.591	0.442	0.947	0.329	0.958	0.574	0.441	0.247	0.023	0.205
SOM	r	0.284	0.275	0.041	-0.190	0.034	0.014	-0.115	0.196	0.323	0.190
	p	0.128	0.141	0.829	0.313	0.859	0.940	0.544	0.300	0.082	0.315

L = Lateral, A = Anterior, P = Posterior, SSC = Semicircular Canal, BDI = Beck Depression Inventory, BAI = Beck Anxiety Inventory, DHI = Dizziness Handicap Inventory, SOM = Somatization Score. Pearson correlation is significant at the 0.05 level (2-tailed).

vestibular system neurotransmitters, and emotional state pathways (1).

Psychological Test Results and Vestibular Findings: Our study showed no significant differences in BDA, BAI, and SOM scores between patients with and without vestibular test findings. Both groups exhibited mild to moderate depression, anxiety, and somatization. In Group I, these findings could be due to psychogenic symptoms secondary to vestibular disorders, while in Group II, dizziness might be due to psychological factors. No significant correlation was found between vestibular findings and psychological test results, which aligns with Best et al. (35) who also found no direct link between vestibular test results and psychological symptoms in patients with dizziness. In our clinical approach, all patients presenting with dizziness undergo comprehensive audiological and vestibular evaluation, regardless of initial diagnostic assumptions, to distinguish peripheral, central, or psychogenic origins. This inclusive strategy reflects real-world clinical diversity. The presence of dizziness in patients with normal vestibular test results (Group II) may indeed influence psychological findings. However, this subgroup represents a clinically relevant population, and their inclusion highlights the importance

of integrating subjective and psychological assessments into the diagnostic pathway for dizziness.

Recent studies have increasingly emphasized the role of psychological factors in dizziness severity, particularly among patients with vestibular pathologies. Rutenkröger et al. (2024) (22) reported that higher levels of depression and anxiety were significantly correlated with increased DHI scores in patients with vestibular schwannoma. Similarly, Inoue et al. (2023)(36) and Kim et al. (2024) found that psychiatric symptoms were highly prevalent in patients with vestibular disorders such as vestibular migraine (37), with clinically significant anxiety reported in nearly half of the cases. Omara et al. (2022)(38) further demonstrated that a substantial proportion of dizzy patients experience comorbid anxiety and depression, often simultaneously. Consistent with these findings, our study identified moderate levels of depression and anxiety in both groups, regardless of objective vestibular test results. The lack of significant differences in BDE scores between vestibular-positive and vestibular-negative groups may reflect the multifactorial and perceptual nature of dizziness, where subjective distress is not always aligned with measurable vestibular dysfunction. These results underscore the importance of including

psychological assessment in routine dizziness evaluations and support our study's objective of highlighting subjective factors as key diagnostic and therapeutic considerations.

(2) vHIT Findings and Psychological Measures: Our study found no significant correlation between vHIT results and anxiety, depression, or somatization. However, a relationship was found with DHI scores. Gurgel et al. (5) and Subaşı et al. (39) found links between psychological factors and vestibular dysfunction. However, this was not observed in our study due to the exclusion of conditions such as hearing loss or tinnitus. This might have reduced the impact of vestibular dysfunction on vHIT results, as mild findings were observed in our patients (3).

Subjective Assessments and Dizziness Perception: A significant difference in dizziness perception, as measured by the DHI, was found between patients with and without abnormal vestibular findings. Dizziness perception was higher in patients with regular vestibular tests, aligning with Yip & Strupp and Zamysłowska-Szmytko et al. (40), who found that psychological factors influence dizziness perception in patients with normal vestibular findings. Psychological factors often influence dizziness perception more than vestibular findings when tests are inconclusive. Piker et al. (41) found that psychological comorbidities correlated with self-reported dizziness disability, and Schmid et al. (42) showed strong correlations between DHI scores and emotional sub-scores. Our findings support these results, suggesting that subjective assessments should guide further diagnostic and psychological evaluations for patients with dizziness.

The relationship between anxiety and balance disorders involves shared neural pathways, which may contribute to dizziness caused by psychological factors. Saman et al. (43) noted that many patients with dizziness also require psychological support. This underscores the importance of psychological evaluation in patients with dizziness and expected vestibular test results.

We see exciting potential for future studies to refine our patient grouping methods. For instance, we could compare PPPD with other potentially confusing patients, such as those with presbycusis, to further enrich our understanding. Future studies could improve patient grouping considering symptom severity and triggers.

CONCLUSION

Psychological assessments in patients with dizziness may serve as a valuable tool in guiding further vestibular testing and facilitating referrals for psychological evaluation, particularly when vestibular findings are inconclusive.

Acknowledgments

We would like to express our sincere gratitude to all the patients who participated in this study. Their patience, cooperation, and willingness to contribute to this research were invaluable, and we deeply appreciate their involvement.

Authorship contributions

Hanifi Korkmaz: Conceptualized the study, designed the methodology, and conducted the data collection. Ahmet Kutluhan: Provided expertise in vestibular assessments, supervised the clinical procedures, and contributed to the interpretation of the test results. Banu Mujdeci: Analyzed the data, contributed to the statistical analysis, and drafted sections related to depression, anxiety, and somatization. Erkan Karatas Reviewed and edited the manuscript, ensuring academic rigor, and coordinated the collaboration between the authors. All authors read and approved the final manuscript.

Data availability statement

The datasets generated and/or analyzed during the current study are not publicly available due to privacy restrictions but are available from the corresponding author upon reasonable request.

Declaration of competing interest

The authors declare no financial interests, connections, or other situations that could potentially raise questions of bias regarding the work reported, its conclusions, implications, or opinions. Furthermore, there are no pertinent commercial interests, sources of funding, or affiliations with any organization, department, or individual that could influence the content of this article. The authors also confirm the absence of personal relationships or direct academic competition that may impact the objectivity or integrity of the presented work.

Ethics

Ethical approval was obtained from the İnönü University of Medical Clinical Research Ethics Committee (Protocol number: 2017/29, Date:17.01.2018/11).

Funding

The authors report that there is no funding source for the work.

REFERENCES

1. Neuhauser HK. Epidemiology of vertigo. Current opinion in neurology. 2007;20(1):40-6.
2. Cullen KE. The vestibular system: multimodal integration and encoding of self-motion for motor control. Trends Neurosci. 2012;35(3):185-96.
3. Borel L, Lopez C, Péruch P, Lacour M. Vestibular syndrome: a change in internal spatial representation. Neurophysiologie Clinique/Clinical Neurophysiology. 2008;38(6):375-89.
4. Best C, Tschan R, Eckhardt-Henn A, Dieterich M. Who is at risk for ongoing dizziness and psychological strain after a vestibular disorder? Neuroscience. 2009;164(4):1579-87.
5. Gurgel LG, Dourado MR, Moreira TdC, Serafini AJ, Menegotto IH, Reppold CT, et al. Correlation between vestibular test results and self-reported psychological complaints of patients with vestibular symptoms. Brazilian Journal of otorhinolaryngology. 2012;78:62-7.
6. Strupp M, Brandt T. Diagnosis and treatment of vertigo and dizziness. Dtsch Arztebl Int. 2008;105(10):173-80.
7. Patel M, Arshad Q, Roberts RE, Ahmad H, Bronstein AM. Chronic symptoms after vestibular neuritis and the high-velocity vestibulo-ocular reflex. Otology & Neurotology. 2016;37(2):179-84.
8. Yip CW, Strupp M. The Dizziness Handicap Inventory does not correlate with vestibular function tests: a prospective study. Journal of neurology. 2018;265:1210-8.
9. Phillips JS, FitzGerald JE, Bath AP. The role of the vestibular assessment. J Laryngol Otol. 2009;123(11):1212-5.
10. Post RE, Dickerson LM. Dizziness: a diagnostic approach. Am Fam Physician. 2010;82(4):361-8, 9.
11. Tirelli G, Rigo S, Bullo F, Meneguzzi C, Gregori D, Gatto A. Saccades and smooth pursuit eye movements in central vertigo. ACTA otorhinolaryngologica italica. 2011;31(2):96.
12. Newman-Toker DE, Hsieh Y-H, Camargo Jr CA, Pelletier AJ, Butchy GT, Edlow JA, editors. Spectrum of dizziness visits to US emergency departments: cross-sectional analysis from a nationally representative sample. Mayo Clinic Proceedings; 2008: Elsevier.
13. Nishikawa D, Wada Y, Shiozaki T, Shugyo M, Ito T, Ota I, et al. Patients with vertigo/dizziness of unknown origin during follow-ups by general otolaryngologists at outpatient town clinic. Auris Nasus Larynx. 2021;48(3):400-7.
14. Hoffman RM, Einstadter D, Kroenke K. Evaluating dizziness. Am J Med. 1999;107(5):468-78.
15. Eckhardt-Henn A, Best C, Bense S, Breuer P, Diener G, Tschan R, et al. Psychiatric comorbidity in different organic vertigo syndromes. J Neurol. 2008;255(3):420-8.
16. Yardley L, Beech S, Weinman J. Influence of beliefs about the consequences of dizziness on handicap in people with dizziness, and the effect of therapy on beliefs. Journal of psychosomatic research. 2001;50(1):1-6.
17. Gofrit SG, Mayler Y, Eliashar R, Bdolah-Abram T, Ilan O, Gross M. The association between vestibular physical examination, vertigo questionnaires, and the electronystagmography in patients with vestibular symptoms: a prospective study. Annals of Otology, Rhinology & Laryngology. 2017;126(4):315-21.
18. Herdman D, Norton S, Pavlou M, Murdin L, Moss-Morris R. Vestibular deficits and psychological factors correlating to dizziness handicap and symptom severity. Journal of psychosomatic research. 2020;132:109969.
19. Kirbac A, Kaya E, Incesulu SA, Carman KB, Yazar C, Ozen H, et al. Differentiation of peripheral and non-peripheral etiologies in children with vertigo/dizziness: The video-head impulse test and suppression head impulse paradigm. International Journal of Pediatric Otorhinolaryngology. 2024;179:111935.
20. Vorobyev A, Farrelly S, Hartis A, Monsch E, Strange C, Rizk H, et al. Optimizing Stroke Assessment of Dizziness: The Role and Impact of Video Head Impulse Testing. Stroke: Vascular and Interventional Neurology. 2024;4:e12984_350.
21. Luchikhin L, Kunel'skaya N, Guseva A, Dovlatova E, Chistov S. The diagnostic significance of the clinical methods for the investigation into the oculomotor reactions to dizziness. Vestnik otorinolaringologii. 2015;80(2):8-11.
22. Rutenkröger M, Scheer M, Rampp S, Strauss C, Schönfeld R, Leplow B. Associations between Psychological Factors and Long-Term Dizziness Handicap in Vestibular Schwannoma Patients: A Cross-Sectional Study. medRxiv. 2024:2024.10.19.24315803.
23. Jacobson GP, Piker EG, Hatton K, Watford KE, Trone T, McCaslin DL, et al. Development and preliminary findings of the dizziness symptom profile. Ear and hearing. 2019;40(3):568-76.
24. Staab JP, Eckhardt-Henn A, Horii A, Jacob R, Strupp M, Brandt T, et al. Diagnostic criteria for persistent postural-perceptual dizziness (PPPD): Consensus document of the committee for the Classification of Vestibular Disorders of the Bárány Society. Journal of Vestibular Research. 2017;27(4):191-208.
25. Garrison D, Barth L, Kaylie D, Riska K. Symptoms, audiometric and vestibular laboratory findings, and imaging in a concurrent superior canal dehiscence syndrome and vestibular schwannoma: a case report. Journal of the American Academy of Audiology. 2020;31(01):076-82.
26. Behrbohm H, Kaschke O. Ear, nose, and throat diseases: with head and neck surgery: Thieme; 2009.
27. Kerber KA, Baloh RW. The evaluation of a patient with dizziness. Neurol Clin Pract. 2011;1(1):24-33.
28. Wu C-N, Luo S-D, Chen S-F, Huang C-W, Chiang P-L, Hwang C-F, et al. Applicability of Oculomotor Tests for Predicting Central Vestibular Disorder Using Principal Component Analysis. Journal of Personalized Medicine. 2022;12(2):203.

29. Mossman B, Mossman S, Purdie G, Schneider E. Age dependent normal horizontal VOR gain of head impulse test as measured with video-oculography. *Journal of Otolaryngology-Head & Neck Surgery*. 2015;44:1-8.
30. Vereeck L, Truijen S, Wuyts FL, Van de Heyning PH. The dizziness handicap inventory and its relationship with functional balance performance. *Otology & neurotology*. 2007;28(1):87-93.
31. Karapolat H, Eyigor S, Kirazlı Y, Celebisoy N, Bilgen C, Kirazlı T. Reliability, Validity and Sensitivity to Change of Turkish Dizziness Handicap Inventory (DHI) in Patients with Unilateral Peripheral Vestibular Disease. *Journal of International Advanced Otology*. 2009;5(2).
32. Beck AT, Ward CH, Mendelson M, Mock J, Erbaugh J. An inventory for measuring depression. *Archives of general psychiatry*. 1961;4(6):561-71.
33. Ulusoy M, Sahin NH, Erkmen H. Turkish version of the Beck Anxiety Inventory: psychometric properties. *Journal of cognitive psychotherapy*. 1998;12(2):163.
34. Holi M. Assessment of psychiatric symptoms using the SCL-90: Helsingin yliopisto; 2003.
35. Best C, Eckhardt-Henn A, Diener G, Bense S, Breuer P, Dieterich M. Interaction of somatoform and vestibular disorders. *Journal of Neurology, Neurosurgery & Psychiatry*. 2006;77(5):658-64.
36. 井上亜希, 西村信一, 藤本千里, 岩崎真一. めまい疾患における日常生活障害度に関連する心理学的特性について. *Equilibrium Research*. 2023;82(2):98-104.
37. Kim TS, Lee WH, Heo Y. Prevalence and contributing factors of anxiety and depression in patients with vestibular migraine. *Ear, Nose & Throat Journal*. 2024;103(5):305-12.
38. Omara A, Basiouny EM, Shabrawy ME, Shafei RRE. The correlation between anxiety, depression, and vertigo: a cross-sectional study. *The Egyptian Journal of Otolaryngology*. 2022;38(1):143.
39. Subasi B, Yildirim N, Akbey ZY, Karaman NE, Arik O. Correlations of Clinical and Audio-Vestibulometric Findings with Coexisting Anxiety and Depression in Meniere's Disease Patients. *Audiol Neurotol*. 2023;28(2):75-83.
40. Zamysłowska-Szmytko E, Politański P, Jozefowicz-Korczyńska M. Dizziness handicap inventory in clinical evaluation of dizzy patients. *International Journal of Environmental Research and Public Health*. 2021;18(5):2210.
41. Piker EG, Jacobson GP, McCaslin DL, Grantham SL. Psychological comorbidities and their relationship to self-reported handicap in samples of dizzy patients. *Journal of the American Academy of Audiology*. 2008;19(04):337-47.
42. Schmid D, Allum J, Sleptsova M, Welge-Lüssen A, Schaefert R, Meinlschmidt G, et al. Relation of anxiety and other psychometric measures, balance deficits, impaired quality of life, and perceived state of health to dizziness handicap inventory scores for patients with dizziness. *Health and quality of life outcomes*. 2020;18:1-15.
43. Saman Y, McLellan L, McKenna L, Dutia MB, Obholzer R, Libby G, et al. State Anxiety Subjective Imbalance and Handicap in Vestibular Schwannoma. *Front Neurol*. 2016;7:101.
44. Swamy SN, Yuvaraj P, Pruthi N, Thennarasu K, Rajasekaran AK. Comprehensive normative data for objective vestibular tests. *Cureus*. 2023;15(6).

Research Article

INVESTIGATION OF THE EFFECT OF 25(OH)D3 LEVELS ON THE DISEASE SEVERITY AND THE COURSE OF THE TREATMENT IN ACTIVE PULMONARY TUBERCULOSIS PATIENTS

 Esma Seda AKALIN KARACA^{1*},  Gönenç ORTAKÖYLÜ²

¹ University of Health Sciences, Goztepe Training and Research Hospital, İstanbul, TURKIYE

² University Of Health Sciences, İstanbul Yedikule Health Research Center for Pulmonology And Thoracic Surgery, İstanbul, TURKIYE

*Correspondence: esmasedaakalin@gmail.com

ABSTRACT

Aim: Tuberculosis (TB) remains a significant global health problem, with emerging evidence linking vitamin D deficiency to increased susceptibility and disease progression. Vitamin D regulates calcium, phosphorus, and bone metabolism while playing a crucial role in immune responses, particularly in macrophage activation and antimicrobial defense. This study aimed to assess the relationship between serum 25(OH)D3 levels and clinical, radiological, and treatment outcomes in TB patients.

Materials and Methods: A prospective study involving 70 newly diagnosed TB patients (aged 18-69 years) and 20 healthy controls was conducted over ten months. TB diagnosis was confirmed through clinical, radiological, and microbiological findings, including ARB smear and M. tuberculosis culture positivity. Participants underwent physical examinations, routine blood tests, and serum 25(OH)D3 level measurements. Vitamin D levels were categorized as deficient (<10 ng/mL), insufficient (10-24 ng/mL), or adequate (25-80 ng/mL).

Results: The mean serum 25(OH)D3 level in TB patients (22.01±9.24 ng/mL) was significantly lower than in controls (37.8±18 ng/mL, p<0.001). Among TB patients, 61.5% had deficient or insufficient levels, with severe deficiency (<10 ng/mL) observed in 6 individuals. Higher 25(OH)D3 levels correlated positively with hemoglobin, hematocrit, albumin, and calcium, and negatively with WBC count. Patients with higher 25(OH)D3 levels exhibited better radiological improvement after one month of treatment (p<0.05, r= -0.223).

Conclusion: The study concludes that low 25(OH)D3 levels are associated with greater TB severity and delayed recovery, emphasizing the need for further research on vitamin D supplementation in TB management.

Keywords: tuberculosis; vitamin D; 25(OH)D3; progression; outcomes

Received: 03 January 2025

Revised: 21 April 2025

Accepted: 24 April 2025

Published: 23 June 2025



Copyright: © 2025 by the authors. Published by Aydın Adnan Menderes University, Faculty of Medicine and Faculty of Dentistry. This article is openly accessible under the Creative Commons Attribution-NonCommercial 4.0 International (CC BY-NC 4.0) License.

INTRODUCTION

Tuberculosis (TB) remains an important public health problem as one of the most common infectious diseases worldwide. According to the WHO 2019 Global Tuberculosis Control Report Data, Turkey has a disease incidence of 13 per thousand, and estimated number of multi-drug resistant cases is 330 (1).

TB is a chronic granulomatous infectious disease that involves all organ systems, most often the lungs, and 98% of the cases are infected with *Mycobacterium tuberculosis* strains, although a lesser degree of infection is related to other *Mycobacterium* species *M. bovis* and *M. africanum*. Approximately 5% of those infected can develop progressive primary disease following the primary infection (2). Individuals with the greatest risk of developing the primary disease are infants and children under five years of age (3). Progressive primary tuberculosis is also frequently seen in immunocompromised adults with advanced HIV infection or AIDS (4).

The relationship between vitamin D deficiency and insufficiency and the development of and susceptibility to TB has been evaluated in various studies (5-7). The most likely explanation is that 1,25-dihydroxycholecalciferol, the active form of vitamin D, binds to its receptor to regulate the expression of genes crucial for immune function and cytokine production. Additionally, the anti-mycobacterial response triggered by specific toll-like receptors (TLRs) in macrophages relies on 25(OH)D levels and genetic variations in the vitamin D binding protein (DBP) and its receptor. Overall, vitamin D plays a key role in the body's immune defense against TB infection by promoting the production of antimicrobial peptides like cathelicidin, and enhancing the phagocytic activity of monocytes and macrophages.

Vitamin D is one of the most important physiological regulators of calcium, phosphorus and bone metabolism. It has a synergistic effect with parathormone (PTH) in the regulation of serum calcium level and contributes to bone mineralization (8). It has also been shown to play a role in the formation of cellular and humoral immune responses, increasing lysosomal enzyme activity in the macrophages, and facilitates the cytotoxic effect via phagocytosis (9).

M. tuberculosis is an intracellular pathogen, located in macrophages in particular and decreased monocyte-macrophage function plays an important role in the pathogenesis of TB infection (10).

In this study, we aimed to evaluate the effect of 25 Hydroxy Vitamin D3 (25(OH)D3) levels on the degree, course, and treatment of microbiological and radiological findings in patients with recently diagnosed TB, who are positive for acid-resistant bacteria (ARB) staining of sputum samples.

MATERIALS AND METHODS

In this prospective study, recently diagnosed 70 TB patients were evaluated in a year between January and October in a tertiary care hospital. The study was conducted in accordance with the Declaration of Helsinki, and informed consent was obtained from all participants.

The study group consisted of 70 patients with active pulmonary tuberculosis diagnosed with clinical, radiological and bacteriological findings of the TB infection [ARB smear (+), culture (+)] with an age interval of 18-69 years. The sputum samples of the patients were analyzed for the presence of ARB, and following the decontamination process, mycobacterium culture was performed using the Löwenstein - Jensen broth and MIGIT tubes. Patients with a positive result for *M. tuberculosis* complex were included in the study.

All TB patients were given anti-TB therapy of isoniazid, rifampin, pyrazinamide, ethambutol or streptomycin. The patients who were positive for resistance to anti-TB drugs were excluded. Healthy control samples were obtained from 20 volunteers aged between 25-69 years without any comorbidities. 25 (OH)D3 levels were measured in the serum samples of these individuals.

The medical data of the patients diagnosed with active pulmonary tuberculosis were collected and physical examinations were performed. BMI was calculated by measuring the height and weight of the patients. Routine analytical examinations included complete blood count (CBC), and serum levels of fasting blood glucose, blood urea nitrogen, creatinine, AST, ALT, ALP, Total Protein, Albumin, Total cholesterol, Ca, Na, K, Cl, and 25(OH)D3. Blood samples were taken before anti-TB treatment was initiated.

Radiological evaluation of the cases was performed by posterior-anterior chest radiography, and the radiological grading of the disease was evaluated. Microbiological and radiological evaluations were performed at the beginning of the treatment, and the end of the first and second months of treatment, and the response to the treatment was noted.

Twenty healthy gender and age-matched volunteers selected from the outpatient patients applied to our center were included as the control group. Patients were classified according to the extent and type of chest radiograph changes, and a total score was calculated individually depending on the number of the lobes involved, presence of visible cavities or pleural involvement, the number and diameter of the visible cavities according to the modified radiological scale by Somoskovi et al (11).

We evaluated initial serum 25(OH)D3 levels and blood chemistry analyses and routine CBC were performed. The relationship between 25(OH)D3 levels and demographic characteristics, biochemical parameters, sputum smear/culture results and radiological grading of the patients were evaluated. The blood samples were centrifuged at 3000 rpm for 15 minutes, the supernatant was taken into opaque tubes in order to protect from light during the collection and storage of the samples, and kept at -40 until the day of analysis. Serum 25 (OH)D3 levels were measured using a high-pressure liquid chromatography [HPLC, Hewlett Packard (Spectrophotometric, fluorometric and electrochemical detector)], with a commercial HPLC assay (ImmuChrom HPLC, Deutschland). The limit of detection (LOD) and the limit of quantification (LOQ) values were 1.76 ng/mL and 4.28 ng/mL, respectively. Serum 25(OH)D3 levels were categorized into three subgroups according to the reference range determined by the manufacturer as follows: <10 ng/ml as 25(OH)D3 deficiency; 10-24 ng/mL as 25(OH)D3 insufficiency, and 25-80 ng/mL as an adequate level of serum 25(OH)D3.

Statistical Analysis

Statistical analyzes were performed using Minitab 16 (Minitab, State College, Pennsylvania) software. The normality of the data was checked using the Kolmogorov-Smirnov test. The data are shown in the tables as Mean±Standard Deviation (SD). The student's t-test was used for the comparison of the variables, and Person's correlation coefficient test was used for the evaluation of a correlation between the study variables. The confidence level was determined as 95% CI, and a p-value <0.05 was considered statistically significant.

RESULTS

The mean age of the study group was 39.7 ± 16.8 years. Forty-six of the patients were women and 24 were men. Twenty healthy volunteers were included in the study as a control group with a mean age of 42.3 ± 14.5 years. The

mean 25(OH) D3 level was 22.01 ± 9.24 ng/ml in the study group, and 37.8 ± 18 ng /ml in the control group ($p < 0.001$) (Table 1).

Table 1. Comparison of 25(OH)D3 levels between the study and control groups

Variables	Study group (n=70)	Control group (n=20)	p value
Age	39.7 ± 16.8	42.3 ± 14.5	0.512
25(OH)D3 (ng/ml)	22.01 ± 9.24	37.8 ± 18	0.001

We established a cut-off value of 25 ng/dl for the diagnosis of 25(OH)D3 deficiency and insufficiency, and 27 (38.5%) of the patients were above, whereas 43 (61.5%) of the patients were below the threshold value. Six patients (13.9%) of this group were evaluated as 25 (OH)D3 deficiency with their analyte levels below 10 ng/dl. We did not find a relationship between the study variables among the two groups (Table 2).

While we subgrouped the patients as 25(OH)D3 deficiency, insufficiency, and adequacy, a significant difference was found in the comparison of albumin, Ca, Na, WBC values ($p < 0.05$). There was no significant difference in terms of age, BMI and serum biochemical tests in comparison to the group with severe 25(OH)D3 deficiency with the group with an adequate level of 25(OH)D3 (Table 3). We also found a negative correlation between WBC and 25(OH)D3 levels, and a positive correlation between Hb, Hct, Total protein, Albumin, and Ca values (Table 4).

25 (OH)D3 levels of 33 patients with positive smear findings were found to be 21.88 ± 9.27 ng/ml when compared to the 22.32 ± 9.35 ng/ml of 37 smear-negative individuals ($p = 0.84$). At the end of the second month of treatment, the mean 25(OH)D3 levels of 6 patients with positive smear result were found to be 20.33 ± 6.74 ng/ml, whereas and the mean 25 (OH)D3 levels of 64 smear-negative cases was 22.27 ± 9.49 ng/ml ($p=0.62$).

We observed a negative correlation between the radiological grade at the end of the first month of the treatment and 25(OH)D3 level, and the radiological response to treatment was found to be more efficient at the first month in the patients with higher levels of 25 (OH)D3 ($p < 0.05$, $r = -0.223$).

Table 2. Comparison of the study variables according to 25(OH)D3 Deficiency & Insufficiency and Adequate Levels of 25(OH)D3 status

Variables	25(OH)D3 Deficiency & Insufficiency (< 25 ng/ml) (n=43)		Adequate Levels of 25(OH)D3 (≥ 25 ng/ml) (n=27)		P value
	Mean	\pm SD	Mean	\pm SD	
Age	41.64	18.01	33.95	13.53	0.139
BMI	20.89	3.48	22.14	2.51	0.281
WBC (10^3)	10.59	3.79	8.25	2.00	0.48
Hb (g/dl)	12.05	1.97	12.91	1.68	0.13
HCT (%)	36.57	5.62	39.11	4.72	0.11
PLT (10^3)	358.1	116.6	314.4	105.3	0.089
Glucose (mg/dl)	125	84.8	97.67	18.65	0.50
Urea (mg/dl)	27.79	14.37	27.05	8.2	0.803
Creatinine (mg/dl)	0.70	0.31	0.71	0.18	0.995
AST (U/L)	30.23	22.73	23.81	13.35	0.92
ALT (U/L)	27.98	32.14	22.52	19.09	0.817
ALP (U/L)	101.35	52.32	87.55	24.17	0.30
Total Protein (g/dl)	7.09	0.66	7.36	0.41	0.78
Albumin (g/dl)	3.48	0.75	4	0.46	0.65
Total cholesterol (mg/dl)	156.26	47.56	158.62	38.08	0.23
HDL-C (mg/dl)	34.95	19.85	45.9	17.7	0.19
LDL-C (mg/dl)	99.62	43.96	93	33	0.30
Triglycerides (mg/dl)	121.6	52.6	122.7	54.1	0.56
Ca (mg/dl)	8.74	0.81	9.27	0.67	0.99
Na (mEq/L)	134.43	4.81	136.71	2.94	0.74
K (mEq/L)	4.41	0.47	4.43	0.36	0.82
Cl (mEq/L)	99.34	4.32	101.43	4.69	0.69
Initial Radiological severity score	7.47	3.37	6.64	0.81	0.54
Radiological severity score on the 1st month of the treatment	6.35	3.48	5.08	0.74	0.33
Radiological severity score on the 2nd month of the treatment	5.46	3.39	4.09	0.68	0.17

DISCUSSION

In our study, we aimed to determine the serum 25(OH)D3 level in recently diagnosed ARB positive TB patients and to investigate its effect on anti-TB treatment response. When the serum 25(OH)D3 levels were compared between 70 sputum smear ARB positive cases and 20 healthy adults,

the mean 25(OH)D3 level was found to be significantly lower in TB patients in accordance with previous publications.

TB is a disease known since the ancient years, however, the epidemic has become an important public and medical concern after the industrial revolution when people started to live in cities under intense and harsh conditions (12). The presence of diseases that compromise immunity such as HIV infection, malnutrition, vitamin D deficiency, the long-term intake of immunosuppressive drugs and TNF-alpha inhibitors facilitate the emergence of the disease and worsens the course of the disease.

Vitamin D is key a hormone that regulates calcium and phosphorus metabolism. Recently, effective studies are being conducted on the representation of vitamin D in the development of chronic diseases such as malignancies, diabetes mellitus, and metabolic syndrome (13). Furthermore, in-vitro studies have shown that vitamin D and its metabolites might play an important role in the regulation of granulomatosis reactions and increase the ability to inhibit the growth of mycobacterium species through the activation of alveolar macrophages (14).

There is a variety of meta-analysis and prospective study reports suggesting that TB patients had lower vitamin D levels than the healthy population. In their study, Sato et al. found that 87% of active tuberculosis patients had vitamin D deficiency, whereas another study conducted in India had shown that low vitamin D levels were found to be associated with the development of disease in smear-positive patients (15, 16). 25 (OH) D3 levels were found lower in children with tuberculosis infection, and vitamin D deficiency increased the risk of TB.

In our study, we observed a negative correlation between the WBC count and 25(OH)D3 level, and a positive correlation between Hb, Hct, total protein, albumin and Ca values and 25(OH)D3 levels, suggesting that vitamin D deficiency might be increasing the inflammatory response and delaying the recovery process. Reports show that WBC values were higher and RBC values were lower in TB patients with vitamin D deficiency and that Vitamin D deficient patients had a longer duration of sputum smear ARB positivity (17, 8). Although vitamin D deficiency might not be the sole factor in the pathogenesis and disease severity of TB, the studies reported decreased antimycobacterial activity caused by Vitamin D deficiency is linked to increased inflammatory response and accelerated proliferation of *M. tuberculosis* (19). On the

Table 3. Comparison of the study variables according to 25(OH)D3 Deficiency, Insufficiency and Adequacy status.

Variables	25(OH)D3 Deficiency		25(OH)D3 Insufficiency		Adequate Levels of 25(OH)D3
	<10 ng/ml	p value*	10-24 ng/ml	p value**	25-80 ng/ml
Age	33±14.35	0.032	41.78±17.94	0.078	34.08±13.3
BMI	18.44±1.2	0.237	21.123±3.6	0.164	22±2.7
WBC (10 ³)	12.89±6.9	0.112	10.68±3.58	0.004	8.07±1.82
Hb (g/dl)	10.13±2.27	0.042	12.05±1.85	0.199	13.14±1.75
HCT (%)	31.92±6.82	0.073	36.49±5.34	0.153	39.64±4.8
PLT (10 ³)	419.5±151.2	0.118	357±119	0.204	310.6±101.5
Glucose (mg/dl)	96.25±15.88	0.279	129.8±94.2	0.085	97.42±18.84
Urea (mg/dl)	19.75±4.92	0.835	28.95±14.92	0.936	26.75±7.71
Creatinine (mg/dl)	0.45±0.1	0.93	0.72±0.32	0.771	0.704±0.18
AST (U/L)	53.25±14.31	0.136	29.3±23.66	0.339	24.54±12.2
ALT (U/L)	20.67±7.23	0.513	26.59±31.19	0.54	24.21±18.23
ALP (U/L)	94.8±25.3	0.879	104.35±57.23	0.135	87.5±23.16
Total Protein (g/dl)	6.575±0.9	0.237	7.1±0.62	0.085	7.42±0.45
Albumin (g/dl)	2.97±0.74	0.057	3.44±0.73	0.004	4.05±0.47
Total cholesterol (mg/dl)	117±22.6	0.848	158.54±46.95	0.826	164.33±43.05
HDL-C (mg/dl)	28.3±22.6	0.234	36.5±19.6	0.216	45.9±17.7
LDL-C (mg/dl)	93.3±55.9	0.994	101.1±42.6	0.586	93±33
Triglycerides (mg/dl)	171±89.7	0.388	110.7±36	0.54	122.7±54.1
Ca (mg/dl)	8.45±0.71	0.392	8.67±0.81	0.009	9.279±0.655
Na (mEq/L)	131.75±3.86	0.068	134.24±5.08	0.05	136.79±2.78
K (mEq/L)	4.65±0.66	0.103	4.37±0.46	0.438	4.37±0.33
Cl (mEq/L)	97.75±4.57	0.143	99±4.39	0.147	101.29±4.37

* p value obtained from the comparison of 25(OH)D3 deficiency and adequacy; ** p value obtained from the comparison of 25(OH)D3 insufficiency and adequacy

other hand, Wejse et al. concluded that additional treatment for the amelioration of Vitamin D status did not yield an efficient treatment response in their randomized double-blind study (20).

The immune system can detect many pathogens and *M. tuberculosis* via the activity of TLRs and with pathogen-related molecular patterns (PAMPs) (21). PAMPs presented by *M. tuberculosis* associate with TLR2 /1 dimers of macrophages, resulting in the up-regulation of both CYP27b1 and vitamin D receptor (VDR). Besides, IL-15 is responsible for CYP27b1 induction, which provides the conversion of 25(OH)D3 to 1, 25 (OH)D2, activation of VDR, and induction of cathelicidin. The cathelicidin gene LL-37 encodes a Vitamin D-dependent anti-microbial peptide, that requires a vitamin D activity in humans. Thus, vitamin D binding provides the LL-37-mediated immune response to *M. tuberculosis*. It has been shown that the cathelicidin gene is expressed in respiratory epithelium cells, vitamin D-dependent cathelicidin is found in many cell lines, such as bronchial epithelium cells (22). While the immunity in the pathogenesis of TB is provided by cytokines secreted by Th 1 cells, macrophage

activation, and granuloma formation, the Th2 response causes a delayed-type hypersensitivity reaction that aggravates tissue damage.

The link between low vitamin D levels and delayed TB treatment response may be influenced by several factors. Limited sun exposure during colder seasons — when TB incidence is higher — reduces vitamin D synthesis. Additionally, groups with higher TB rates, such as children, the elderly, and immigrants, often have lower serum vitamin D levels, along with potential nutritional, digestive, and absorption issues. Age-related decline in kidney function also impairs the body's ability to produce vitamin D, leading to lower blood 25-hydroxyvitamin D concentrations. Historically, cod liver oil and sunlight, both rich sources of vitamin D, were used to treat TB, highlighting the long-recognized importance of vitamin D in managing the disease.

While we established a cut-off value of 25 ng/ml for the determination of vitamin D deficiency and insufficiency, the WBC count was significantly higher in the group with vitamin D deficiency and insufficiency, as well as the

significant difference in albumin, Ca, Na, K levels. However, we did not find a relationship between 25(OH)D3 levels of patients and sputum smear negativity. Studies report conflicting data on vitamin D levels and its effect on sputum and culture negativity in TB patients (23, 24). It was also reported that TaqI VDR polymorphism, the dose of the given vitamin D and other clinical differences should be taken into consideration when investigating the efficiency of vitamin D supplementation in active tuberculosis cases (25).

Table 4. The correlation between the study variables and the 25(OH)D3 levels.

Variables	Correlation coefficient	P value
Age	-0.215	0.075
BMI	0.15	0.22
WBC (10 ³)	-0.32	0.007
Hb (g/dl)	0.258	0.032
HCT (%)	0.269	0.025
PLT (10 ³)	-0.204	0.092
Glucose (mg/dl)	-0.159	0.193
Urea (mg/dl)	-0.065	0.598
AST (U/L)	-0.145	0.236
ALT (U/L)	-0.058	0.635
ALP (U/L)	-0.109	0.375
Total Protein (g/dl)	0.293	0.014
Albumin (g/dl)	0.352	0.003
Total cholesterol (mg/dl)	0.125	0.304
Ca (mg/dl)	0.255	0.035
Na (mEq/L)	0.206	0.09
K (mEq/L)	-0.128	0.295
Cl (mEq/L)	0.199	0.101
Initial Radiological severity score	-0.18	0.144
Radiological severity score on the 1st month of the treatment	-0.239	0.05
Radiological severity score on the 2nd month of the treatment	0.283	0.2

One important finding of our study is that the radiological severity of the disease on the different time points as the initiation of the treatment, end of the first month of the treatment and end of the second month of treatment was in concordance with 25(OH)D3 level. We observed a better radiological improvement at the end of the first month of the treatment in patients with higher levels of 25(OH)D3.

Similarly, in their randomized controlled study, Nursyam et al. showed that in their 67 TB patients, radiological recovery was better in the group in which they added vitamin D supplementation to the TB treatment.

Although seasonal variations might be expected in 25(OH)D3 levels, we did not detect a season-based difference in our study group. In a similar study conducted by Maceda et al., shared a similar data of TB patients, contrary to the expectations (26).

CONCLUSION

In this study, the relationship between 25 (OH)D3 levels and the clinical course of active tuberculosis patients was investigated. We suggest that 25 (OH)D3 level might be affecting the clinical course and the disease severity of the active pulmonary TB. However, there is a great need for comprehensive studies in TB patients, where vitamin D levels, disease prevalence and response to treatment are evaluated, and the effect of vitamin D supplementation on treatment is examined.

Acknowledgments

None.

Authorship contributions

SAK: Data collection, interpretation, writing; GO: Supervision; critical review

Data availability statement

Data is available upon request.

Declaration of competing interest

None.

Ethics

Obtained from the institutional review board (24.12.2012 / 6128).

Funding

None.

REFERENCES

1. Global tuberculosis report. World Health Organization. 2024. Available at : <https://www.who.int/teams/global-tuberculosis-programme/tb-reports> Accessed: 30. December 2024
2. Tobin EH, Tristram D. Tuberculosis. [Updated 2024 Aug 11]. In: StatPearls [Internet]. Treasure Island (FL): StatPearls Publishing; 2024 Jan-. Available from: <https://www.ncbi.nlm.nih.gov/books/NBK441916/>






3. Newton SM, Brent AJ, Anderson S, Whittaker E, Kampmann B. Paediatric tuberculosis. *Lancet Infect Dis*. 2008 Aug;8(8):498-510. doi: 10.1016/S1473-3099(08)70182-8.
4. Taghipour A, Azimi T, Javanmard E, Pormohammad A, Olfatifar M, Rostami A, Tabarsi P, Sohrabi MR, Mirjalali H, Haghighi A. Immunocompromised patients with pulmonary tuberculosis; a susceptible group to intestinal parasites. *Gastroenterol Hepatol Bed Bench*. 2018 Winter;11(Suppl 1):S134-S139.
5. Eleteby R, Elsharkawy A, Mohamed R, Hamed M, Kamal Ibrahim E, Fouad R. Prevalence of vitamin D deficiency and the effect of vitamin D3 supplementation on response to anti-tuberculosis therapy in patients with extrapulmonary tuberculosis. *BMC Infect Dis*. 2024 Jul 9;24(1):681. doi: 10.1186/s12879-024-09367-0.
6. Cai L, Hou S, Huang Y, Liu S, Huang X, Yin X, Jiang N, Tong Y. The Potential Role of Vitamin D in the Development of Tuberculosis in Chinese Han Population: One Case-Control Study. *Front Med (Lausanne)*. 2022 Jul 25;9:849651. doi: 10.3389/fmed.2022.849651.
7. Nouri-Vaskeh M, Sadeghifard S, Saleh P, Farhadi J, Amraii M, Ansarin K. Vitamin D Deficiency among Patients with Tuberculosis: a Cross-Sectional Study in Iranian-Azari Population. *Tanaffos*. 2019 Jan;18(1):11-17.
8. Khazai N, Judd SE, Tangpricha V. Calcium and vitamin D: skeletal and extraskeletal health. *Curr Rheumatol Rep*. 2008 Apr;10(2):110-7. doi: 10.1007/s11926-008-0020-y.
9. Di Rosa M, Malaguarnera M, Nicoletti F, Malaguarnera L. Vitamin D3: a helpful immuno-modulator. *Immunology*. 2011 Oct;134(2):123-39. doi: 10.1111/j.1365-2567.2011.03482.x.
10. Rajaram MV, Brooks MN, Morris JD, Torrelles JB, Azad AK, Schlesinger LS. Mycobacterium tuberculosis activates human macrophage peroxisome proliferator-activated receptor gamma linking mannose receptor recognition to regulation of immune responses. *J Immunol*. 2010 Jul 15;185(2):929-42. doi: 10.4049/jimmunol.1000866.
11. Somoskövi A, Zissel G, Zipfel PF, Ziegenhagen MW, Klaucke J, Haas H, Schlaak M, Müller-Quernheim J. Different cytokine patterns correlate with the extension of disease in pulmonary tuberculosis. *Eur Cytokine Netw*. 1999 Jun;10(2):135-42.
12. Martini M, Riccardi N, Giacomelli A, Gazzaniga V, Besozzi G. Tuberculosis: an ancient disease that remains a medical, social, economical and ethical issue. *J Prev Med Hyg*. 2020 Apr 30;61(1 Suppl 1):E16-E18. doi: 10.15167/2421-4248/jpmh2020.61.1s1.1475.
13. Álvarez-Mercado AI, Mesa MD, Gil Á. Vitamin D: Role in chronic and acute diseases. *Encyclopedia of Human Nutrition*. 2023:535-44. doi: 10.1016/B978-0-12-821848-8.00101-3.
14. Greenstein RJ, Su L, Brown ST. Vitamins A & D inhibit the growth of mycobacteria in radiometric culture. *PLoS One*. 2012;7(1):e29631. doi: 10.1371/journal.pone.0029631.
15. Sato S, Tanino Y, Saito J, Nikaido T, Inokoshi Y, Fukuhara A, Fukuhara N, Wang X, Ishida T, Munakata M. Relationship between 25-hydroxyvitamin D levels and treatment course of pulmonary tuberculosis. *Respir Investig*. 2012 Jun;50(2):40-5. doi: 10.1016/j.resinv.2012.05.002.
16. Jaimni V, Shasty BA, Madhyastha SP, Shetty GV, Acharya RV, Bekur R, Doddamani A. Association of Vitamin D Deficiency and Newly Diagnosed Pulmonary Tuberculosis. *Pulm Med*. 2021 Jan 15;2021:5285841. doi: 10.1155/2021/5285841.
17. Zhang X, Zhang Y, Xia W, Liu Y, Mao H, Bao L, Cao M. The relationship between vitamin D level and second acid-fast bacilli (AFB) smear-positive during treatment for TB patients was inferred by Bayesian network. *PLoS One*. 2022 May 4;17(5):e0267917. doi: 10.1371/journal.pone.0267917.
18. Ganmaa D, Munkhzul B, Fawzi W, Spiegelman D, Willett WC, Bayasgalan P, Baasansuren E, Buyankhishig B, Oyun-Erdene S, Jolliffe DA, Xenakis T, Bromage S, Bloom BR, Martineau AR. High-Dose Vitamin D3 during Tuberculosis Treatment in Mongolia. A Randomized Controlled Trial. *Am J Respir Crit Care Med*. 2017 Sep 1;196(5):628-637. doi: 10.1164/rccm.201705-0936OC.
19. Coussens AK, Martineau AR, Wilkinson RJ. Anti-Inflammatory and Antimicrobial Actions of Vitamin D in Combating TB/HIV. *Scientifica (Cairo)*. 2014;2014:903680. doi: 10.1155/2014/903680.
20. Wejse C, Gomes VF, Rabna P, Gustafson P, Aaby P, Lisse IM, Andersen PL, Glerup H, Sodemann M. Vitamin D as supplementary treatment for tuberculosis: a double-blind, randomized, placebo-controlled trial. *Am J Respir Crit Care Med*. 2009 May 1;179(9):843-50. doi: 10.1164/rccm.200804-567OC.
21. Zihad SMNK, Sifat N, Islam MA, Monjur-Al-Hossain ASM, Sikdar KMYK, Sarker MMR, Shilpi JA, Uddin SJ. Role of pattern recognition receptors in sensing Mycobacterium tuberculosis. *Heliyon*. 2023 Oct 4;9(10):e20636. doi: 10.1016/j.heliyon.2023.e20636.
22. Chung C, Silwal P, Kim I, Modlin RL, Jo EK. Vitamin D-Cathelicidin Axis: at the Crossroads between Protective Immunity and Pathological Inflammation during Infection. *Immune Netw*. 2020 Feb 11;20(2):e12. doi: 10.4110/in.2020.20.e12.
23. Zhang J, Chen C, Yang J. Effectiveness of vitamin D supplementation on the outcome of pulmonary tuberculosis treatment in adults: a meta-analysis of randomized controlled trials. *Chin Med J (Engl)*. 2019 Dec 20;132(24):2950-2959. doi: 10.1097/CM9.0000000000000554.
24. Junaid K, Rehman A, Saeed T, Jolliffe DA, Wood K, Martineau AR. Genotype-independent association between profound vitamin D deficiency and delayed sputum smear conversion in pulmonary tuberculosis. *BMC Infect Dis*. 2015 Jul 21;15:275. doi: 10.1186/s12879-015-1018-5.
25. de Souza Freitas R, Fratelli CF, de Souza Silva CM, de Lima LR, Stival MM, da Silva ICR, Scherz Funghetto S. Association of Vitamin D with the TaqI Polymorphism of the VDR Gene in Older Women Attending the Basic Health Unit of the Federal District,

DF (Brazil). J Aging Res. 2020 Sep 24;2020:7145193. doi: 10.1155/2020/7145193.

26. Maceda EB, Gonçalves CCM, Andrews JR, Ko AI, Yeckel CW, Croda J. Serum vitamin D levels and risk of prevalent tuberculosis, incident tuberculosis and tuberculin skin test conversion among prisoners. Sci Rep. 2018 Jan 17;8(1):997. doi: 10.1038/s41598-018-19589-3

Research Article

EVALUATION OF THE EFFECTIVENESS OF DIFFERENT CLEANING METHODS FOR REMOVABLE SPACE MAINTAINERS

 Ceren SAĞLAM^{1*},  Dilşah ÇOĞULU¹,  Ayla Beyza ÇENGEL²,  Yasemin YİĞİT³,
 Ataç UZEL⁴

¹ Ege University Faculty of Dentistry, Department of Pediatric Dentistry, İzmir, TURKIYE

² Ege University Faculty of Dentistry, Grade 5 Student, İzmir, TURKIYE

³ Private Dentist, Muğla, TURKIYE

⁴ Ege University Faculty of Science, Department of Biology, Basic and Industrial Microbiology Section, İzmir, TURKIYE

*Correspondence: sglmceren@gmail.com

ABSTRACT

Aim: The present study aimed to evaluate the antimicrobial effectiveness of different cleaning methods in reducing microbial colonization on space maintainer appliances.

Materials and Methods: Acrylic blocks (5×5×3 cm) were fabricated for the study. The surfaces of these blocks were sterilized using 70% ethanol and subsequently air-dried. A standardized microorganism suspensions (*Streptococcus mutans* ATCC 10449 and *Candida albicans* ATCC 60193) were prepared at a density of OD600 = 0.01, and 400 µL of the suspension was applied to the surfaces of the acrylic blocks. The blocks were then covered with sterile plastic films (4×4 cm) and incubated at 37°C for 24 hours. After incubation, microbial load was quantified, and five different cleaning protocols were applied to the block surfaces. The groups were as follows; Group1: Control (No treatment), Group2: Toothbrush+liquid soap, Group3: Toothbrush+toothpaste, Group4: Toothbrush+liquid soap+cleanser tablet, Group5: Toothbrush+toothpaste+cleanser tablet, Group6: Cleanser tablet only. All blocks were rinsed in sterile phosphate buffered saline, and the residual microbial load was determined by inoculation on to Brain Heart Infusion Agar (for *S. mutans*) and Sabouraud Dextrose Agar (for *C. albicans*). Data analysis was performed using SPSS 25.0 software program by the chi-square and t-tests.

Results: All cleaning methods significantly reduced the colonization of both *S. mutans* and *C. albicans* (p=0.01). Among the tested methods, Group 5 demonstrated the highest antimicrobial efficacy, followed by Groups 4>6>3>2, respectively.

Conclusion: This study highlights the effectiveness of various cleaning methods in reducing microbial colonization on removable space maintainers. The combination of mechanical cleaning with a toothbrush and the use of cleanser tablets showed superior efficacy.

Keywords: Space maintainer, *Streptococcus mutans*, *Candida albicans*

Received: 23 December 2024

Revised: 03 April 2025

Accepted: 14 April 2025

Published: 23 June 2025



Copyright: © 2025 by the authors. Published by Aydın Adnan Menderes University, Faculty of Medicine and Faculty of Dentistry. This article is openly accessible under the Creative Commons Attribution-NonCommercial 4.0 International (CC BY-NC 4.0) License.

INTRODUCTION

Early loss of primary teeth can lead to space loss, the mesialization of adjacent teeth, resulting in a decrease in arch length, and malocclusions. Space maintainers have long been used for the management of space loss in primary and mixed dentition, maintain arch length and prevent malocclusion (1–3). Space maintainers can be categorized as a removable and a fixed one; unilateral or bilateral, and functional or nonfunctional (4). The selection of an appropriate space maintainer depends on various factors, including the stage of dental development, the dental arch, the location and size of the missing tooth, the age and the cooperation of the patient, and the condition of the adjacent teeth (1,3–5).

Space maintainers can contribute to plaque accumulation and pose challenges in maintaining proper oral hygiene, which may lead to the development of gingivitis (2,4). Additionally, they come into direct contact with the oral microflora, facilitating the formation of microbial biofilms on their surfaces (2,6). To prevent microbial retention, patients using space maintainers should be more careful to maintain optimal oral hygiene (2,7).

In cases where oral hygiene is insufficiently maintained, orthodontic appliances (e.g., space maintainers) can lead to plaque accumulation (8–10). The use of space maintainers has been associated with an increase in bacterial concentrations within the oral environment, as well as a reduction in buffering capacity, pH levels, and salivary flow rate (8,11). *Streptococcus mutans*, which is strongly associated with early enamel demineralization, exhibits elevated salivary levels in conditions promoting its colonization. While some studies report an increase in *S. mutans* during orthodontic treatment, others do not observe such a trend (8,10,11). *Candida* species, commonly found in the oral cavity, are known to colonize surfaces such as cement, enamel, and dentin, acting as reservoirs for microbial spread. Despite extensive research on the effects of orthodontic appliances on the oral microbiota, there is limited focus on the impact of removable appliances and fixed space maintainers (8,12). Studies have shown that patients using removable appliances exhibit elevated salivary levels of *Candida albicans*, which increases the likelihood of developing candidiasis and stomatitis (13).

Removable orthodontic appliances that are not effectively cleaned pose a risk of cross-infection for clinicians, technicians, and patients (14). Various chemical and mechanical cleaning methods are employed to eliminate

microorganisms on the surface of removable orthodontic appliances (15). While products such as sodium hypochlorite, peroxide and enzymes are used in chemical cleaning methods; toothbrushes and ultrasonic cleaning products are used in mechanical cleaning. Studies also showed that the combination of chemical and mechanical cleaning has a positive effect on cleaning these appliances (15,16).

Despite the widespread use of space maintainers, there is no consensus on the most effective cleaning protocols, particularly for removable appliances. This lack of standardization increases the risk of microbial accumulation and subsequent oral infections, underscoring the need for evidence-based cleaning methods. The aim of the present study is to address this gap by evaluating the antimicrobial efficacy of various cleaning methods for space maintainers, with a specific focus on clinically significant microorganisms such as *Streptococcus mutans* and *Candida albicans*.

MATERIALS AND METHODS

Study Design and Sample Preparation

The present study aimed to evaluate the effectiveness of various cleaning methods and their combinations in reducing microbial retention on acrylic materials used in space maintainers. A total of 30 cold acrylic blocks, each measuring 5x5x3 cm, were prepared by a single operator to ensure consistency in methodology. These blocks were sterilized prior to inoculation with microbial cultures and subjected to various cleaning treatments. The cleaning methods included toothbrush (Colgate Extra Clean soft, ABD), toothpaste (Colgate Anti-caries, ABD), liquid soap (Palmolive, Colgate-Palmolive, ABD), and cleanser tablet (Corega Orthodontics, GlaxoSmithKline, ABD), which were tested in the experimental groups. A detailed description of these groups is presented in Table 1.

Microbiological Procedures

Following the preparation of the cold acrylic materials (n=30) for use in the study, the microbiological procedure was initiated. The microorganisms and culture media utilized are outlined below:

Microorganisms: *Streptococcus mutans* ATCC 10449 and *Candida albicans* ATCC 60193

Culture Media: Brain Heart Infusion Agar (BHIA) (Difco) and Sabouraud Dextrose Agar (SDA) (Difco)

These media were selected for their proven efficacy in promoting the growth of the target microorganisms, ensuring reliable and reproducible results. The experiments were conducted with two replicates, following a modified JIS Z 2801 standard.

Table 1. Different cleaning methods tested in the study

Groups	Cleaning Methods
Group 1	Control Group-No Treatment
Group 2	Toothbrush-Colgate Extra Clean soft (Colgate-Palmolive, ABD) Liquid soap (Palmolive, Colgate-Palmolive, ABD)
Group 3	Toothbrush-Colgate Extra Clean soft (Colgate-Palmolive, ABD) Toothpaste-Colgate Anti-caries (Colgate-Palmolive, ABD)
Group 4	Toothbrush-Colgate Extra Clean soft (Colgate-Palmolive, ABD) Liquid soap (Palmolive, Colgate-Palmolive, ABD) Cleanser tablet-Corega Orthodontics (GlaxoSmithKline, ABD)
Group 5	Toothbrush-Colgate Extra Clean soft (Colgate-Palmolive, ABD) Toothpaste-Colgate Anti-caries (Colgate-Palmolive, ABD) Cleanser tablet-Corega Orthodontics (GlaxoSmithKline, ABD)
Group 6	Cleanser tablet-Corega Orthodontics (GlaxoSmithKline, ABD)

The acrylic block surfaces were sterilized using 70% ethanol (v/v) and subsequently dried. After sterilization, the surfaces were inoculated with the microbial suspension (*Streptococcus mutans* ATCC 10449 and *Candida albicans* ATCC 60193), with the concentration adjusted to OD₆₀₀=0.01. A total of 400 µl of the microbial suspension was applied to each surface, which was then covered with sterile plastic films measuring 4cm×4cm. The samples were incubated in a humid atmosphere at 37°C for 24 hours.

Experimental Procedures

After the 24-hour incubation period, the surfaces of the samples were subjected to five different treatment groups, which included cleaning agents and/or their combinations as listed in Table 1. The control group received no treatment. The protocols for using the cleaning methods in each group are presented in Table 2. The selected cleaning methods and combinations were chosen to replicate real-life cleaning practices, ensuring the clinical relevance of the study findings.

Table 2. Clinical procedures for the different cleaning methods

Groups	Clinical procedures
Control Group	No treatment
Toothbrush liquid soap	– A pea-sized amount of liquid soap was applied to the brush, and the surface of the samples was cleaned with three brush strokes. After cleaning, the samples were rinsed with water.
Toothbrush toothpaste	– A pea-sized amount of toothpaste was applied to the brush, and the surface of the samples was cleaned with three brush strokes. The samples were then rinsed with water.
Toothbrush liquid soap – cleanser tablet	– A pea-sized amount of liquid soap was applied to the brush, and the surface of the samples was cleaned with three brush strokes. Afterward, the samples were rinsed with water. An effervescent tablet was dissolved completely in one glass of water, and the samples were immersed in the effervescent solution for three minutes. The samples were then rinsed with water.
Toothbrush toothpaste – cleanser tablet	– A pea-sized amount of toothpaste was applied to the brush, and the surface of the samples was cleaned with three brush strokes. The samples were then rinsed with water. An effervescent tablet was dissolved completely in one glass of water, and the samples were immersed in the effervescent solution for three minutes. The samples were then rinsed with water.
Cleanser tablet	An effervescent tablet was dissolved completely in one glass of water, and the samples were immersed in the effervescent solution for three minutes. The samples were then rinsed with water."

After the cleaning procedures, all samples were rinsed with sterile phosphate-buffered saline (PBS) to recover any residual microorganisms from the surfaces. The recovered microorganisms were then cultured on Brain Heart Infusion Agar (BHIA) for *S. mutans* and Sabouraud Dextrose Agar (SDA) for *C. albicans* to assess the final microbial load. The *S. mutans* plates were incubated in a CO₂ incubator at 5% CO₂. The reduction in microbial load was calculated in logarithmic values, comparing the results to the control group. According to the JIS Z 2801 standard, a reduction of at least 2 log units was considered indicative of antimicrobial efficacy.

Statistical Analysis

Data analysis was performed using SPSS 25.0 software program by the chi-square and t-tests. Results were reported with 95% confidence intervals, and statistical significance was set at p<0.05.

RESULTS

The results of the present study demonstrated that all cleaning methods assessed significantly reduced the colonization of *S. mutans* and *C. albicans* ($p=0.01$). The most effective cleaning method for reducing both *S. mutans* (Table 3) and *C. albicans* (Table 4) colonization was found to be Group 5, which utilized a combination of toothbrush, toothpaste, and cleanser tablet. The effectiveness of the cleaning methods decreased in the following order: Group 4>Group 6>Group 3>Group 2, showing a gradual decline in antimicrobial efficacy across the different cleaning protocols.

Table 3. The efficacy of different cleaning methods on *S. mutans* colonization

Groups	Baseline (log)	Post-treatment (log)	Reduction (log)
Group 1	5.42	5.42	-
Group 2	5.42	3.39	2.03
Group 3	5.42	3.32	2.10
Group 4	5.42	2.96	2.46
Group 5	5.42	2.79	2.63
Group 6	5.42	3.02	2.40

Table 4. The efficacy of different cleaning methods on *C. albicans* colonization

Groups	Baseline (log)	Post-treatment (log)	Reduction (log)
Group 1	5.29	5.29	-
Group 2	5.29	3.29	2.00
Group 3	5.29	3.26	2.03
Group 4	5.29	2.85	2.44
Group 5	5.29	2.65	2.64
Group 6	5.29	2.96	2.33

DISCUSSION

The present study evaluated the effectiveness of various cleaning methods in removing microbial adherence, specifically *S. mutans* and *C. albicans*, on cold acrylic materials commonly used in space maintainers. The cleaning agents selected; liquid soap, toothbrush, toothpaste, cleanser tablets, and/or their combinations were applied, and the subsequent microbial loads were quantified. The results revealed that all cleaning methods effectively reduced microbial colonization on the cold acrylic surfaces, with the combination of a toothbrush with toothpaste and cleanser tablets emerging as the most effective approach.

The use of orthodontic appliances notably disrupts oral hygiene and contributes to the development of retentive

areas, which in turn promotes the plaque and biofilm accumulation. Orthodontic treatments, through the incorporation of bands, brackets, wires, and acrylic resins, create environments contribute to the retention of food particles and microorganisms, ultimately influencing the oral microbiota (8–12). Research by Kundu et al. (8) highlighted a significant increase in the levels of *Streptococcus mutans* following the placement of both fixed and removable space maintainers. Similarly, Topaloğlu et al. (11) found that orthodontic appliances, by providing retention sites, facilitate the colonization of *Candida* species, thereby altering the microbial environment of the oral cavity. Pithon et al. (17) further emphasized that the size and surface roughness of acrylic materials could influence microbial growth by acting as reservoirs for food debris. Additionally, study by Budtz-Jorgensen and Bertram suggested that the increased prevalence of *Candida* colonization following the use of removable appliances may be attributed to the inherent affinity of *Candida* species for plastic polymers (8,18,19).

The oral cavity harbors a diverse range of microbial species, with *S. mutans* and *C. albicans* being two key microorganisms often implicated in oral health-related issues. *S. mutans* is widely recognized as a primary etiological agent of dental caries and is among the most frequent contaminants of orthodontic appliances. *C. albicans*, commonly present in the oral microbiota, has been linked to various oral pathologies, including candidiasis (18). Rammohan et al. (9) further emphasized the importance of oral hygiene in the context of orthodontic appliances, noting that microbial adhesion, particularly of *S. mutans* and *C. albicans*, is significantly higher on these appliances. Based on these findings, *S. mutans* and *C. albicans* were specifically selected for the present study due to their clinical relevance.

Brushing is widely regarded as the most preferred mechanical method for cleaning removable orthodontic appliances (20,21). Eichenauer et al. (20) reported that many orthodontists in Germany favor brushing with toothpaste for the maintenance of removable appliances. Similarly, in a study by Tsolakis et al. (21), it was emphasized that regular brushing is universally recommended by orthodontists for cleaning orthodontic appliances. Furthermore, a significant proportion of orthodontists also suggest supplementary cleaning methods such as denture cleaners, disinfection solutions, and vinegar in conjunction with brushing. In another study by Duyck et al. (15), which compared the effectiveness of toothbrush cleaning and ultrasonic cleaning with or without effervescent tablets, no

significant impact of effervescent tablets on biofilm formation was observed. Consistent with these findings, the present study demonstrated that the combined use of a toothbrush with toothpaste and cleanser tablet was more effective than the other cleaning methods.

Charavet et al. observed that commercial cleaning tablets had a notable effect on biofilm removal. Their study further indicated that one of the tablets tested exhibited a bacteriostatic, rather than a bactericidal, effect on *Candida* species. They also pointed out that manual brushing, as reported in the studies they reviewed, was not directly compared with antimicrobial agents but was primarily used as an initial cleaning step. Charavet et al. emphasized that manual brushing plays a critical role as the foundational cleaning method (22). Similarly, the present study included brushing as the initial cleaning step and evaluated its effectiveness in combination with other cleaning agents, providing a comparative analysis of various cleaning protocols.

In a clinical study by Farhadifard et al. (23), three different cleaning methods were compared; manual brushing as the control group, a combination of brushing and cleanser tablets in the second group, and brushing combined with a propolis-based mouthwash in the third group. The results indicated that the combination of brushing with cleanser tablets was more effective than the other methods. Similarly, Diedrich et al. (24), in their comparative study evaluating toothbrush and toothpaste, cleanser tablets, and ultrasonic devices, concluded that toothbrush and toothpaste were effective for cleaning accessible surfaces, while cleanser tablets and ultrasonic devices were superior in cleaning hard-to-reach areas. These findings are consistent with the results of the present study, where the combination of brushing and cleanser tablets proved to be the most effective method for significantly reducing microbial colonization.

Despite the increasing use of space maintainers, there is a lack of standardized cleaning protocols. The present study provides critical insights into the comparative efficacy of different cleaning methods, contributing to the development of evidence-based guidelines for oral hygiene maintenance in patients with removable appliances.

CONCLUSION

In conclusion, all cleaning methods evaluated in the present study were effective in reducing microbial colonization on acrylic blocks. Mechanical cleaning with a

toothbrush was identified as a crucial component of the cleaning process, with the addition of cleanser tablets further enhancing cleaning efficacy. Notably, no standardized cleaning protocol for space maintainers has been established in the literature, and previous studies have also failed to propose a universally accepted approach.

Future research should focus on exploring the long-term effects of various cleaning protocols, as well as evaluating additional microbial species, to optimize oral hygiene strategies during the use of removable space maintainers. Additionally, further studies are needed to investigate patient adherence to these cleaning methods in daily use and to assess their long-term impact on microbial populations and appliance durability.

Acknowledgments

The authors would like to thank Assoc. Prof. Dr. Timur KÖSE for his valuable contributions to the statistical analysis.

Authorship contributions

Surgical and Medical Practices: CS, AÇ, YY and AU; Concept: DÇ, Design: DÇ and AU; Data Collection or Processing: CS, DÇ, AÇ and AU; Analysis or Interpretation: CS, DÇ and AU; Literature Search: CS and DÇ; Writing: CS and DÇ. All authors read and approved the final manuscript.

Data availability statement

The data that support the findings of this study are available from the corresponding author, [CS], upon reasonable request.

Declaration of competing interest

The authors deny any conflicts of interest related to this study.

Ethics

This study does not require Ethics Committee Approval.

Funding

None.

REFERENCES

1. Ramakrishnan M, Dhanalakshmi R, Subramanian EMG. Survival rate of different fixed posterior space maintainers used

- in Paediatric Dentistry – A systematic review. Saudi Dent J. 2019;31:165-172.
2. Gökcek Taraç M. Are Plaque Disclosing Agents Effective for Improving Self-Performed Dental Hygiene in Patients with Space Maintainers? A Randomized Controlled Clinical Trial. Eur J Ther. 2024;30:616-625.
3. Gurcan AT, Koruyucu M, Kuru S, Sepet E, Seymen F. Effects of Fixed and Removable Space Maintainers on Dental Plaque and DMFT/dft Values. Odovtos - Int J Dent Sci. 2021;23:137-147.
4. Gumber P, Sarawgi A, Dutta S, Goenka P. Simple Fixed Functional Space Maintainer. Int J Clin Pediatr Dent. 2014;7:225-228.
5. Kargul B, Çağlar E, Kabalay U. Glass fiber-reinforced composite resin as fixed space maintainers in children: 12-Month clinical follow-up. J Dent Child. 2005;72:109-112.
6. Kilian M, Chapple ILC, Hannig M, et al. The oral microbiome - An update for oral healthcare professionals. Br Dent J. 2016;221:657-666.
7. Oliveria ML, Pazinato J, Zanatta FB. Are oral hygiene instructions with aid of plaque - disclosing methods effective in improving self-performed dental plaquecontrol? A systematic review of randomized controlled trials. Int J Dent Hyg. 2021;19:239-254.
8. Kundu R, Tripathi AM, Jaiswal JN, Ghoshal U, Palit M, Khanduja S. Effect of fixed space maintainers and removable appliances on oral microflora in children: An in vivo study. J Indian Soc Pedod Prev Dent. 2016;34:3-9.
9. Rammohan S, Juvvadi S, Gandikota C, Challa P, Manne R, Mathur A. Adherence of Streptococcus mutans and Candida albicans to different bracket materials. J Pharm Bioallied Sci. 2012;4:212.
10. Lara-Carrillo E, Montiel-Bastida NM, Sánchez-Pérez L, Alanís-Tavira J. Effect of orthodontic treatment on saliva, plaque and the levels of Streptococcus mutans and Lactobacillus. Med Oral Patol Oral Cir Bucal. 2010;15.
11. Topaloglu-Ak A, Ertugrul F, Eden E, Ates M, Bulut H. Effect of orthodontic appliances on oral microbiota-6 month follow-up. J Clin Pediatr Dent. 2011;35:433-436.
12. Pathak AK, Sharma DS. Biofilm associated microorganisms on removable oral orthodontic appliances in children in the mixed dentition. J Clin Pediatr Dent. 2013;37:335-340.
13. Hibino K, Wong RWK, HÄgg U, Samaranayake LP. The effects of orthodontic appliances on Candida in the human mouth. Int J Paediatr Dent. 2009;19:301-308.
14. Aydoğan Akgün F. Cleaning Methods and Materials for Removable Orthodontic Appliances: A Questionnaire Study. Black Sea J Heal Sci. 2021;4:136-140.
15. Duyck J, Vandamme K, Krausch-Hofmann S, et al. Impact of denture cleaning method and overnight storage condition on denture biofilm mass and composition: A cross-over randomized clinical trial. PLoS One. 2016;11:1-16.
16. Cruz PC, de Andrade IM, Peracini A, et al. The effectiveness of chemical denture cleansers and ultrasonic device in bio film removal from complete dentures. J Appl Oral Sci. 2011;19:668-673.
17. Pithon MM, dos Santos RL, Alviano WS, Ruellas AC de O, Araújo MT de S. Quantitative assessment of S. mutans and C. albicans in patients with Haas and Hyrax expanders. Dental Press J Orthod. 2012;17:1-6.
18. Arendorf T, Addy M. Candidal carriage and plaque distribution before, during and after removable orthodontic appliance therapy. J Clin Periodontol. 1985;12:360-368.
19. Budtz-Jorgensen E, Bertram. U. Denture Stomatitis. I. The Etiology in Relation to Trauma and Infection.; 1970.
20. Eichenauer J, Serbesis C, Ruf S. Reinigung herausnehmbarer kieferorthopädischer Apparaturen - eine Umfrage. J Orofac Orthop. 2011;72:389-395.
21. Tsolakis A, Kakali L, Prevezanos P, Bitsanis I, Polyzois G. Use of different cleaning methods for removable orthodontic appliances: A questionnaire study. Oral Heal Prev Dent. 2019;17.
22. Charavet C, Graveline L, Gourdain Z, Lupi L. What are the cleaning and disinfection methods for acrylic orthodontic removable appliance? A systematic review. Children. 2021;8:1-13.
23. Farhadifard H, Sohilifar S, Bakhshaei A. Plaque Removal Efficacy of 3 Cleaning Methods for Removable Orthodontic Appliances: A Crossover Randomized Clinical Trial. Turkish J Orthod. 2021;34:170-175.
24. Diedrich P, Aachen. Keimbeseidlung und verschiedene Reinigungsverfahren kieferorthopädischer Geräte. Fortschr Kieferorthop. 1989;50:231-239.S

Research Article

THE SUCCESS OF POST-ENDODONTIC RESTORATIONS USING DIFFERENT RESTORATIVE MATERIALS: A TWO- YEAR FOLLOW-UP STUDY

 Sait GÜLLÜ¹,  Emre ÇULHA^{1*},  Uğur AYDIN¹,  Muazzez Naz BAŞTÜRK ÖZER¹

¹Department of Endodontics, Faculty of Dentistry, Gaziantep University, Gaziantep, Turkey

*Correspondence: emreculha@hotmail.com

ABSTRACT

Objective: Coronal restoration following endodontic therapy is critical for success. Restorations after endodontic treatment should minimize fractures of residual hard tissues, and maintain dental function. The aim of this study was to evaluate the success of post-endodontic restorations using various restorative materials over a two-year period.

Materials and Methods: The study involved 60 individuals aged 18 to 40. The patients were randomly divided into three groups. Conventional composite restorations were used to restore the first group. The second group was treated with a fiber-reinforced composite covered in composite resin. The third group was reconstructed using endocrowns. The restorations were prospectively investigated for two years.

Results: In the composite restoration group, two restorations and one tooth were fractured, with two polishable surfaces found on a single restoration. In the fiber-reinforced composite restoration group, one restoration fragmented and one polishable surface was found. In the endocrown restoration group, 2 endocrowns had decementation. No significant difference was observed in periodontal examination including gingival pocket depth, plaque and bleeding indices assessment ($p > 0.05$). There were no marginal discrepancies and no caries in any of the restorations. At the last appointment, patient satisfaction was evaluated in terms of aesthetics and function using a visual analog scale.

Conclusion: All groups had a 100% survival rate over the two-year follow-up period. According to the patients, there was no functional difference between the restoration groups ($p > 0.05$); however, aesthetically, restorations with endocrowns were more successful ($p < 0.05$).

Keywords: Endocrown, Fiber-Reinforced Composite, Composite, Canal Treatment, Post-Endodontic Restoration

Received: 10 September 2024

Revised: 09 April 2025

Accepted: 03 June 2025

Published: 23 June 2025



Copyright: © 2025 by the authors. Published by Aydın Adnan Menderes University, Faculty of Medicine and Faculty of Dentistry. This article is openly accessible under the Creative Commons Attribution-NonCommercial 4.0 International (CC BY-NC 4.0) License.

INTRODUCTION

The quality of coronal restoration in endodontically treated teeth (ETT) is critical for long-term tooth prognosis. A successful coronal restoration lowers the risk of tooth loss by minimizing bacterial microleakage into the obturated root canal system. However, ETT has poorer outcomes than vital teeth, primarily associated with periodontal problems and vertical root or cusp fractures (1). 11% of the ETT was extracted owing to improper restorations (2). When restored with veneers, these teeth attain survival rates similar to vital ones because microleakage is minimized and tooth structure is preserved. However, the success rate is reduced when they are reconstructed with composite resin (CR) alone (3). Endocrown restorations, which receive support from the pulp chamber and are less intrusive than post-supported prosthetic crowns, have become increasingly popular with the advancement of minimally invasive dentistry.

Endocrowns provide the appropriate distribution of stress inside the coronal restoration and the uniform transmission of occlusal pressures (4). The manufacture of endocrowns on computer aided design-computer aided manufacturing (CAD-CAM) systems has allowed for more suitable restorations to be performed in less time. Compared to traditional procedures, the positive aspects of endocrowns are that they offer better aesthetic and functional outcomes, are less expensive, and require less time to complete (5). Glass ceramics reinforced with lithium disilicate (LD), one of the dental materials utilized for fabricating endocrowns, have enhanced crystal content to strengthen the substructure ceramics. Nevertheless, there is little information on the longer-term survival and success of endocrowns (6). As a different approach, fiber-reinforced composites (FRCs) are inserted beneath the restorations to improve the physical characteristics of ETT restored with CRs. Utilizing FRCs improves the fracture resistance of the tooth structure when applied to ETT (7).

This study was targeted to assess the clinical and radiographic survival and success rates of endocrown, FRC, and CR after root canal treatment over 2 years. In our study, follow-up was based on prosthetic, periodontal, radiographic, and patient satisfaction criteria. The null hypothesis predicted that there would be no difference in success rates among the different restoration types.

MATERIALS AND METHODS

The Scientific Studies Review and Ethics Board of Gaziantep University approved this study at its meeting

on November 27, 2017, with decision number 2017/389. Participants were enrolled after receiving appropriate information and providing written consent, in accordance with the Helsinki Declaration (2013 revision). All stages of the clinical study are presented in the workflow diagram in Figure 1.

This study comprised 60 systemically healthy people aged 18 to 40. Preoperative data for each tooth were documented, including demographic information and the clinical status of each tooth. After rubber dam isolation, Specialized ultrasonic tips and a long-shaft round diamond bur were used to prepare a conservative cavity access. Root canals were explored to the apical foramen using pre-curved stainless steel #8 or #10 K-files (Maillefer, Bailague, Switzerland). Working length was determined using an electronic apex locator (Root ZX Morita, Tokyo, Japan) and confirmed with digital periapical radiography. All canals were prepared using an M-Wire alloy rotary system (ProTaper Next, Maillefer, Bailague, Switzerland) with a tip size of up to #25 and variable taper. Irrigation was carried out with 5.25% sodium hypochlorite (Imicryl, Konya, Turkey) through side-vented 30-G needles. The root canals were irrigated with 17% EDTA solution (Werax, İzmir, Turkey) for 3 minutes. The canals were dried with sterile paper points, then obturated using the lateral condensation technique with gutta-percha cones (Maillefer, Bailague, Switzerland) and AH Plus sealer (Dentsply DeTrey, Konstanz, Germany).

After root canal obturation, a different investigator evaluated the marginal integrity, surface characteristics, as well as the periodontal and radiographic findings.

Inclusion criteria were as follows:

- A molar tooth requiring root canal treatment
- Radiographic continuity of the lamina dura
- An acceptable crown-to-root ratio
- No root fractures, cracks, or periapical lesions
- Presence of a MOD cavity in the tooth
- Good oral hygiene and compliance with hygiene recommendations
- Absence of periodontal disease

Exclusion criteria included:

- Presence of any systemic health problems
- Tooth mobility greater than Grade I

After initial screening, all eligible participants were randomly assigned to one of three groups based on the type of post-endodontic restoration. Allocation was concealed using a randomization program (www.randomizer.org).

Composite Restoration Group

Unsupported enamel that was prone to fracture on the cavity walls was removed and smoothed until a satisfactory length-to-thickness ratio was obtained. The Supermat Matrix System (Hawe Neos Dental, Switzerland) was applied to the molar tooth with the help of appropriately sized wooden interdental wedges to create proper contacts both mesially and distally. 37% phosphoric acid (Ivoclar Vivadent AG, Schaan, Liechtenstein) was applied to the cavity surface for 15 seconds, rinsed for 15 seconds, and finally dried. G-bond adhesive (GC Corporation Tokyo, Japan) was applied to the created cavity, allowed to dry for 20 seconds, and then polymerized with an LED light device (Valo Cordless, South Jordan, USA) for 40 seconds. A hybrid resin composite (Essentia Universal, GC Germany, Bad Homburg, Germany) was placed in layers of approximately 1.2 mm depth. Finally, CR was polished with a bur and composite finishing discs.

Fiber-reinforced Resin Supported Composite Restoration Group

The underlying structure (EverX Posterior, GC Corporation, Tokyo, Japan) was utilized, with short E-fibers. 37% phosphoric acid was coated over the cavity surface for 15 seconds, rinsed, and dried. G-bond adhesive (GC Corporation Tokyo, Japan) was applied to the cavity, waited 20 seconds, then dried with air and polymerized for 40 seconds with an LED light. The composite material was then used to form the mesial and distal marginal walls. Following that, the FRC material was placed in 3-4 mm increments based on the approximate cavity depth and held for 20 seconds. After that, a hybrid resin composite (Essentia Universal, GC Germany, Bad Homburg, Germany) was applied to the 1.5-2 mm thick FRC. The restoration was polymerized for 40 seconds with an LED light device prior to being polished with a polishing bur and composite finishing discs.

Endocrown Restoration Group

In this research, LD blocks (IPS e.max CAD PC/FC, Ivoclar Vivadent AG, Schaan, Liechtenstein) were chosen as endocrown restorative materials. The sealer and gutta-percha residues at the canal orifices were cleaned out using a tiny carbide diamond bur. The root canal orifices and cavity floor were covered with 1 mm of flowable CR to keep them on a level surface. The pulp chamber of the tooth obtained a central pulp cavity depth of 2-4 mm, and the undercuts of the internal surfaces in the cavity chamber were filled with CR. To create a restoration-appropriate entry way, the coronal walls were set up to extend occlusally at a 4° angle.

Patient data was uploaded into the software system (Dentsply Sirona Dental Systems, Bensheim, Germany) according to the manufacturer's guidelines. The intra-oral scanning was performed independently for the lower and upper jaws, and the occlusion was recorded (Figure 2). The model part was selected, the margin parts and boundaries of the tooth were determined, then the entry route was selected, the preparation analyzed, and the design created by selecting the 'design' mode (the restoration form, contact information, and closure were all organized). Following these steps, the restoration was produced on a milling device (Sirona Dental Systems, Bensheim, Germany).

During the clinical phase, the restoration was adjusted to the cavity. A diamond bur (Dentsply, Bensheim, Germany) was utilized to form the proximal contacts, followed by the margins, and the abraded areas were finished off with a polishing rubber. The restoration glazing procedure involved applying paste and liquid and firing in the porcelain oven in 'p51' mode. The interior portion of the restoration was treated with 9.5% hydrofluoric acid (Porcelain Etchant, Bisco Inc., Schaumburg, Germany) for 60 seconds, rinsed with water, and dried, then silane (Monobond N, Ivoclar Vivadent AG, Schaan, Liechtenstein) was applied for 60 seconds. The cavity was filled with resin cement (Variolink Esthetic, Ivoclar Vivadent AG, Schaan, Liechtenstein), and the restoration was immediately fitted. LED light was used briefly to clean the remaining resin, then applied for 20 seconds to each surface of the restoration to harden it properly (Figure 3). Proximal surfaces were inspected with dental floss, and the remaining resin cement was extracted. The presence of remaining cement was confirmed by a periapical film using the parallel radiography method.

Prosthetic and periodontal records of the restorations were organized biannually for a period of two years. At the last follow-up, patient satisfaction with aesthetics and function was assessed using the Visual Analogue Scale (VAS).

Prosthetic evaluation

Margin integrity

1. Acceptable standards:

The probe revealed no fractures or grooves along the margin.

There is a slight imperfection along the margin, but no decay; repair is possible but not required.

The probe is positioned only in one direction.

2. Unacceptable conditions:

An edge that is beyond repair.

Discoloration along the pulpal margin of the restoration.
Residual cement.
Loose or broken restoration.
Decay along the entire margin.
Fractured enamel structure.
Surface characteristics
Acceptable conditions:
The surface is smooth.
The surface is moderately rough but can be polished.
Large surface imperfections that cannot be repaired.
A fractured surface.
Extensive porosity.

Periodontal Evaluation:

Gingival pocket depth, plaque index, bleeding index, and gingival index were assessed. Pocket depth was measured using a standardized probe in six tooth areas: distobuccal, distolingual, lingual, mesiobuccal, mesiolingual, and mid-buccal.

Plaque index:

0: No visible plaque.
1: No apparent plaque, but can be confirmed with a probe.
2: Moderate plaque near the gingival margin.
3: Plaque formation on the tooth surface and at the gingival margin.

Survival and Success of Restorations:

Survival was assessed based on marginal fractures, minor imperfections, and polishable roughness; broken enamel, irreparable restorations, and extensive porosity were considered failures.

Patient Satisfaction:

Patient satisfaction was assessed using the Visual Analogue Scale (VAS) at the final follow-up. Patients were placed in an undisturbed environment and given a scale with 10 horizontal boxes numbered from 0 to 10, then asked to evaluate both the aesthetic and functional aspects of their restorations. Patients were asked to score from 1 (lowest) to 10 (highest) on various factors, including functionality, aesthetic satisfaction, discomfort, ease of oral hygiene, and bleeding.

Statistical Analysis

The data was statistically analyzed using SPSS (IBM SPSS Statistic Version 22, Chicago, Illinois, USA). The Shapiro-Wilk test determined the normality of the data distribution. Normally distributed data was evaluated with one-way ANOVA and post-hoc Tukey HSD tests. The Kruskal-Wallis test was used to assess groups that did not have a

normal distribution. The statistical significance level was set at <0.05 .

RESULTS

The mean age of those included in the study was 27.98 ± 1.54 years, of which 58.3% ($n=35$) were female and 41.7% ($n=25$) were male.

Findings Related to Gingival Pocket Depth

When the pocket measurements of the groups before and 6 months, 1 year, and 2 years after the procedure were evaluated, the post-operative measurements of all groups were statistically similar to preoperative measurements ($p > 0.05$).

Findings Regarding Patient Satisfaction

Patient satisfaction results showed that there was no significant difference between the groups in terms of function ($p > 0.05$) (Table 1). However, the endocrown provided significantly more aesthetic satisfaction than the other groups at the end of the 2-year follow-up ($p < 0.05$). Findings related to the plaque index and the gingival index

Table 1. Patient satisfaction values of composite, fiber-reinforced composite, and endocrown restoration groups in a two-year period

Patient Satisfaction	Composite	Fiber-reinforced composites	Endocrown
Aesthetic	5.89 ± 0.29^a	5.70 ± 0.28^a	9.10 ± 0.16^b
Functional	8.26 ± 0.31^x	8.15 ± 0.22^x	8.75 ± 0.20^x

Different superscript lowercase letters in the same row indicate statistically significant differences between groups. $p < 0.05$; Analysis of variance, Tukey posthoc test

No significant difference was observed between the groups in the measurements regarding the plaque index and the gingival index ($p > 0.05$).

Findings related to the survival rate and success of the restorations

In our study, two out of 20 endocrowns experienced decementation. One decemented after 6 months, while the other decemented in the 3rd month, was recemented, and then decemented again 5 days later. In the CR group, two restorations had fractures, one tooth was fractured, and one showed slight surface roughness. In the FRC group, one restoration fractured, and one showed slight surface roughness.

DISCUSSION

There was no strong evidence to determine the optimal material or procedure for restoring the coronal part of teeth. The fact that 27% of clinical failures of ETT were connected with tooth fractures backs up the idea that ETT has a considerably higher risk of fracture than vital teeth (8). The primary reason is the reduction of hard tissue during access cavity and root canal preparation. The positioning of the tooth, whether posterior or anterior, influences the final restoration decision, as the loads on the restoration differ in these locations. Literature indicates that the fracture rate of mandibular first molars is twice that of maxillary first molars (9). Additionally, converting an occlusal cavity to a mesio-occlusal-distal (MOD) cavity in posterior teeth significantly reduces fracture resistance (10). Therefore, our study focused on ETT lower first molars with MOD cavities to better assess the strength differences among restorations.

Fracture resistance correlates directly with the remaining tooth structure. Endocrown restorations demonstrated superior fracture resistance compared to traditional restorations. This is consistent with the 5-year success rates of endocrowns, ranging from 77% to 94% (11). However, various factors, including the design, configuration, size, and elasticity of the restoration material, influence the prognosis of post-endodontic restorations. A comprehensive comparison is difficult since endocrowns and composite resin (CR) restorations have different characteristics. Therefore, this study focused on obtaining long-term follow-up data on the performance of restorations in in-vivo environments. Prospective studies with extended monitoring periods are limited due to the costs, material variations, and insufficient patient recall rates. Clinical studies on the outcomes of healed ETTs report annual failure rates ranging from 0% to 5%, but these results are based on follow-ups of only 3 to 5 years (12,13). As a result, longer-term follow-ups could differentiate between restoration options. As a result, longer-term follow-ups are necessary to distinguish between restoration options. According to Opdam et al., a more meaningful comparison of restoration prognosis can be made after 5 to 10 years of observation (14).

Two of the 20 endocrown restorations in this study experienced decementation. Improper polymerization of the cement applied to ceramic restorations can impair polymerization quality, especially when the thickness of the endocrown is excessive (15). The two decementations observed in our investigation could be related to the increased thickness of the restorations, which reduced the

polymerization of the resin cement. Another explanation for decementation could be the formation of a sclerotic dentin layer, where minerals accumulate in the dentinal tubules, obstructing them. The hybrid layer in sclerotic dentin is thinner, leading to weaker bonding. Additionally, the resin-dentin interface within the endocrown cavity may degrade over time due to ongoing chemical processes. The varying shape of the cavity makes it difficult to control moisture, minimize shrinkage stresses during polymerization, and eliminate the smear layer during adhesive application. To prevent decementation, clinicians should follow the adhesion protocol and use materials with high adhesion properties, such as lithium disilicate (LD) (16). Also, the pulp chamber floor should be flattened with glass ionomer cement or flowable composite before applying the endocrown. Furthermore, preparing the axial walls of the pulp chamber with a 6° to 12° angle is recommended to minimize debonding (11).

The two-year follow-up of this study revealed no negative impacts on the surface characteristics or margin integrity of the endocrown restorations. Additionally, the survival rate was 100%, consistent with previous studies with follow-up periods of 6, 15, and 36 months (17,18). This success may be attributed to specific characteristics of endocrowns. First, their modulus of elasticity is similar to dentin, allowing for better occlusal stress distribution across the bonded area. In contrast, conventional restorations consist of multiple subunits, such as metal or glass fiber-reinforced supports, ceramic or composite cores, and crowns. This complexity can make load distribution less efficient compared to endocrowns, which, due to their monoblock structure, can better withstand stress (19).

In our study, one tooth and two restoration fractures occurred when assessing the marginal integrity of composite resin (CR) restorations. Additionally, two teeth with CR showed a polishable surface. In the short term, there was no significant difference in the likelihood of tooth loss between ETT restored with CR or an indirect restoration (20). CRs are effective for posterior teeth due to vertical chewing forces and the mechanical anchorage of the pulp chamber. They can also be quickly restored in the mouth and are less abrasive to antagonistic tooth structures compared to ceramic restorations. However, CRs can degrade over time due to hydrolysis, mechanical stress, and leaking of the filler-matrix interfaces, which weaken their mechanical properties. Inadequate polymerization can also compromise the integrity of large CRs. Our study found no significant difference in surface texture between CR and indirect restorations. The surface

quality of CRs depends on factors such as the degree of conversion, finishing, polishing, and the composition of the filling material (21). Clinical failure of CRs may result from inadequate fracture resistance or weak resistance to crack progression under functional and para-functional stresses. In our study, CRs fractured more frequently than FRCs. However, the study's null hypothesis was supported because the failure rate of CRs did not differ significantly from that of FRCs. FRCs, especially those with fibers like polyethylene and glass fibers, improve the marginal integrity and fracture resistance of CRs by providing reinforcement beneath the restoration (22). This improvement may be due to the isotropic reinforcement provided by EverX Posterior, which uses irregularly organized short glass fibers to strengthen the tooth in multiple directions. Short fiber fillers, as noted by Garoushi et al., can limit crack development and increase fracture resistance (23). Furthermore, the less rigid E-glass fibers in EverX Posterior offer better adaptability to dentin and CR, while the thixotropic viscosity of FRC ensures it stays in place when inserted into maxillary molars. Consequently, the FRC substructure helps transmit forces from the polymer matrix to the E-glass fibers, enhancing the restoration's durability.,

In the 6-month periodontal evaluation of this study, no statistically significant differences were observed in pocket depth, plaque index, or gingival index. This can be attributed to the fact that the participants were periodontally healthy and maintained good oral hygiene. Additionally, the LD ceramics used for the endocrowns may contribute to a reduced plaque retention rate (24). Furthermore, endocrowns have supragingival margins, which make it easier to control plaque and assess the restoration margins compared to CRs and FRCs (25).

Similar to many studies, the present research showed that endocrowns offer better aesthetics than conventional restorations after two years, based on patient preferences (16,19). This can be attributed to the fact that the morphological features of the endocrowns were designed in a computer environment using thousands of tooth shapes stored in the program's database. Moreover, the LD crystal content and the monoblock structure of endocrowns likely contributed to superior light transmission compared to FRC and CR, enhancing patients' aesthetic satisfaction.

CONCLUSION

Although there was no statistical difference in our study, the use of FRCs under the CRs prevents restoration

fractures. All restoration groups had a 100% survival rate over the two-year follow-up period. Endocrowns have become the materials preferred by patients in terms of both aesthetics and durability.

Acknowledgments

This study was presented as an oral presentation at the 3rd International Dentistry Congress of Konya Necmettin Erbakan University held on 24-26 May.

Authorship contributions

SG and UA created the idea/concept and the design of the study. SG, EÇ and UA undertook the control and supervision of the study. SG and MNBÖ carried out the data collection and processing. SG, UA and MNBÖ performed the analysis and interpretation of the results. EÇ carried out literature review. EÇ and MNBÖ wrote the article. EÇ and UA carried out the critical review. EÇ provided the references. SG collected the materials of the study.

Data availability statement

The data that support the findings of this study are available from the corresponding author upon reasonable request.

Declaration of competing interest

The authors deny any conflict of interest related to this study. We affirm that we have no financial affiliation, or involvement with any commercial organization with a direct financial interest in the subject or materials discussed in this manuscript, nor have any such arrangements existed in the past three years.

Ethics

Ethical approval for this study was obtained from The Scientific Studies Review and Ethics Board of Gaziantep University (27/10/ 2017, decision number 2017/389).

Funding

This research did not receive any specific grant from funding agencies in the public, commercial, or not-for-profit sectors.

REFERENCES

1. Landys Borén D, Jonasson P, Kvist T. Long-term survival of endodontically treated teeth at a public dental specialist clinic. *J Endod.* 2015;41(2).
2. Sjögren U, Hägglund B, Sundqvist G, Wing K. Factors affecting the long-term results of endodontic treatment. *J Endod.* 1990;16(10).

3. Tang W, Wu Y, Smales RJ. Identifying and Reducing Risks for Potential Fractures in Endodontically Treated Teeth. Vol. 36, Journal of Endodontics. 2010.
4. Gulec L, Ulusoy N. Effect of Endocrown Restorations with Different CAD/CAM Materials: 3D Finite Element and Weibull Analyses. Biomed Res Int. 2017;2017.
5. Dietschi D, Duc O, Krejci I, Sadan A. Biomechanical considerations for the restoration of endodontically treated teeth: a systematic review of the literature, Part II (Evaluation of fatigue behavior, interfaces, and in vivo studies). Quintessence Int. 2008;39(2).
6. Zheng Z, He Y, Ruan W, Ling Z, Zheng C, Gai Y, et al. Biomechanical behavior of endocrown restorations with different CAD-CAM materials: A 3D finite element and in vitro analysis. Journal of Prosthetic Dentistry. 2021;125(6).
7. Khan SI, Anupama R, Deepalakshmi M, Kumar KS. Effect of two different types of fibers on the fracture resistance of endodontically treated molars restored with composite resin. J Adhes Dent. 2013;15(2).
8. Setzer FC, Boyer KR, Jeppson JR, Karabucak B, Kim S. Long-term prognosis of endodontically treated teeth: A retrospective analysis of preoperative factors in molars. J Endod. 2011;37(1).
9. Assif D, Gorfil C. Biomechanical considerations in restoring endodontically treated teeth. J Prosthet Dent. 1994;71(6).
10. Costa LCS, Pegoraro LF, Bonfante G. Influence of different metal restorations bonded with resin on fracture resistance of endodontically treated maxillary premolars. Journal of Prosthetic Dentistry. 1997;77(4).
11. Al-Dabbagh RA. Survival and success of endocrowns: A systematic review and meta-analysis. Vol. 125, Journal of Prosthetic Dentistry. 2021.
12. Van Dijken JWV, Hasselrot L, Örmén A, Olofsson AL. Restorations with extensive dentin/enamel-bonded ceramic coverage. A 5-year follow-up. Eur J Oral Sci. 2001;109(4).
13. Murgueitio R, Bernal G. Three-Year Clinical Follow-Up of Posterior Teeth Restored with Leucite-Reinforced IPS Empress Onlays and Partial Veneer Crowns. Journal of Prosthodontics. 2012;21(5).
14. Opdam NJM, Bronkhorst EM, Loomans BAC, Huysmans MCDNJM. 12-year survival of composite vs. amalgam restorations. J Dent Res. 2010;89(10).
15. Soares CJ, Da Silva NR, Fonseca RB. Influence of the feldspathic ceramic thickness and shade on the microhardness of dual resin cement. Oper Dent. 2006;31(3).
16. Govare N, Contrepolis M. Endocrowns: A systematic review. Vol. 123, Journal of Prosthetic Dentistry. 2020.
17. Decerle N, Bessadet M, Munoz-Sanchez ML, Eschevins C, Veyrune J, Nicolas E. Evaluation of Cerec endocrowns: a preliminary cohort study. Eur J Prosthodont Restor Dent. 2014;22(2).
18. Otto T. Computer-Aided Direct All-Ceramic Crowns: Preliminary 1-Year Results of a Prospective Clinical Study. Int J Periodontics Restorative Dent. 2004;24(5).
19. Sedrez-Porto JA, Rosa WL de O da, da Silva AF, Münchow EA, Pereira-Cenci T. Endocrown restorations: A systematic review and meta-analysis. Vol. 52, Journal of Dentistry. 2016.
20. de Kuijper MCFM, Cune MS, Özcan M, Gresnigt MMM. Clinical performance of direct composite resin versus indirect restorations on endodontically treated posterior teeth: A systematic review and meta-analysis. Vol. 130, Journal of Prosthetic Dentistry. 2023.
21. Chung K hung. Effects of finishing and polishing procedures on the surface texture of resin composites. Dental Materials. 1994;10(5).
22. Luthria A, Sirekha A, Hegde J, Karale R, Tyagi S, Bhaskaran S. The reinforcement effect of polyethylene fibre and composite impregnated glass fibre on fracture resistance of endodontically treated teeth: An in vitro study. Journal of Conservative Dentistry. 2012;15(4).
23. Garoushi S, Vallittu PK, Lassila L V. Fracture toughness, compressive strength and load-bearing capacity of short glass fibre-reinforced composite resin. Chin J Dent Res. 2011;14(1).
24. Kamonwanon P, Hirose N, Yamaguchi S, Sasaki JJ, Kitagawa H, Kitagawa R, et al. SiO₂-nanocomposite film coating of cad/cam composite resin blocks improves surface hardness and reduces susceptibility to bacterial adhesion. Dent Mater J. 2017;36(1).
25. Robbins JW. Restoration of the endodontically treated tooth. Dent Clin North Am. 2002;46(2).

Research Article

A COMPARATIVE ANALYSIS OF ANGULAR CEPHALOMETRIC MEASUREMENTS USING VISTADENT AND NEMOCEPH DIGITAL SOFTWARE

 Fundagül BİLGİÇ ZORTUK^{1*},  Eyüp Burak KÜÇÜK¹

¹Hatay Mustafa Kemal University, Faculty of Dentistry, Department of Orthodontics, Hatay, Türkiye

*Correspondence: fbilgic@mku.edu.tr

ABSTRACT

Objective: The aim of this investigation was to compare the reliability of two different software programs, Vista Dent and NemoCeph for digital cephalometric tracing when used for angular measurements on 2D digital cephalometric radiographs.

Methods: A total of 300 cephalometric radiographs were chosen for this study. The Vista dent and Nemoceph computerized softwares programs were used to obtain cephalometric measurements from lateral cephalograms. The SNA and SNB angle values obtained by the two methods were evaluated through independent sample T-test and and the Mann-Whitney U Test was done to compare GoGn-SN angle between the two different computerized softwares programs. The Pearson correlation analysis was used to evaluate the consistency between the two measurement method.

Results: It shows no statistical difference between the values of the SNA, SNB, and GoGn-SN angles performed by the Vista dent and Nemoceph software ($p > 0.05$). It was obtained strong correlations between all the variables.

Conclusions: The measurements from the two computer-assisted cephalometric analysis are consistent. Clinicians can confidently use either of these programs.

Keywords: VistaDent, Nemoceph, Steiner analysis, Cephalometric radiographs

Received: 17 February 2025

Revised: 21 March 2025

Accepted: 07 April 2025

Published: 23 June 2025



Copyright: © 2025 by the authors. Published by Aydın Adnan Menderes University, Faculty of Medicine and Faculty of Dentistry. This article is openly accessible under the Creative Commons Attribution-NonCommercial 4.0 International (CC BY-NC 4.0) License.

INTRODUCTION

Lateral cephalograms play an important role in dentistry. Indeed, cephalometric measurements represent a key method for planning orthodontic treatment. Cephalometric evaluation is also used for case diagnosis, evaluation of treatment progress and growth, and prediction of surgical outcomes following treatment of dentofacial deformities. To accomplish all this, skeletal, dental, and soft tissue anatomical features need to be determined via a landmark identification and manual cephalometric analysis process for analyzing X-ray images. However, such an analysis requires an expert in the field of orthodontics and entails a time-consuming process (1,2).

Cephalometric measurements, which were traditionally performed manually, especially in the field of orthodontics, are now being replaced by digital cephalometric measurement programs. In fact, advances in computer technology have resulted in a greater adoption of digital systems for both viewing and analyzing cephalograms (3). These digital methods represent a sector of technology facilitating systems to obtain data, automatically calculate angles and linear measurements, and reduce mistakes in both landmark line drawing and measurements, and all with minimal human intervention (4). In addition, digital methods allow measurements to be carried out quickly, treatment plans to be easily determined, and images to be easily stored, reproduced, and sent anywhere in the world (5). Hence, the cost-efficient replication of radiographs and their rapid superimposition are among the advantages of such methods (6).

Various digital methods and computer software are now used for cephalometric tracing to assess the legitimacy and consistency of linear and angular measurements performed by programs such as Quick Ceph 2000 (Sarasota, Florida, USA), NemoCeph (Madrid, Spain), FACAD (Beilkegaten, Linköping, Sweden), Vista Dent (Woodbridge, Canada), and OnyxCeph (Neidelwaldstr, Chemnitz, Germany). The use of such software greatly supports orthodontic professionals in performing cephalometric evaluations and developing accurate diagnostic and treatment plans (7).

These technological advances have provided faster and better outcomes, which have helped to enhance clinical practices. However, despite the technological advances, there are still several types of errors (errors in the patient's head position and magnification) still occur in the cephalometric measurement process and need to be

identified. To address this issue, the present study aims to evaluate the reliability of angular measurements obtained from two-dimensional (2D) direct digital cephalometric radiographs. More specifically, this study is carried out to find out the validity of the free of cost and readily available imaging software such as VistaDent (Woodbridge, Canada) and NemoCeph (Madrid, Spain) for digital cephalometric tracing, by comparing its reliability of two different software programs. The null hypothesis is that the parameters obtained with Vista Dent and NemoCeph will be consistent with each other.

MATERIALS AND METHODS

The present research design was approved by the institutional ethical committee (approval no. 2022/02). The inclusion criteria for this study were a fully erupted permanent dentition, good-quality radiographs, and no previous history of orthodontic treatment. The exclusion criteria were patients with gross asymmetry, any dental syndromes, a history of orthodontic treatment and/or orthognathic surgery, and poor-quality radiographs. A total of 300 radiographs were collected based on the inclusion and exclusion criteria from archive of the orthodontics department of Hatay Mustafa Kemal University. For this study, the lateral cephalometric radiographs were obtained using a Vatech PaX-i SC digital panoramic and cephalometric imaging device (Gyeonggi, Korea). Direct digital exposures were made with 72 kV, 10 mA and a total scanning time of 20.2 s. Each radiograph was taken with the patient's Frankfort horizontal plane aligned parallel to the floor, and the jaws in centric occlusion.

Digital tracing

In the process of digital cephalometric measurement, digital cephalogram images were imported into the NemoCeph NX 2021 (Nemotec, Madrid, Spain) and Vista Dent software (GAC International, Inc., Bohemia, New York, USA). The images were calibrated by digitizing two points on the ruler within the digital image using the software provided by the manufacturer. Following digitization of the six anatomical landmarks, the Vista Dent and the NemoCeph programs automatically generated the measurements. (Table 1).

Statistical analysis

The statistical analyses were conducted using version 20.0 of the Statistical Package for the Social Sciences (SPSS Inc., Chicago, Illinois, USA). The Shapiro–Wilk test was used to inspect the normality of the data distribution. The sella, nasion, A point (SNA; $80^\circ \pm 2^\circ$) and sella, nasion B point

(SNB; $78^{\circ} \pm 2^{\circ}$) angles were revealed to be normally distributed, although the GoGn-SN angle ($36^{\circ} \pm 2^{\circ}$) was not normally distributed. Thus, an independent samples t-test was performed to compare the SNA and SNB angle values and a Mann-Whitney U test was conducted to compare the GoGn-SN angles between the NemoCeph and Vista Dent tracings, as shown in Table 2.

Two weeks after the initial measurements were completed, 50 digital radiographs and the associated measurements were repeated with the NemoCeph and Vista Dent software to determine the intraexaminer reliability using the intraclass correlation coefficient (ICC) for each measurement (8). Moreover, a clinically significant difference was identified when the discrepancy in the angular and linear measurements exceeded 2° or 2 mm, respectively.⁹ The Pearson correlation was used to evaluate the consistency between the two measurement methods (Table 3).

Table 1. Description of cephalometric landmarks and measurements used in this study.

Landmark (abbreviation)	Definition
Sella (S)	Center of the pituitary fossa of the sphenoid bone
Nasion (Na)	Most anterior point on the frontonasal suture in the midsagittal plane
Point A (A)	Deepest point of the curve of the anterior border of the maxilla
Point B (B)	Most posterior point in the concavity along anterior border of the symphysis
Gonion (Go)	Point along angle of the mandible, midway between lower border of mandible and posterior ascending ramus
Gnation (Gn)	The most antero-inferior point on the contour of the chin, right in the middle of the lower edge of the mandible
Measurements	
SNA ($^{\circ}$)	SN to NA angle
SNB ($^{\circ}$)	SN to NB angle
SN/GoGn ($^{\circ}$)	SN to GoGn angle

RESULTS

The ICC values ranged from 0.797 to 0.998, indicating good to excellent agreement between the two software programs. The differences in the SNA, SNB, and GoGn-SN angles between the two cephalometric analysis programs are shown in Table 2. In this regard, the differences in the measurements of the SNA, SNB, and GoGn-SN were not statistically significant between Vista Dent and NemoCeph ($p < 0.05$). The Pearson correlation analysis revealed a strong correlation between all the variables (i.e., strong correlation; Table 3).

Table 2. Comparison of the cephalometric measurements between the Vista dent and Nemoceph computerized softwares.

	Vistadent		Nemoceph		p
	Mean	SD	Mean	SD	
^a SNA ($^{\circ}$)	79.9	4.29	79.27	4.45	0.48
^a SNB ($^{\circ}$)	76.81	4.17	77.23	4.14	0.98
^b SN-GoGn ($^{\circ}$)	32.88	6.53	33.51	6.89	0.21

SD Standard deviation, ^aThe results of paired t test, ^bThe results of Mann-Whitney U Test

Table 3. Pearsons correlation: Comparison of mean values obtained from the Vista dent and Nemoceph computerized softwares.

Parameters being correlated	N	Correlation(r)	p
SNA ($^{\circ}$)	300	0.970	<0.001
SNB ($^{\circ}$)	300	0.972	<0.001
SN-GoGn ($^{\circ}$)	300	0.931	<0.001

DISCUSSION

The lateral cephalogram is an essential tool for both evaluating skeletal growth and planning treatment and long-term follow-up of pre- and post-treatment changes (9). Due to the advancement of technology, the manual cephalometric tracing method is gradually being replaced by computer-based software, such as NemoCeph and Vista Dent (10,11). By using computer-assisted digital cephalometric analysis systems, the time required for tracing and analysis can be reduced, the inter- and intra-examiner errors can be eliminated, and the cephalometric results can be stored, used, and retrieved (12).

In computer-assisted cephalometric analysis, the location of landmarks is manually determined on the digital images, the cephalometric analysis is conducted using computer, and the cephalometric software program calculates the distances and angles automatically (13). However, these software programs are still associated with the potential for errors, irrespective of the clinician's experience who performs the manual landmark identification, which may lead to problems, for example, when transferring results (14,15).

The increasing use of digital cephalometric software has led to a need to compare the different software programs. Hence, this study aimed to evaluate the reliability of three angular measurements performed on 2D lateral cephalometric images derived from two rendering programs. Steiner's analysis was chosen for this study due to its widespread use as one of the most commonly applied cephalometric methods (16). All the measurements were performed by a single investigator with approximately 19 years of experience in cephalometric tracing. This approach was chosen to ensure standardization and minimize the errors that could

arise between different operators, given the observation that the inter-examiner error rate is exceeds the intra-examiner error rate. Moreover, performing 10 tracings daily also contributed to reducing the investigator's stress and minimizing the errors (17).

According to the results of this study, the measurements obtained using the 2D VistaDent and NemoCeph tracing methods showed no statistical variations ($p > 0.05$). These results should be interpreted as indicating that Vista Dent and NemoCeph software can be used in place of each other, with no or only minimal systematic bias (18).

In many prior studies in which NemoCeph and manual tracing have been compared, no significant differences were found, suggesting that NemoCeph can be reliably used for cephalometric measurements (12,19). Comparable studies have also been conducted on desktop software such as AOCeph, NemoCeph, Quick Ceph, Dolphin, FACAD, Vista Dent and AutoCEPH. It was reported that the precision and dependability of the examined software to be comparable to manual cephalometric tracing, rendering the software suitable for use in diagnosis of the case, treatment planning, and assessment of treatment progress and results in clinical and research environments (17,19,20). However, the drawbacks of these desktop cephalometric software programs include the necessity of using them on a desktop or laptop, the high cost, and the need for an internet connection (12).

Still, Gorracci et al.(21) demonstrated the high consistency of cephalometric measurements taken using the iPad-based software SmileCeph, the desktop application NemoCeph, and manual tracing. In a study by Paul et al.(22), automated tracing (WebCeph) was associated with a higher number of landmark recognition errors compared to manual or semi-automatic tracing (NemoCeph), although both WebCeph and NemoCeph were found to be more reliable than manual tracing, with NemoCeph also demonstrating higher efficacy. For the present study, NemoCeph software was used due to its advantage over conventional tracing methods in terms of reducing observer errors (7).

Limitations

The study only used Steiner's analysis, which limits the generalizability of the findings. Using parameters from different analyses could lead to more valuable results.

CONCLUSION

The result of this study shows that the digital tracing with the NemoCeph had equal accuracy in comparison to the Vista Dent. This study determined that the measurements obtained from the two computer-assisted cephalometric analysis programs (NemoCeph and Vista Dent) currently in use are compatible with each other, indicating that both programs can be reliably used by clinicians.

Acknowledgments

Not Applicable.

Authorship contributions

Zortuk FB: Conceptualization, Methodology, Software, Validation, Formal analysis, Investigation, Resources, Data Curation, Writing – original draft preparation, Writing – review and editing, Visualization, Supervision. Küçük EB: Writing – original draft preparation, Writing – review and editing, Visualization, Supervision.

Data availability statement

The data used in this paper is publically available through Hatay Mustafa Kemal University's research repository.

Declaration of competing interest

No conflict of interest was declared by the authors.

Ethics

The present study was approved by the institutional ethical committee (approval no. 2022/02).

Funding

The authors declared that this study received no financial support.

REFERENCES

1. Aksoy S, Kelahmet U, Hincal E, Oz U, Orhan K. Comparison of linear and angular measurements in CBCT scans using 2D and 3D rendering software. *Biotechnology & Biotechnological Equipment* 2016;30:777-84.
2. Sangmin J, and Lee KC. Comparison of cephalometric measurements between conventional and automatic cephalometric analysis using convolutional neural network. *Prog Orthod* 2021;22:1-8.
3. Faliya N, Mamatha J, Doshi J, Gandhi P, Mathakiya L, Bind P. Comparing the Efficacy between OneCeph digital software versus Manual Cephalometric Tracing. *J Adv Health* 2021; 2:2-13.

4. Liu JK, Chen YT, Cheng KS. Accuracy of computerized automatic identification of cephalometric landmarks. *Am J Orthod Dentofacial Orthop* 2000;118:535-40.
5. Forsyth DB, Shaw WC, Richmond S, Roberts CT. Digital imaging of cephalometric radiographs, Part 2: image quality. *Angle Orthod* 1996; 66: 43-50.
6. Harrell WE Jr. 3-D Diagnosis and treatment planning in orthodontics. *Semin Orthod* 2009;15:35-41.
7. Rawat S, Jadhav VV, Paul P. A Comparative Analysis of Skeletal and Dental Parameters in Bilateral Cleft Lip and Palate vs. Non-bilateral Cleft Lip and Palate Patients in the Central Indian Population: A NemoCeph Study. *Cureus* 2024;16:2-13.
8. Portney LG, Watkins MP. Foundations of clinical research: applications to practice. New Jersey, Prentice Hall; 2000. p. 11-5.
9. Kumar V, Ludlow J, Cevidanes LHS, Mol A. In vivo comparison of conventional and cone beam CT synthesized cephalograms. *Angle Orthod* 2008;78:873-9.
10. Pavan KM, Praveen KN, Murthy S. Model analysis on a smartphone. *J Clin Orthod* 2012; 46:356-8.
11. Keim RG, Gottlieb EL, Vogels DS 3rd, Vogels PB. 2014 JCO study of orthodontic diagnosis and treatment procedures, Part 1: results and trends. *J Clin Orthod* 2014; 48:607-30.
12. Mohan A, Sivakumar A, Nalabothu P. Evaluation of accuracy and reliability of OneCeph digital cephalometric analysis in comparison with manual cephalometric analysis: A cross-sectional study. *BDJ open* 2021;7:1-4.
13. Khatoon B, Hill KB, Walmsley AD. Can we learn, teach and practise dentistry anywhere, anytime? *Br Dent J* 2013;215:345-7.
14. Richardson A. A comparison of traditional and computerized methods of cephalometric analysis. *Eur J Orthod* 1981;3:15-20.
15. Turner PJ, Weerakone S. An evaluation of the reproducibility of landmark identification using scanned cephalometric images. *J Orthod* 2001;28: 221-9.
16. Steiner, C. C. Cephalometrics for you and me. *Am J Orthod* 1953;39:729-55.
17. Erkan M, Gurel HG, Nur M, Demirel B. Reliability of four different computerized cephalometric analysis programs. *Eur J Orthod* 2011; 34:318-21.
18. Yassir YA, Nabbat SA, and Hamdan HA. Evaluation of Semi-Automated Software and Application for Cephalometric Analysis. *International Medical Journal* 2021;28:16-20.
19. Paixao MB, Sobral MC, Vogel CJ, Martin de Araujo T. Comparative study between manual and digital cephalometric tracing using Dolphin Imaging software with lateral radiographs. *Dent Press J Orthod* 2010;15:123-30.
20. Santoro M, Jarjoura K, Cangialosi TJ. Accuracy of digital and analogue cephalometric measurements assessed with the sandwich technique. *Am J Orthod Dentofac Orthoped* 2006;129:345-51.
21. Goracci, C, Ferrari M. Reproducibility of measurements in tablet-assisted, PC- aided, and manual cephalometric analysis. *Angle Orthod* 2014;84:437-42.
22. Paul L, Tania SDM, Rathore S, Missier S, Shaga B. Comparison of accuracy and reliability of automated tracing Android app with conventional and semiautomated computer aided tracing software for cephalometric analysis - a cross-sectional study. *Int J Orthod Rehabil* 2022,13:39-51.

Research Article

CLINICOPATHOLOGICAL SIGNIFICANCE OF IMMUNOHISTOCHEMICAL PD-L1 AND ANDROGEN RECEPTOR EXPRESSIONS IN TRIPLE NEGATIVE BREAST CANCERS

● Büşra EKİNCİ^{1*}, ● Nesibe KAHRAMAN ÇETİN¹, ● İbrahim Halil ERDOĞDU¹, ● İbrahim
METEOĞLU¹

¹Department of Pathology, Aydın Adnan Menderes University Faculty of Medicine, Aydın, TURKIYE

*Correspondence: busraekinci16@gmail.com

ABSTRACT

Objective: Triple negative breast cancers (TNBC), a subset of breast cancers are high-grade, and related to younger age, higher risk of recurrence, higher incidence of metastases and poorer prognosis. Currently, there is increasing evidence of a dynamic interaction between the breast cancer and immune system. Luminal Androgen Receptor (LAR) subtype is dependent on Androgen Receptor (AR) signaling and represents a novel subtype of TNBC with a distinct prognosis that offers an opportunity for the development of targeted therapeutics. In this study, we aimed to investigate the immunohistochemical expression of Programmed death ligand 1(PD-L1) and AR and their correlations with clinical parameters in TNBC.

Materials and Methods: Sixtyfour patients who received a primary diagnosis of TNBC from surgical material at Aydın Adnan Menderes University Faculty of Medicine Hospital Department of Pathology between 2013-2019 were available for this study. Demographic and histopathological characteristics were obtained from archival reports. PD-L1 and AR immunohistochemical stains were applied to sections prepared from the blocks.

Results: The mean age was 53,47±15,044(range 28-84 years). The percentage of PD-L1 positivity was %57,8 and AR positivity was %26,6. There was a significant correlation PD-L1 positivity with Ki67 proliferation index(p=0.009), and lymphovascular invasion(p=0.009) and no correlation between PD-L1 and other parameters. No significant correlation was found between AR and clinicopathologic parameters.

Conclusion: PD-L1 and AR are important prognostic markers for TNBC and identify important groups for targeted therapies. PD-L1 positive cases are associated with poor prognostic markers and further studies in larger groups are needed for both markers.

Keywords: Triple negative breast cancer, PD-L1, AR, Ki67, immunohistochemistry.

Received: 30 January 2025

Revised: 25 March 2025

Accepted: 07 April 2025

Published: 23 June 2025



Copyright: © 2025 by the authors. Published by Aydın Adnan Menderes University, Faculty of Medicine and Faculty of Dentistry. This article is openly accessible under the Creative Commons Attribution-NonCommercial 4.0 International (CC BY-NC 4.0) License.

INTRODUCTION

Triple negative breast cancer (TNBC) is a subset of breast cancers that lack expression of the progesterone receptor (PR), estrogen receptor (ER) and human epidermal growth factor receptor 2 (HER2). According to hormone receptor positive breast cancer TNBC is related to younger age, higher risk of recurrence, higher incidence of metastases and poorer prognosis (1). Despite the wide range of morphologies, the majority of TNBCs are high-grade, with tumor cells showing large nuclear size, solid growth pattern and geographic necrosis (2). This molecular heterogeneity has led to the lack of FDA-approved targeted therapies for TNBC (3).

Programmed death ligand 1 (PD-L1) is a transmembrane glycoprotein of haplotype 1 of the immunoglobulin superfamily, so named because of its association with the apoptotic program. PD-L1 is widely expressed on the surface of B lymphocytes, natural killer cells, monocytes, vascular endothelial cells and macrophages (4). It was also upregulated in tumor cell lines such as ovarian cancer, lymphoma and melanoma, suggesting a close relationship with tumor initiation and development (4). There is increasing evidence of a dynamic interaction between the immune system and breast cancer (5). PD-L1 immunohistochemical expression in breast cancer is about %10-30 and TNBC shows the highest percentage of PD-L1 positivity (6). Taken together, identifying the PD-1/PD-L1 pathway is of clinical importance.

Lehmann et al identified four subtypes of TNBC, each displaying unique ontologies. The TNBC subtypes include two basal-like (BL1 and BL2), mesenchymal (M) and luminal androgen receptor (LAR) (3). The LAR subtype is enriched for hormone-regulated pathways and is dependent on androgen receptor (AR) signaling, is distinct from unselected TNBC, is predominantly subclassified in the non-basal subset, and represents a novel subtype of TNBC with a distinct prognosis that offers an opportunity for the development of targeted therapeutics (7).

In this study, we aimed to investigate the immunohistochemical expression of PD-L1 and AR and their correlations with clinical parameters in TNBC and to determine the groups suitable for targeted therapy.

MATERIALS AND METHODS

Sixtyfour patients who received a primary diagnosis of TNBC from surgical material at Aydın Adnan Menderes University Faculty of Medicine Hospital Department of

Pathology between 2013 and 2019 were available for this study. Demographic and histopathological characteristics were obtained from archival reports. Hematoxylin and eosin-stained sections of each patient were re-evaluated. Blocks with the most tumor cells and the least necrosis were selected (Figure 1).

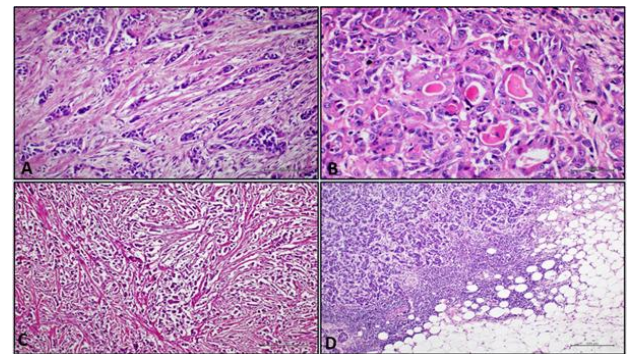


Figure 1. A. Invasive breast carcinoma, no special type x100 HPF, Hematoxylin&Eosin. B. Acinic cell carcinoma x200 HPF, Hematoxylin&Eosin. C. Invasive micropapillary carcinoma, x100 HPF, Hematoxylin&Eosin. D. Invasive breast carcinoma medullary pattern, x100 HPF, Hematoxylin&Eosin

In addition, ER, PR, HER2, Ki67 immunohistochemistry slides were reviewed according to the American Society of Clinical Oncology/American Society of Pathologists (ASCO/CAP) breast cancer guidelines.

PD-L1 and AR immunohistochemical staining

Three-micron sections of 64 formalin-fixed, paraffin-embedded tissue blocks were cut and mounted on positively charged poly-L-lysine (Micro Slides Snowcoat X-tra, Surgipath, Richmond, IL, USA) coated slides and stored overnight in an oven at 37 degrees Celsius. Immunohistochemistry was performed using the avidin-biotin complex system. PD-L1 (Anti-Programmed Death Ligand 1 [22C3] monoclonal mouse, code: 22C3, 1/20-1/50 dilution, Agilent Technologies, Santa Clara, CA) and AR (Anti-Androgen Receptor antibody [AR 441] monoclonal mouse, code: AR441, 1/25-1/50 dilution, ABCAM, Cambridge, UK) stainings were applied to selected sections. Finally, the slides were sealed with mounting solution. Positive control evaluation for PD-L1 and AR was performed using positively stained tissue. Tonsil tissue was used for PD-L1 and non-neoplastic breast tissue for AR. Immunohistochemical staining was evaluated by light microscopy (Olympus BX53, Tokyo, Japan) at x100, x200 and x400 magnifications. Photomicrographs were taken using a high-resolution video camera (Olympus DP 22, Japan) attached to an Olympus BX-53 model microscope (Olympus Co., Tokyo, Japan).

Immunohistochemical PD-L1 staining was evaluated on tumor tissue. The presence of complete membranous

staining in at least %1 of tumor cells was classified as positive. Cytoplasmic or incomplete membranous staining was considered as negative (Figure 2).

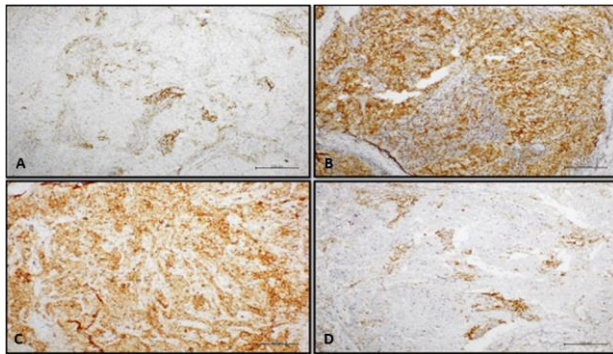


Figure 2. PD-L1 immunohistochemical complet membranous staining positive at different rates in different triple negative breast cancer sites, x100 HPF: **A** and **D**- Examples of focal staining, **B** and **C**- Examples of diffuse staining

Immunohistochemical AR staining was evaluated on tumor tissue. The percentage of stained cells was determined in 1000 tumor cells. The presence of %10 or more nuclear staining was classified as positive. Cytoplasmic or less than %10 nuclear staining was considered as negative (Figure 3).

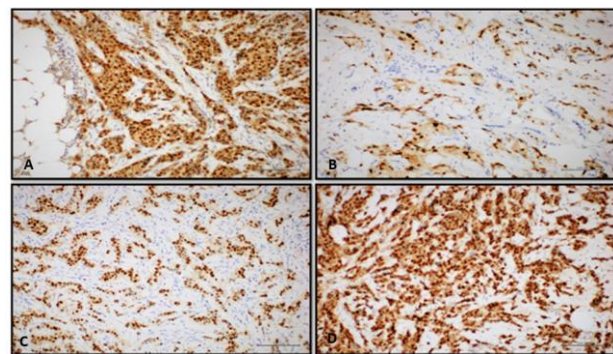


Figure 3. AR immunohistochemical nuclear staining positive at different rates in different triple negative breast cancer sites, x100 HPF: **A** and **D**- Examples of focal diffuse staining, **B** and **C**- Examples of diffuse staining.

Statistical analysis

Statistical analyses were performed using SPSS 22.0 Package Program. Descriptive statistics were performed for all parameters entered as a dataset. Descriptive statistics were expressed as number and percentage for categorical variables, minimum and maximum for numerical variables, mean and standard deviation. Due to insufficient sample size for some parameters, the Mann-Whitney U test was used for binary variables that did not show a normal distribution, and the one-way ANOVA test was used for multiple variables. Box-whisker plots were

generated for the parameters that showed statistically significant differences as a result of the Mann-Whitney U and one-way ANOVA tests. The alpha level of statistical significance was accepted as $p \leq 0.05$.

RESULTS

Clinical and histopathological findings

64 patients included in this study. The clinicopathologic features of the cases are summarized in Table 1.

Table 1. Clinicopathologic features of triple negative breast cancer cases

		Mean±SD (Minimum- Maximum)	
Age		53.47±15.044 (28-84)	
Tumor Size		2.764±1.8635 (0,4-9)	
		n	%
Surgery	Lumpectomy	46	71.9
	Mastectomy	18	28.1
Type	Right	36	56.2
	Left	28	43.8
Localization	Retro areolar	3	4.7
	Lower outer quadrant	8	12.5
	Lower inner quadrant	5	7.8
	Upper outer quadrant	38	59.4
	Upper inner quadrant	10	15.6
	quadrant		
Histologic Type	IBC, NST	49	76.5
	IMK	7	10.9
	IBC Medullary pattern	6	9.4
	ILK	1	1.6
	Asinic cell carcinoma	1	1.6
Histologic Grade	1	1	1.6
	2	21	32.8
	3	42	65.6
pT	1	35	54.7
	2	21	28.1
	3	7	10.9
	4	1	1.6
pN	0	36	56.3
	1	18	28.1
	2	7	10.9
	3	3	4.7

SD: Standard deviation, IBC: Invasive breast carcinoma, NST: No special type, IMK: Invasive micropapillary carcinoma, ILK: Invasive lobular carcinoma

At the time of diagnosis, 28 (43.8%) patients had lymph node metastasis. 40 (62.5%) patients had histopathologic lymphatic and vascular invasion. 23 (35.9%) patients had concomitant ductal carcinoma in situ (DCIS). 52 (81.3%) patients had a Ki67 index greater than 20%. 4 (6.3%) patients had tumors at surgical margins.

PD-L1 expression

Immunohistochemical PD-L1 staining was positive in 37 cases (57.8%) and negative in 27 cases (42.2%). The relationship of the cases with clinical parameters

according to PD-L1 immunohistochemical staining is summarized in the Table 2. Distant metastasis was observed in 5 PD-L1 positive cases and DCIS in 11 cases. Lymphovascular invasion was observed in 26 of 37 PD-L1 positive cases ($p=0.009$).

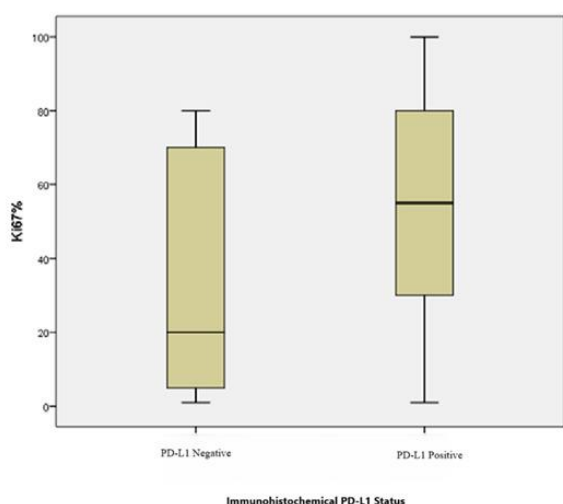


Figure 4. Association between immunohistochemical PD-L1 Status and Ki67 Proliferation index

In other words, there was a significant correlation between PD-L1 and lymphovascular invasion. In addition, the mean Ki67 of PD-L1 positive cases was 55.43, while the mean Ki67 of PD-L1 negative cases was 35.14 ($p=0.009$). A significant correlation between PD-L1 and Ki67 increase was also observed (Figure 4).

AR expression

Immunohistochemical AR staining was positive in 17 cases (26.6%) and negative in 47 cases (73.4%). The relationship of the cases with clinical parameters according to AR immunohistochemical staining is summarized in the Table 3. Lymphovascular invasion was detected in 10 (58.8%) AR positive cases ($p=0.717$), distant metastasis in 3 (17.6%) ($p=0.623$) and DCIS in 6 (35.3%) ($p=0.949$). The mean Ki67 of AR positive cases was 44.13 ± 30.84 , while that of negative cases was 42.85 ± 31.39 ($p=0.937$). There was no significant relationship between AR and clinicopathological parameters.

DISCUSSION

Currently, breast cancer management and classification is based on histological grade, stage, metastasis status as well as molecular subtyping of the tumor. Molecular subtyping is performed by immunohistochemical

Estrogen Receptor (ER), Progesterone Receptor (PR), Human Epidermal Growth Factor Receptor (HER2) and

Table 2. Association between PD-L1 positivity and clinicopathologic parameters

		Positive Mean \pm SD		Negative Mean \pm SD		p
Age		54.32 \pm 14.95		53.77 \pm 14.16		0.835
Tumor size		3.14 \pm 2.06		2.51 \pm 1.72		0.310
		n	%	n	%	
Surgery	Lumpectomy	24	64.8	22	81.5	0.7
	Mastectomy	13	35.2	5	18.5	
Localization	Retroareolar	1	2.7	2	7.4	0.947
	Lower quadrant	8	21.6	5	18.5	
	Upper quadrant	28	75.7	20	74.1	
Laterality	Right	20	54.1	16	59.2	0.526
	Left	17	45.9	11	40.8	
Histological type						
	IBC NST	29	78.4	20	74.1	0.727
	ILK	1	2.7	0	0	
	IMK	4	10.8	3	11.1	
	IBC medullary pattern	3	8.1	3	11.1	
	ACC	0	0	1	3.7	
Histologic Grade						
	1	1	2.7	0	0	0.589
	2	10	27	11	40.8	
	3	26	70.3	16	59.2	
pT	1	16	43.3	19	70.4	0.32
	2	15	40.5	6	22.2	
	3	5	13.5	2	7.4	
	4	1	2.7	0	0	
pN	0	20	54.1	16	59.2	0.64
	1	9	24.3	9	33.4	
	2	5	13.5	2	7.4	
	3	3	8.1	0	0	

SD: Standard deviation, IBC: Invasive breast carcinoma, NST: No special type, IMK: Invasive micropapillary carcinoma, ILK: Invasive lobular carcinoma, ACC: Acinic cell carcinoma

Ki67 proliferation index (8, 9). TNBC usually presents as of high-grade invasive carcinoma and has a higher rate of early recurrences, often with distant metastases and is associated with poorer prognosis. It is more common in younger premenopausal women (10). Menopause is an important risk factor for breast cancer and has different molecular characteristics. In one study, TNBCs accounted for the majority of cases under 30 years of age (9). Despite the progress about tumor biology, clinical outcomes for TBNC unfortunately remain unsatisfactory (10). In our study the youngest patient was 24 years old and the average age was about 53 years. The 6 molecular subtypes

identified by Lehmann et al. according to gene expression profile show different clinical course and different responses to treatment (3). However, response to current target therapies is still poor and the systemic treatment option is cytotoxic drugs. It is necessary to find new markers to elucidate better treatment responses and drug resistance (11). Therefore, our study evaluates PD-L1 and AR immunohistochemical staining and provides new information for classification and targeted therapies in TNBCs, a heterogeneous group.

Evasion of antitumor immunity is a hallmark of cancer development and progression. Tumors use multiple mechanisms to evade recognition by the host immune system, including expression of the negative T-cell regulatory molecule PD-L1 (12). PD-L1 is a transmembrane protein expressed on both tumor-

therapies are being investigated and developed for a variety of tumor types, including breast cancer (2). PD-L1 positivity in breast cancer is mostly associated with triple negative subtype (14). Importantly increased PD-L1 expression on the surface of TNBC cells had functional consequences on T cells including decreasing their proliferation and increasing apoptosis (12).

In a systematic analysis by Stovgaard et al. summarizing 37 studies with immunohistochemical PD-L1 application in breast cancers including different numbers of patients between 64-3916, positivity was found between 0-83%. (15). In our study PD-L1 expression was %57.8. This may be due to the size of the tumoral area evaluated in different studies, the lack of a standardized evaluation system and the use of different clones. Wimberly et al. showed that PD-L1 expression level can give 4-fold different results between different areas even in a breast cancer patient. Intratumoral heterogeneity has also been demonstrated in other organs. (14). Because of this clear heterogeneity, it is necessary to evaluate PD-L1 in resected material in blocks containing a large tumor area. In our study, the blocks with the most tumors among the resected specimens were used.

Immunohistochemical Ki67 is a proliferation marker and its application is essential especially in TNBCs as it provides information about prognosis and survival (11). In our study there was a significant correlation between PD-L1 positivity and Ki67 proliferation index ($p=0.009$). Many studies in the literature have found a positive correlation between PD-L1 immunohistochemical positivity and Ki67 proliferation index (6, 11, 16, 17). Lymphovascular invasion is the pathway of tumor spread, and it shows aggressive tumor behavior by causing tumors to differentiate between adjacent lymphatics and blood vessels (18). In our study there was also a significant association between PD-L1 expression and lymphovascular invasion ($p=0.009$). Various studies have investigated the relationship between PD-L1 and prognosis, but different results have been obtained. The prognostic value of PD-L1 is not clear (11, 15). In our study, as PD-L1 positivity increased, Ki67 proliferation index and lymphovascular invasion increased. This suggests that PD-L1 positivity has a poor prognostic value. Therefore, the targeted treatment regimen for this PD-L1-positive subset of TNBC is even more important.

Another promising and potential marker in TNBCs is the AR (11). AR is a type 1 nuclear receptor and acts as an intranuclear transcription factor responsible for gene expression. It is present in numerous tissues in both sexes,

Table 3. Association between AR positivity and clinicopathologic parameters

		Positive Mean \pm SD		Negative Mean \pm SD		P
Age		54.32 \pm 14.95		53.77 \pm 14.16		
Tumor size		3.14 \pm 2.06		2.51 \pm 1.72		
		n	%	n	%	
Surgery	Lumpectomy	11	64.8	35	74.5	0.447
	Mastectomy	6	35.2	12	25.5	
Localization	Retroareolar	1	5.9	2	4.3	0.126
	Lower quadrant	1	5.9	15	31.9	
	Upper quadrant	15	88.2	30	63.8	
Laterality	Right	13	76.5	23	48.9	0.072
	Left	4	23.5	24	51.1	
Histological type	IBC NST	15	88.2	34	72.3	0.202
	ILK	-	-	1	2.1	
	IMK	2	11.8	5	10.6	
	IBC	-	-	6	12.9	
	medullary pattern ACC	-	-	1	2.1	
Histologic Grade	1	1	5.9	-	-	0.413
	2	6	35.2	15	31.9	
	3	10	58.9	32	68.1	
pT	1	12	70.6	23	48.9	0.265
	2	3	17.6	18	38.2	
	3	1	5.9	6	12.9	
	4	1	5.9	-	-	
pN	0	11	64.8	25	53.2	0.723
	1	3	17.6	15	31.9	
	2	3	17.6	4	8.5	
	3	-	-	3	6.4	

SD: Standard deviation, IBC: Invasive breast carcinoma, NST: No special type, IMK: Invasive micropapillary carcinoma, ILK: Invasive lobular carcinoma, ACC: Acinic cell carcinoma

infiltrating lymphocytes and cancer cells. The binding of PD-L1 on tumor cells to PD-1 on T lymphocytes is one of the potential mechanisms for tumor escape from the immune system (13). Immune-checkpoint blockade

including bone, liver, brain, and breast (18). While other nuclear steroid hormone receptors, ER and PR, are widely used, the biological role of AR is still under investigation (19). The expression of the antigen AR has been documented in approximately 70–90% of breast cancers. Furthermore, the expression of this antigen varies between 10% and 50% in TNBC (20). AR is thought to have an inhibitory effect in luminal subtype breast cancer but stimulates tumor growth in TNBC. (21). Although there is evidence for AR in breast cancer pathogenesis, its role in TNBC is not clear (19). Although AR expression can be expressed in all molecular subtypes, it is mainly characteristic of the LAR subtype. It is expressed in 10-90% of TNBCs (11). In studies using a cutoff of 10% for AR positivity, this positivity was found between 17.1-38% (22-26). In this study we used a cutoff of 10% and found %26,6 of TNBCs expressed AR, which was in line with previous reports. The absence of a universally applicable principle is attributable to the considerable heterogeneity observed in the results of diverse studies, thereby giving rise to an ambiguous relationship between AR and TNBC (21).

AR is expressed in two types of mammary epithelial cells. One is luminal epithelial cells and the other is metaplastic apocrine cells. In the latter, the cells are mostly components of fibrocystic disease and most of them are ER and PR negative. In the former it commonly expressed with ER, PR. Although tumors arising from these different origins have common AR expression, their morphology and treatment response are likely to be different (19). According to the literature, AR positivity in several studies has been associated with less aggressive biological behavior, such as lower clinical stage, lower histologic grade, lower mitosis count and lymphovascular invasion (19, 25, 27, 28). Numerous other studies have found significant associations between AR expression and poor prognostic clinicopathological parameters such as large tumor diameter, high tumor grade, high clinical stage, high number of lymph node metastases (27, 29-32). However, the results from our study showed no statistical significance between clinical or pathological parameters and AR status. These include the histological subtype, laterality, tumor localization, tumor grade, tumor size, tumor stage, nodal status, Ki-67 score and lymphovascular invasion. The differences seen in the results are clearly related to the different methods used. These differences are likely due to the cutoff used, the number of patients, and the histopathologic scoring of AR. However, many studies in the literature have shown that there is no association between clinical and pathologic parameters and AR, which is consistent with our study (11, 18, 21, 33).

In a study of 125 patients, immunohistochemistry for AR and PD-L1 in TNBC was performed and a significant relationship was found between them. High tumor and nuclear grade was observed in cases where they were simultaneously expressed, while in cases where they were negative, an association with metastasis was observed (11). In another study of 197 patients, PD-L1 was found to be 3 times more positive in AR-positive patients (13). In our study, no significant correlation was found between AR and PD-L1. This may be related to the small number of patients compared to the above mentioned studies.

CONCLUSION

Response to current target therapies in TNBC is poor and the systemic treatment option is cytotoxic drugs. Molecular heterogeneity has led to the lack of FDA-approved targeted therapies for TNBC. It is necessary to find new markers to elucidate better treatment responses and drug resistance. Therefore, our study provides new information for targeted therapies by evaluating PD-L1 and AR immunohistochemical staining. Immune-checkpoint blockade therapies are being investigated and developed for a variety of tumor types, including breast cancer. PD-L1 positivity in breast cancer is mostly associated with triple negative subtype. Our study highlighted that due to intratumoral heterogeneity, PD-L1 should be evaluated from blocks containing large tumor areas. There was a significant correlation PD-L1 positivity with Ki67 proliferation index ($p=0.009$), and lymphovascular invasion ($p=0.009$). PD-L1 positive cases appear to be associated with a poor prognosis and thus associated with lower overall survival. However, this disadvantage can be overcome with monoclonal antibody therapies directed against PD-L1. AR is thought to have an inhibitory effect in luminal subtype breast cancer but stimulates tumor growth in TNBC. Many studies in the literature have shown that there is no association between clinical and pathologic parameters and AR, which is consistent with our study. However, there are conflicting studies and the relationship between AR and TNBC needs to be clarified. In TNBCs, PD-L1 and AR are two important markers that will determine the appropriate group for treatment and prognosis, and standardization in studies and evaluation in larger cohorts is essential.

Acknowledgments

None

Authorship contributions

All authors contributed to the study conception and design. Material preparation, data collection and analysis

were performed by Büşra Ekinici. The first draft of the manuscript was written by Büşra Ekinici. Finding and designing the topic of the project, statistics and control was done by Nesibe Kahraman Çetin, İbrahim Halil Erdoğan, İbrahim Meteoglu. All authors commented on previous versions of the manuscript. All authors read and approved the final manuscript.

Data availability statement

The data that support the findings of this study are available on request from the corresponding author.

Declaration of competing interest

The authors have no relevant financial or non-financial interests to disclose.

Ethics

This study was approved by the Ethics Committee for Noninvasive Clinical Trials of Aydın Adnan Menderes University. Approval number 2018/1343.

Funding

This study was supported by Aydın Adnan Menderes University Scientific Research Projects Unit, grant number TTF-18032.

REFERENCES

- Zhao S, Ma D, Xiao Y, Li XM, Ma JL, Zhang H, Xu XL, Lv H, Jiang WH, Yang WT, Jiang YZ, Zhang QY, Shao ZM. Molecular Subtyping of Triple-Negative Breast Cancers by Immunohistochemistry: Molecular Basis and Clinical Relevance. *Oncologist*. 2020;25(10):e1481-e91.
- Author AB AC, Author EF. WHO Classification of Tumours Editorial Board. Breast tumours [Internet]. Lyon (France): International Agency for Research on Cancer; 2019. Available from: <https://tumourclassification.iarc.who.int/chapters/32>.
- Lehmann BD, Jovanović B, Chen X, Estrada MV, Johnson KN, Shyr Y, Moses HL, Sanders ME, Pietenpol JA. Refinement of triple-negative breast cancer molecular subtypes: implications for neoadjuvant chemotherapy selection. *PloS one*. 2016;11(6):e0157368.
- Li F, Ren Y, Wang Z. Programmed death 1 Ligand 1 expression in breast cancer and its association with patients' clinical parameters. *Journal of cancer research and therapeutics*. 2018;14(1):150-4.
- Muenst S, Schaerli A, Gao F, Däster S, Trella E, Drieser R, Muraro M, Zajac P, Zanetti R, Gillanders W. Expression of programmed death ligand 1 (PD-L1) is associated with poor prognosis in human breast cancer. *Breast cancer research and treatment*. 2014;146:15-24.
- Angelico G, Broggi G, Tinnirello G, Puzzo L, Vecchio GM, Salvatorelli L, Memeo L, Santoro A, Farina J, Mulé A. Tumor infiltrating lymphocytes (TILs) and PD-L1 expression in breast cancer: a review of current evidence and prognostic implications from pathologist's perspective. *Cancers*. 2023;15(18):4479.
- Rampurwala M, Wisinski KB, O'Regan R. Role of the androgen receptor in triple-negative breast cancer. *Clinical advances in hematology & oncology: H&O*. 2016;14(3):186.
- Erdoğan İH, Gürel D. Evaluation of Somatic PIK3CA Mutations Detected by Next-generation Sequencing in Breast Cancer Cases. *Meandros Medical & Dental Journal*. 2023;24(4).
- Erdoğan İH, Orenay-Boyacıoğlu S, Boyacıoğlu O, Gürel D, Akdeniz N, Meteoglu I. Variation Analysis in Premenopausal and Postmenopausal Breast Cancer Cases. *Journal of Personalized Medicine*. 2024;14(4):434.
- Vagia E, Mahalingam D, Cristofanilli M. The Landscape of Targeted Therapies in TNBC. *Cancers (Basel)*. 2020;12(4).
- Medić-Milijić N, Jovanović I, Nedeljković M, Marković I, Spurnić I, Milovanović Z, Ademović N, Tomić T, Tanić N, Tanić N. Prognostic and Clinical Significance of PD-L1, EGFR and Androgen Receptor (AR) Expression in Triple-Negative Breast Cancer (TNBC) Patients. *Life (Basel)*. 2024;14(6).
- Mittendorf EA, Phillips AV, Meric-Bernstam F, Qiao N, Wu Y, Harrington S, Su X, Wang Y, Gonzalez-Angulo AM, Akcakanat A. PD-L1 expression in triple-negative breast cancer. *Cancer immunology research*. 2014;2(4):361-70.
- Tung N, Garber JE, Hacker MR, Torous V, Freeman GJ, Poles E, Rodig S, Alexander B, Lee L, Collins LC, Schnitt SJ. Prevalence and predictors of androgen receptor and programmed death-ligand 1 in BRCA1-associated and sporadic triple-negative breast cancer. *NPJ Breast Cancer*. 2016;2:16002.
- Wimberly H, Brown JR, Schalper K, Haack H, Silver MR, Nixon C, Bossuyt V, Pusztai L, Lannin DR, Rimm DL. PD-L1 Expression Correlates with Tumor-Infiltrating Lymphocytes and Response to Neoadjuvant Chemotherapy in Breast Cancer. *Cancer Immunol Res*. 2015;3(4):326-32.
- Stovgaard ES, Dyhl-Polk A, Roslind A, Balslev E, Nielsen D. PD-L1 expression in breast cancer: expression in subtypes and prognostic significance: a systematic review. *Breast cancer research and treatment*. 2019;174:571-84.
- Botti G, Collina F, Scognamiglio G, Rao F, Peluso V, De Cecio R, Piezzo M, Landi G, De Laurentiis M, Cantile M, Di Bonito M. Programmed Death Ligand 1 (PD-L1) Tumor Expression Is Associated with a Better Prognosis and Diabetic Disease in Triple Negative Breast Cancer Patients. *Int J Mol Sci*. 2017;18(2).
- Bae SB, Cho HD, Oh MH, Lee JH, Jang SH, Hong SA, Cho J, Kim SY, Han SW, Lee JE, Kim HJ, Lee HJ. Expression of Programmed Death Receptor Ligand 1 with High Tumor-Infiltrating Lymphocytes Is Associated with Better Prognosis in Breast Cancer. *J Breast Cancer*. 2016;19(3):242-51.
- Dubrava AL, Kyaw PSP, Newman J, Pringle J, Westhuyzen J, La Hera Fuentes G, Shakespeare TP, Sakalkale R,

- Aherne NJ. Androgen Receptor Status in Triple Negative Breast Cancer: Does It Correlate with Clinicopathological Characteristics? Breast Cancer (Dove Med Press). 2023;15:359-71.
19. Rampurwala M, Wisinski KB, O'Regan R. Role of the androgen receptor in triple-negative breast cancer. Clin Adv Hematol Oncol. 2016;14(3):186-93.
20. Gerratana L, Basile D, Buono G, De Placido S, Giuliano M, Minichillo S, Coinu A, Martorana F, De Santo I, Del Mastro L, De Laurentiis M, Puglisi F, Arpino G. Androgen receptor in triple negative breast cancer: A potential target for the targetless subtype. Cancer Treat Rev. 2018;68:102-10.
21. Prutianu I, Giușcă SE, Gafton B, Chifu MB, Terinte C, Antonescu A, Popovici L, Căruntu ID. Triple-negative breast cancer: from classical clinicopathological features to androgen receptor profile. Rom J Morphol Embryol. 2024;65(2):209-16.
22. Zakaria F, El-Mashad N, Mohamed D. Androgen receptor expression as a prognostic and predictive marker in triple-negative breast cancer patients. Alexandria journal of medicine. 2016;52(2):131-40-40.
23. Payandeh M, Shazad B, Madani S, Ramezani M, Sadeghi M. Androgen Receptor Expression and its Correlation with Other Risk Factors in Triple Negative Breast Cancers: a Report from Western Iran. Asian Pac J Cancer Prev. 2016;17(7):3321-4.
24. Lyalkin SA, Verevkina NO, Alekseyenko OO, Syvak LA. Prognostic role of androgen receptor expression in patients with metastatic triple negative breast cancer. Exp Oncol. 2020;42(2):140-3.
25. Jam S, Abdollahi A, Zand S, Khazaeipour Z, Omranipour R, Najafi M. Androgen Receptor Expression in Triple-Negative Breast Cancer. Archives of Breast Cancer. 2019;92-5. Available from: <https://www.archbreastcancer.com/index.php/abc/article/view/249>.
26. Adamo B, Ricciardi GRR, Ieni A, Franchina T, Fazzari C, Sanò MV, Angelico G, Michele C, Tuccari G, Adamo V. The prognostic significance of combined androgen receptor, E-Cadherin, Ki67 and CK5/6 expression in patients with triple negative breast cancer. Oncotarget. 2017;8(44):76974.
27. Teoh PY, Tan GC, Mahsin H, Wong YP. Androgen receptor expression in triple negative breast carcinoma and its association with the clinicopathological parameters. Malays J Pathol. 2019;41(2):125-32.
28. Riaz N, Idress R, Habib S, Lalani EN. Lack of Androgen Receptor Expression Selects for Basal-Like Phenotype and Is a Predictor of Poor Clinical Outcome in Non-Metastatic Triple Negative Breast Cancer. Front Oncol. 2020;10:1083.
29. Sunar V, Dogan HT, Sarici F, Ates O, Akin S, Baspinar B, Aksoy S, Altundag K. Association between androgen receptor status and prognosis in triple negative breast cancer. J BUON. 2018;23(5):1325-30.
30. Liu Y-X, Zhang K-J, Tang L-L. Clinical significance of androgen receptor expression in triple negative breast cancer-an immunohistochemistry study. Oncology letters. 2018;15(6):10008-16.
31. Cabezas-Quintario M, Zenzola V, Arguelles M, Perez-Fernandez E. Androgen receptor as prognostic marker in triple-negative breast cancer patients. J Med Surg Pathol. 2018;3(4):1-6.
32. Astvatsaturyan K, Yue Y, Walts AE, Bose S. Androgen receptor positive triple negative breast cancer: Clinicopathologic, prognostic, and predictive features. PLoS One. 2018;13(6):e0197827.
33. Asano Y, Kashiwagi S, Goto W, Tanaka S, Morisaki T, Takashima T, Noda S, Onoda N, Ohsawa M, Hirakawa K. Expression and clinical significance of androgen receptor in triple-negative breast cancer. Cancers. 2017;9(1):4.

Research Article

TEMPERATURE CHANGE IN THE PULP CHAMBER INDUCED BY DIFFERENT LIGHT CURING UNITS IN SIMULATED DEEP CAVITIES

 Yağmur KILIÇ^{1*},  Mustafa Mert TULGAR¹

¹Department of Endodontology, Faculty of Dentistry, Izmir Katip Çelebi University, Izmir, TURKIYE

*Correspondence: yagmursati@icloud.com

ABSTRACT

Objective: The objective of this study was to evaluate the effect of various types of photopolymerization devices on the temperature of the pulp chamber during the adhesive bonding phase.

Materials and Methods: To this purpose, cavities with a mesiodistal diameter of 5 mm, a buccolingual diameter of 3.5 mm, and a residual dentin thickness of 1.2 mm at the cavity base were prepared. Polymerization lights were applied for 20 seconds using three different devices. The temperature change within the pulp chamber was quantified using a thermocouple, with data collected at 10 and 20 seconds utilized for assessment. The mean intra-pulp temperature in the O-Light, Deepcure-L, and Valo groups at the 10th second was 39.9°C, 41.1°C, and 38.7°C and at the 20th second, had temperatures of 42.4°C, 44.3°C, and 40.4°C, respectively.

Result: A statistically significant difference was observed between the Deepcure-L and Valo groups ($p < .01$) in terms of maximum temperature, increase in pulp chamber temperature, and temperature at the 10th and 20th seconds. The observed changes in pulp chamber temperature between the groups, irrespective of light transmission type, are consistent with the power output of the devices, expressed in mW/cm². All the groups yielded a temperature increase above the limit which has been described critical.

Conclusion: During adhesive bonding phase, lower mW/cm² devices could be preferred in cases where the remaining dentin thickness is reduced.

Keywords: Pulp chamber temperature, Monowave LCU, Polywave LCU, in-vitro

Received: 31 January 2025

Revised: 20 March 2025

Accepted: 21 April 2025

Published: 23 June 2025



Copyright: © 2025 by the authors. Published by Aydın Adnan Menderes University, Faculty of Medicine and Faculty of Dentistry. This article is openly accessible under the Creative Commons Attribution-NonCommercial 4.0 International (CC BY-NC 4.0) License.

INTRODUCTION

Clinicians should be aware of the potential damage to the pulp that can occur during restorative procedures (1). These damages are usually caused by chemical, thermal, and mechanical effects. One primary reason for this is the use of photopolymerization devices during restorative procedures, which may damage the pulp cells due to thermal rather than mechanical effects. During the photopolymerization of resin-based materials, temperature changes of up to 20°C were observed within the material (2–4).

The temperature increase within the pulp is constrained by the isolation provided by the tooth's hard tissues. However, the iatrogenic reduction in the thickness of the dental hard tissues may contribute to the subsequent increase in temperature within the pulp. This makes the pulp prone to thermal damage, particularly in deep carious cavities, as well as cases of direct and indirect pulp capping. In addition to the remaining dentin thickness, the type and thickness of the restorative material used, the power of the photopolymerization device, polymerization time, and the polymerization mode are effective in determining the temperature change in the pulp (5). In a study on primates, Zach and Cohen demonstrated that an increase of 5.5°C in the pulp resulted in necrosis in 15% of the teeth, while increases of 11°C and 16°C caused necrosis in 60% and 100% of the teeth, respectively (6). In contrast, a study on human teeth indicated that a temperature increase of 11.2°C for 2 or 3 minutes did not permanently damage the dental pulp (7).

Many different methodologies have been used to study the thermal changes caused by the Light Curing Unit (LCU) in the pulp. The two most commonly used methods for temperature monitoring are the placement of a thermocouple tip under the resin material or in the pulp chamber of the extracted tooth. The design where the thermocouple tip is placed directly under the restorative material does not reflect the temperature absorption capacity of the tooth hard tissues and thus cannot provide information about the temperature change in the pulp, ultimately making the experiment inadequate to mimic clinical conditions (8). The configuration in which the temperature-measuring tip is situated within the pulp chamber more closely resembles clinical conditions, but it is challenging to implement, and the variability of the remaining dentin thickness further complicates the system (9,10).

After years of using halogen, plasma arc, and argon laser light devices, the second generation of LCUs with an emittance range of 500-1500 mW/cm² was introduced in 2002 (11,12). In 2004, high-performance LCUs reaching 5000 mW/cm² were developed utilizing LED technology (13,14). Although LED technology, which is a cold light source, can provide the necessary emittance and a wavelength of 400-500 nm (nanometers) for polymerization without reaching elevated levels, studies have indicated that temperature increases may cause irreversible damage to the pulp. LED units utilize light guides, either a fiber pipe or a diffuser lens. Fiber pipes, known as fiber guides, are typically found in single-peak (monowave) LCUs that contain a single LED. Diffuser lenses are used in the newer multiple-peak (polywave) units, which feature multiple LEDs to encompass all wavelengths needed for resin polymerization. The LCUs included in the study are the O-Light (DTE Guilin, China) at 1000-1200 mW/cm² with 420nm-490nm wavelength spectrum, the Deepcure-L (3 M ESPE, USA) at 1470 mW/cm² with 430-480 nm wavelength spectrum, and the Valo(Ultradent, USA) at 980 mW/cm² with 385–515 nm wavelength spectrum. Among these LCUs, the Deepcure-L represents single-peak fiber-guided LED models, while the O-Light and Valo are multi-peak LED devices emitting through a lens (Figure 1).



Figure 1. Fiber guided Deepcure-L(A) and polywave O-Light(B) ve Valo(C)

There is limited data on pulp chamber temperature change in cases of reduced residual dentin thickness during the adhesive polymerization phase. The objective of this in vitro study was to evaluate the effect of various modern photopolymerization devices on pulp temperature during

the adhesive bonding phase. The H0 hypothesis stated that there would be no significant difference in the temperature increase of the pulp chamber among different LCUs during light irradiation.

MATERIALS AND METHODS

Approval for this study was obtained from the local ethics committee. The entire study was conducted by the Helsinki Declaration. Data from the study with a similar methodology were used to determine the sample size (15). The sample size was calculated using G*Power software with an alpha level of 0.05 and a beta level of 0.95, resulting in a sample size of 20. Twenty maxillary first molars, extracted for periodontal and prosthodontic reasons no more than six months prior, were included in the study. All samples were stored in a 0.5% chloramine-T solution. The included teeth had mesiodistal diameters between 9.1 and 10.3 mm and buccolingual diameters between 9.7 and 11.7 mm. The occlusal surface of the teeth is reduced for the distance from the cavity surface and cavity floor to be $4.0\text{mm} \pm 0.2\text{mm}$. X-rays were obtained from all included teeth, and teeth with a narrowed pulp chamber were excluded from the study. Teeth that met the inclusion criteria were decoronated at the enamel cementum level (CEJ) or 1 mm below the CEJ using a 0.14 mm thick metal separator. Following decoronation, the pulp chamber was cleaned with an ultrasonic scaling device (P5 Newton; Satelec, Acteon, France) and then washed with 2.5% NaOCl to remove necrotic pulp tissue. To facilitate direct access to the pulp chamber for the temperature-measuring tip of the thermocouple device, the palatal root was shortened to 4 mm, and a straight path was obtained with a #5 Gates Glidden drill. Class 1 cavities with a mesiodistal diameter of 5 mm, a buccolingual diameter of 3.5 mm, and a dentin thickness at the base of 1.2 mm were prepared on the crown piece. The residual dentin thickness was then measured along the cavity floor at 1 mm intervals with a digital caliper.

The temperature change within the pulp chamber was quantified using a CE-licensed and data-logging thermometer (Tasi TA612C, Suzhou, China) via a K-type thermocouple with 0.5 mm diameter tip by 1-second intervals. The thermometer's integrity was confirmed using another calibrated thermometer (Lutron TM-917, Lutron Electronic Enterprise Co. Taiwan) from the University's Central Labs. The thermocouple utilized was capable of measuring temperature changes between -20°C and $+371^{\circ}\text{C}$ with a resolution of 0.1°C and accuracy of $\pm 0.2\%$ + 0.7°C . To facilitate heat transfer, the relevant area for the thermocouple tip in the ceiling of the pulp chamber was

coated with a thin thermal paste with $14,2\text{ W/mK}$ thermoconductivity (Kryonaut, Thermal Grizzly, Lippstadt, Germany). The thermocouple tip was then inserted through the palatal root. The crown piece was secured in its original position on the root using a flowable composite. The root tip was sealed with a gingival resin barrier to maintain the position of the thermocouple along the palatal root and within the pulp chamber. Periapical radiographs were obtained to confirm the position of the thermocouple tip within the setup. The teeth were secured in moist floral foam for oral environment simulation. The internal pulp chamber temperature is regulated at 35°C by the manual dripping of hot water (Figure 2). Before the application, the mW/cm^2 values of all light-curing units were measured three times using a digital power meter (Thorlabs PM130D, USA). During the measurement process, the batteries were maintained at their maximum capacity. For 450-500 nm wavelength, Polywave O-Light had 500 mW/cm^2 , Monowave Deepcure-L had 650 mW/cm^2 , and Polywave Valo had 425 mW/cm^2 average output. These suboptimal values were considered normal given that the optical tip of the testing device is encased within a housing structure with a distance between the LCU tip. Seeing that the observed output ratio between the LCUs was found to be consistent with the manufacturer's specifications, LCUs are found stable for testing.

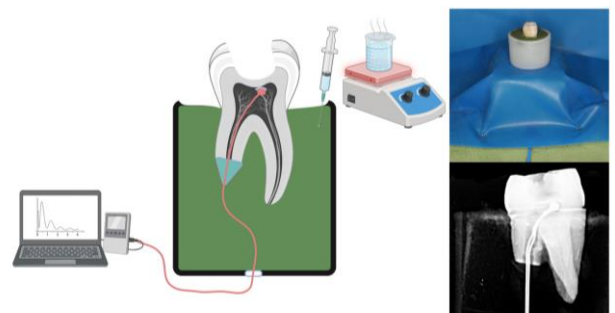


Figure 2. The set-up (upper-right) and pulp chamber temperature experiment illustration (left). Radiographic control for the position of thermocouple tip (lower-right). Created with BioRender.

Polywave O-Light ($1000\text{--}1200\text{ mW/cm}^2$), Monowave Deepcure-L with 1470 mW/cm^2 with fiber conduction, and Polywave Valo with 980 mW/cm^2 emittance power were utilized in 20 samples, respectively, and a total of 60 measurements were conducted. The LCUs are maintained in the same location and angle by a holder device for all the samples, and the irradiation is applied with contact between the LCU and the occlusal cavity. No protective sheath was used with the LCUs. The maximum temperature and the temperature values at the 10th and 20th

seconds were analyzed with the SPSS 20.0 software package, with a significance threshold of 5%. The normality of all collected data was investigated via the Shapiro-Wilk test. The maximum temperature and temperature values at the 10th and 20th seconds among the LCU, which followed a normal distribution, were analyzed using ANOVA. Since the variances were not homogeneously distributed, a post hoc Games-Howel test was performed to investigate differences among the groups. The adjusted significance level was set at 0.01.

RESULTS

The temperature profiles of the samples in the three groups are presented in Figure 1. The mean and maximum intra-pulp, as well as the temperatures at 10th and 20th seconds for each group, are presented in Table 1. The chart of the mean intra-pulp temperature at 20th seconds for the O-Light, Deepcure-L, and Valo groups was 42.4°C, 44.3°C, and 40.4°C, respectively. The mean intra-pulp temperature at 10th seconds was 39.9°C, 41.1°C, and 38.7°C, respectively. The highest intra-pulp temperature data at 10th and 20th seconds were obtained in the Deepcure-L group. Subsequently, the O-Light and Valo groups exhibited the lowest and highest temperatures, respectively. The distribution of the readings is shown in Figure 3. LCUs tested have induced over 5.5°C of difference in all experimental groups, while the 20th second mean temperature of the Valo group remained below the critical threshold of 41°C. The difference between the Deepcure-L and O-Light groups, as well as the difference between the Valo and O-Light groups, in terms of maximum temperature, increase in intra-pulp temperature, and temperature at 10th and 20th seconds was not statistically significant ($p > 0.01$). However, a statistically significant difference was observed between

the Valo group and the Deepcure-L groups ($p < 0.01$), indicating that the Valo group generated less heat in the pulp chamber.

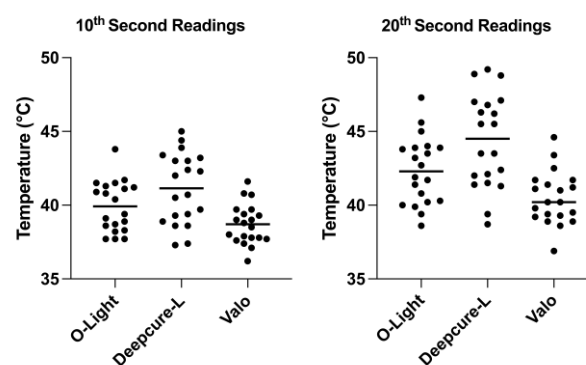


Figure 3. 10th and 20th second readings with means

DISCUSSION

A substantial number of large dentinal tubules are exposed during preparation. The odontoblast extensions within the tubules and the damage to the pulp are caused by several factors, including pressure, the type of cooling, the design of the bur, temperature increase, degree of circulation, dehydration, and so forth. Schuchard (16) and Sato (17) reported that temperature increases may cause structural changes in hard dental tissues and damage to the dental pulp. Especially in cases where the dentin is thin and there is no protective layer on the pulp wall, it is expected that there will be a high-temperature increase in the pulp during the bonding phase for resin materials. Based on the results of the study, the H0 hypothesis was rejected.

To efficiently simulate the closed environment of the pulp chamber and to ensure a clean thermoconductivity by cleaning the pulp remnants within the pulp chamber, the horizontally split crowns were used in the study. Also with this design, a simple gingival resin barrier application to the retrograde palatal entrance was sufficient to retain the K-type thermocouple line and to provide a passive guide to the pulp-dentin junction without the use of adhesive for the thermocouple tip, which would interfere with thermoconductivity. The method we used in our study is similar to the method used by Öztürk et al. (15).

It is established that adhesive materials are toxic to odontoblasts and pulp cells when in direct contact (18). It has been previously demonstrated that at a dentin thickness of 0.7mm, the permeability is significantly reduced in human dentin discs (19). In light of these

Table 1. Minimum, maximum, mean±SD for the pulp chamber temperature of the three different light-curing units tested. The letters a,b indicate significant difference ($p < 0.01$) in pairwise comparisons.

Device	Maximum Temperature	10 th Second	20 th Second
	Max	Mean ± SD	Min Max Mean ± SD
O'light DTE	47.3°C	42.7°C ± 2.3 ^{ab}	37.7°C 43.9°C 39.7°C ± 1.7 ^b
DeepCure L	49.2°C	44.3°C ± 2.1 ^a	37.3°C 45.0°C 41.7°C ± 2.3 ^{ab}
Valo	44.6°C	40.4°C ± 2.3 ^b	36.2°C 41.5°C 38.7°C ± 1.3 ^b
p-value		p=0.00	p=0.00

findings, the lowest threshold for residual dentin thickness in our study is considered to be 0.7mm, beyond which the tooth does not require a biomaterial liner. This makes direct bonding and direct exposure to the LCU clinically relevant. In an in vivo study on tertiary dentin production, Murray et al. reported that tertiary dentin production of 1.5 mm residual dentin thickness samples was 10.6% of 0.5 mm thickness samples. Additionally, the repair response of the pulp was observed to decrease significantly after 1.2 mm residual dentin thickness. The results of this study, when considered alongside those of the aforementioned studies, indicate that the threshold for adhesive bonding without the use of a biomaterial is 1.2 mm. Accordingly, the cavity depths were adjusted following this residual dentin standard (20).

Dental hard tissues, which have lower thermal conductivity and permeability compared to the pulp, play an important role in maintaining the vitality of the pulp (21). A greater thickness of dental hard tissue results in a more substantial insulating effect, which serves to restrict the extent of the intra-pulp temperature increase (21,22). For these reasons, the mesiodistal and buccolingual lengths of the teeth included in our study were selected to be similar. Following the preparation of the cavities, the remaining dentin thicknesses were measured with the assistance of calipers to ensure comparable heat conductivity and permeability due to hard tissues across all samples. The use of three distinct LCUs in each sample ensured that any potential differences in our study results were attributed to the inherent structural characteristics of the samples themselves.

Research has indicated that the basal temperature within the pulp ranges from 34° to 35°C. It has been demonstrated that temperatures exceeding 42.5° to 43°C are sufficient to induce irreversible damage to the pulp, accompanied by a significant increase in reactive blood pressure (21,23,24). All LCUs tested induced a temperature increase exceeding 5.5°C, the threshold for irreversible changes, while only the Valo group remained below the 11°C limit, which induces pulp necrosis in 60% of teeth (6). While an increase in intrapulpal temperature to these levels does not invariably result in irreversible pulpal damage in all cases, the potential for damage may be heightened in the presence of pre-existing pulpal inflammation and limited perfusion. It is also noteworthy that even in cases without permanent damage, the heightened patient sensitization induced by high-temperature changes may increase the clinician's tendency to misdiagnose the treatment as a failed restoration. The findings of this study indicate that the utilization of low-powered polywave units, such as

Valo, could reduce this likelihood by providing a lower increase in pulp chamber temperature in similar deep cavities tested. To emulate the basal temperature observed in clinical settings, the temperature of the setup and the sample was maintained at 35°C throughout the study phases. While microcirculation contributes to regulating intrapulpal temperature, one study showed that its overall impact can be considered negligible due to the low blood volume (21).

In studies, the temperature change in the pulp during the use of LCU has generally been investigated at the time of composite polymerization; however, it has not been investigated in the polymerization of adhesive systems (23,25). The results of our study indicate that the highest temperature increase was observed in the Deepcure-L, O-Light, and Valo groups, in that order. The Deepcure-L device operates at a power level of 1470 mW/cm², while the O-Light and Valo devices operate at 1000-1200 mW/cm² and 980 mW/cm², respectively. It is noteworthy that the preliminary power testing of the O-Light compared to the other manufacturers pointed to a result near 1000 mW/cm² output, which is consistent with, but near the lower limit of the specifications declared by the manufacturer. The intra-pulp temperature changes observed between the groups, regardless of the light transmission type, are consistent with the power of the devices, expressed in mW/cm². The findings of our study indicate that there was no statistically significant difference between the O-Light and Deepcure-L groups, despite the differences in light transmission types and the similarities in power levels. Our results demonstrate that the increase in pulp chamber temperature is not contingent on the type of light transmission (fiber or lens) but is instead directly proportional to the power of the device utilized. To assure pulpal health in the adhesive bonding phase where the remaining dentin is considered thin, a lower mW/cm² LCU can be preferred if multiple devices are present. If there is only one high-output device in a clinical situation, such as the single-peak high mW/cm² group, it is possible to leave a small gap between the LCU tip and the teeth, which will serve to reduce both the emittance and the thermal effect. Concerning this idea, it may be of interest to consider the results of a study that stated a reduction in light irradiance of approximately 28% and a reduction in the degree of conversion of adhesive by approximately 5% with a dentin-LCU distance increase from 4.6 mm to 6.9 mm (26).

Polywave curing units (Valo and O-Light) exhibit a lack of emittance uniformity due to variations in light distribution from different LEDs, resulting in unit-specific hot spots of

high emittance based on the LED chip locations. In contrast, fiber-guided monowave units (Deepcure-L) concentrate emittance primarily on the center beams. The non-uniform energy distribution in polywave curing units is believed to contribute to heterogeneous curing (27). However, there is no clear consensus in the literature regarding the effects of polywave and monowave LCU units on composite polymerization (28–31). Based on our findings, the higher emittance and center beam-focused design of the fiber-guided Deepcure-L unit led to greater temperature increases within the pulp chamber. Therefore, clinicians may consider using these high mW/cm² center beam-focused devices in procedures requiring maximum light penetration, such as bulk composite curing, rather than during the adhesive bonding phase.

Existing studies indicate that photocuring of bonding agents in deep cavities can lead to a significant temperature increase on the dentin surface which is in line with the results of our study (32–34). These studies emphasized the importance of clinicians being mindful of the potential risk of thermal damage to the pulp, particularly when using high-output light sources. No dentin conditioning or adhesive was used on the samples. We decided not to use adhesives in a clinical setting where direct bonding is required because repeated application and removal of the adhesive layer would distort the surface, compromise sample standardization and ultimately affect the readings.

The limitations of this study include its in vitro design, the lack of long-term effects assessment, and the absence of histological analysis. Conducting the study in an in vitro setting does not fully replicate the complex biological and thermal regulation mechanisms found in vivo, particularly pulpal blood flow, which plays a crucial role in heat dissipation. Additionally, the study focused solely on immediate temperature changes during polymerization, without evaluating potential long-term effects on pulpal health, such as delayed inflammation or necrosis.

CONCLUSION

The tested monowave group (Deepcure-L) induced a significantly higher increase than a tested polywave (Valo) group, therefore H0 hypothesis was rejected. The findings of our study indicate that heightened awareness of elevated intra-pulpal temperatures in cases with the thinnest dentin layer may enhance treatment outcomes and pulpal survival. LCUs with high output (>1000 mW/cm²) should be used with caution and it is essential to

consider that the generated heat using LCUs require supplementary protective measures to ensure the maintenance of pulpal health. During adhesive bonding phase, lower mW/cm² devices could be preferred in cases where the remaining dentin thickness is reduced. Further studies are required to gain a comprehensive understanding of the thermal damage caused by LCU devices, utilizing both in vivo and ex vivo functional tissue analysis in conjunction with histology and clinical outcomes.

Acknowledgments

The authors deny any conflicts of interest related to this study.

Authorship contributions

First Author: Concept, Design, Analysis, Literature Search, Writing; Second Author: Design, Data Collection and Processing, Literature Search, Writing.

Data availability statement

The datasets used and/or analyzed during the current study are available from the corresponding author upon reasonable request.

Declaration of competing interest

The authors declare that they have no relevant or material interest that relates to this study.

Ethics

The study protocol was approved by the İzmir Katip Çelebi University Health Research Committee (No: 2024 – SAE--0161) and conducted in accordance with the Declaration of Helsinki.

Funding

The study is not funded by any company or institute.

REFERENCES

1. Ozturk B, Ozturk AN, Usumez A, Usumez S, Özer F. Temperature rise during adhesive and resin composite polymerization with various light curing sources. *Oper Dent*. 2004;29: 325-32
2. McCabe JF. Cure performance of light-activated composites by differential thermal analysis (DTA). *Dent Mater*. 1985;1: 231-4.
3. Lloyd CH, Joshi A, McGlynn E. Temperature rises produced by light sources and composites during curing. *Dent Mater*. 1986;2: 170-4.

4. Masutani S, Setcos JC, Schnell RJ, Phillips RW. Temperature rise during polymerization of visible light-activated composite resins. *Dent Mater.* 1988;4: 174-8.
5. Smail SRJ, Patterson CJW, Mclundie AC, Strang R. In vitro temperature rises during visible - light curing of a lining material and a posterior composite. *J Oral Rehabil.* 1988;15: 361-6.
6. Zach L, Cohen G. Pulp response to externally applied heat. *Oral Surg Oral Med Oral Pathol.* 1965;19: 515-30.
7. Baldissara P, Catapano S, Scotti R. Clinical and histological evaluation of thermal injury thresholds in human teeth: A preliminary study. *J Oral Rehabil.* 1997;24: 791-801.
8. Balestrino A, Verissimo C, Tantbirojn D, García-Godoy F, Soares CJ, Versluis A. Heat generated during light-curing of restorative composites: Effect of curing light, exotherm, and experiment substrate. *Am J Dent.* 2016;29: 234-40.
9. Ratih DN, Palamara JEA, Messer HH. Temperature change, dentinal fluid flow and cuspal displacement during resin composite restoration. *J Oral Rehabil.* 2007;34: 693-701.
10. Miletic V, Ivanovic V, Dzeletovic B, Lezaja M. Temperature changes in silorane-, ormocer-, and dimethacrylate-based composites and pulp chamber roof during light-curing. *J Esthet Restor Dent.* 2009;21: 122-31.
11. Rahiotis C, Patsouri K, Silikas N, Kakaboura A. Curing efficiency of high-intensity light-emitting diode (LED) devices. *J Oral Sci.* 2010;52: 187-195.
12. Flury S, Lussi A, Hickel R, Ilie N. Light curing through glass ceramics with a second- and a third-generation LED curing unit: Effect of curing mode on the degree of conversion of dual-curing resin cements. *Clin Oral Investig.* 2013;17: 2127-37
13. Jandt KD, Mills RW. A brief history of LED photopolymerization. *Dent Mater.* 2013;6: 605-617.
14. Udomthanaporn B, Nisalak P, Sawaengkit P. Shear bond strength of orthodontic bonding materials polymerized by high-intensity LEDs at different intensities and curing times. *Key Eng Mater.* 2017;723: 376-81.
15. Öztürk B, Üşümez A, Öztürk AN, Ozer F. In vitro assessment of temperature change in the pulp chamber during cavity preparation. *J Prosthet Dent.* 2004;9: 436-440.
16. Sato K. Relation between acid dissolution and histological alteration of heated tooth enamel. *Caries Res.* 1983;17: 490-5.
17. Schuchard A. A histologic assessment of low-torque, ultrahigh-speed cutting technique. *J Prosthet Dent.* 1975;34: 644-51.
18. Demirci M, Hiller KA, Bosl C, Galler K, Schmalz G, Schweikl H. The induction of oxidative stress, cytotoxicity, and genotoxicity by dental adhesives. *Dent Mater.* 2008;24: 362-371.
19. Schmalz, G., Arenholt-Bindslev, D. Biocompatibility of dental materials. Vol 1. Berlin: Springer; 2009
20. Murray PE, About I, Lumley PJ, Smith G, Franquin JC, Smith AJ. Postoperative pulpal and repair responses. *J Am Dent Assoc.* 2000;131: 321-29.
21. Lin M, Xu F, Lu TJ, Bai BF. A review of heat transfer in human tooth-Experimental characterization and mathematical modeling. *Dent Mater.* 2010;26: 501-513.
22. Singh R, Tripathi A, Dhiman RK, Kumar D. Intrapulpal thermal changes during direct provisionalization using various autopolymerizing resins: Ex-vivo study. *Med J Armed Forces India.* 2015;71: 313-20.
23. Daronch M, Rueggeberg FA, Hall G, De Goes MF. Effect of composite temperature on in vitro intrapulpal temperature rise. *Dent Mater.* 2007;23: 1283-8.
24. Hannig M, Bott B. In-vitro pulp chamber temperature rise during composite resin polymerization with various light-curing sources. *Dent Mater.* 1999; 15: 275-81.
25. Wang WJ, Grymak A, Waddell JN, Choi JJE. The effect of light curing intensity on bulk-fill composite resins: heat generation and chemomechanical properties. *Biomater Investig Dent.* 2021;8: 137-151.
26. Xu X, Sandras DA, Burgess JO. Shear bond strength with increasing light-guide distance from dentin. *J Esthet and Restor Dent.* 2006;18: 19-27.
27. Torres, C. Modern operative dentistry: Principles for clinical practice. Springer Nature; 2019
28. AlQahtani MQ, AlShaaifi MM, Price RB. Effects of single-peak vs polywave light-emitting diode curing lights on the polymerization of resin cement. *J Adhes Dent.* 2013;15: 547-51.
29. Maghaireh GA, Price RB, Abdo N, Taha NA, Alzraikat H. Effect of thickness on light transmission and vickers hardness of five bulk-fill resin-based composites using polywave and single-peak light-emitting diode curing lights. *Oper Dent.* 2019;44: 96-107.
30. De Oliveira DCRS, Rocha MG, Correr AB, Ferracane JL, Sinhoreti MAC. Effect of beam profiles from different light emission tip types of multiwave light-emitting diodes on the curing profile of resin-based composites. *Oper Dent.* 2019;44: 365-78.
31. Sahadi BO, Price RB, André CB, Sebold M, Bermejo GN, Dibb RGP, et al. Multiple-peak and single-peak dental curing lights comparison on the wear resistance of bulk-fill composites. *Braz Oral Res.* 2018;32: 122.
32. N. Thompson, A. Puckett, S. Phillips and G. Reeves, Potential hazards associated with photocuring dentin bonding agents. Fourteenth Southern Biomedical Engineering Conference, 1995; LA, USA

Research Article

DIAGNOSTIC VALUE OF CIRCULATING miRNA-16-5p AND miRNA-221-3p IN THYROID CANCER

Esin OKTAY^{1*}, Merve Bıyıklı ALEMDAR¹, Bilgin DEMİR¹, İbrahim Halil ERDOĞDU²,
Nesibe Kahraman ÇETİN², İmran Kurt ÖMÜRLÜ³, Engin GÜNEY⁴, Mustafa Gökhan
ÜNSAL⁵

¹Department of Medical Oncology, Adnan Menderes University Faculty of Medicine, Aydın, TURKIYE

²Department of Pathology, Adnan Menderes University Faculty of Medicine, Aydın, TURKIYE

³Department of Biostatistics, Adnan Menderes University Faculty of Medicine, Aydın, TURKIYE

⁴Department of Endocrinology, Adnan Menderes University Faculty of Medicine, Aydın, TURKIYE

⁵General Surgery Specialist, Private Practice, Aydın, TURKIYE

*Correspondence: esinct@gmail.com

ABSTRACT

Objective: The aim of this study is to investigate the usability of microRNA 16-5P and 221-3P levels as biomarkers in the diagnosis of thyroid cancer.

Materials and Methods: Patients who underwent thyroid surgery due to suspicious thyroid nodules were included in the study. A total of 142 patients who agreed to participate in the study had 3-5 cc venous blood taken into EDTA tubes and biochemistry tubes before the operation. In the postoperative period, 68 patients with malignant pathology results and 74 patients with benign pathology results were grouped as the control group. *miRNA-16-5p* and *miRNA-221-3p* levels were measured in serum samples taken from the patients. The levels of miRNA levels in malignant and benign patient groups were analyzed.

Results: The miRNA-16-5p and miRNA-221-3p levels of malignant patients were statistically significantly lower than those of benign patients ($p<0.001$). The analysis showed that miRNA-221-3p and miRNA-16-5p values had diagnostic value in predicting thyroid malignancy. Using a cut-off value of 21.69 for miRNA-221-3p, ROC curve analysis detected 89.7% sensitivity and 71.4% specificity (AUC=0.779, $p<0.001$). Using a cut-off value of 15.34 for miRNA-16-5p, ROC curve analysis detected 32.3% sensitivity and 100% specificity (AUC=0.708, $p<0.001$).

Conclusion: It was observed that *miRNA-221-3p* and *miRNA-16-5p* values had diagnostic value in predicting thyroid malignancy and could be potential biomarkers.

Keywords: miRNA, Biomarkers, Thyroid cancer

Received: 18 April 2025

Revised: 15 June 2025

Accepted: 17 June 2025

Published: 23 June 2025



Copyright: © 2025 by the authors. Published by Aydın Adnan Menderes University, Faculty of Medicine and Faculty of Dentistry. This article is openly accessible under the Creative Commons Attribution-NonCommercial 4.0 International (CC BY-NC 4.0) License.

INTRODUCTION

Thyroid cancer is the most common endocrine malignancy. The most reliable method for preoperative detection of thyroid cancer is currently thyroid fine needle aspiration biopsy (FNAB). There is currently no reliable biomarker that can predict thyroid cancer before surgery (1). MicroRNAs (miRNAs), a class of small non-protein coding RNAs, contribute to the control of gene expression and affect vital processes such as development, cell differentiation, proliferation, and programmed cell death. More than half of miRNA genes are located in genomic regions commonly associated with cancer (especially fragile sites), highlighting their potential role in tumor development (2). Several studies have compared miRNA expression levels in cytological samples and pathological tissue samples from patients with and without papillary thyroid cancer and have revealed different miRNA expression profiles in thyroid cancer tissues (3–6). However, studies evaluating circulating miRNA levels in thyroid cancer patients are still insufficient. miRNA-16-5p is a microRNA that stands out with its tumor suppressor function in various malignancies. It is thought that miRNA-16-5p, which plays a role in basic biological processes such as cell cycle regulation, induction of apoptosis and suppression of proliferation, may also be effective in the pathogenesis of thyroid cancer with similar mechanisms (7). Some studies have shown that miRNA-16-5p levels are significantly reduced in papillary thyroid cancer patients, and it has been suggested that this reduction may be associated with tumor formation and progression (8). Therefore, evaluation of miRNA-16-5p levels may be valuable as a non-invasive biomarker in the early diagnosis of thyroid cancer. miRNA-221-3p is an oncogenic microRNA known to be expressed in many types of cancer. It has been shown that it may contribute to tumor growth by affecting gene pathways that promote cell proliferation and suppress apoptosis (9). Studies on thyroid cancer have shown that miRNA-221-3p levels increase, especially in papillary thyroid carcinoma tissues (10). However, some previous miRNA studies in thyroid cancer patients have yielded contradictory results. The prognostic value of miRNA levels in thyroid cancer and their usability as biomarkers are still controversial. In our study, we aimed to investigate the usability of circulating microRNA levels as biomarkers in the preoperative diagnosis of thyroid cancer.

MATERIALS AND METHODS

Patients who underwent thyroid surgery at Adnan Menderes University Faculty of Medicine Hospital

between November 2019 and November 2020 were included in the study. 68 patients whose postoperative pathology results were malignant and 74 patients who had thyroid surgery for various indications and whose pathology results were benign were included in the study as the control group. A total of 142 patients were included in the study. Prior to the study, approval was obtained from the Adnan Menderes University Faculty of Medicine Clinical Research Ethics Committee (Date of Approval: 10.10.2019 Protocol No: 2019/120). After receiving ethics committee approval, the study was conducted on patients who were decided to undergo surgery and who had thyroid surgery at the Department of General Surgery. The patients and control group were given an explanation of the study's purpose and the procedures to be carried out. Written informed consent forms were prepared regarding the study and their written informed consents were obtained.

Patient selection

Prior to surgery, 3–5 cc of venous blood was collected from patients who consented to participate in the study, using EDTA and biochemistry tubes. Postoperatively, patients were classified as having either benign or malignant conditions based on their pathological findings.

Circulating miRNA expression analysis

Venous blood samples taken from patients were stored at -80 degrees. Samples were isolated using a miRNA-specific kit. miRNA isolation was performed using GeneAll, Hybrid-R miRNA (Cat no:325-150). miRBase database was used in primer design. After the samples were isolated, they were stored at -80°C again. It was performed using 142 miRNA and control primers (U6). Complementary DNA (cDNA) synthesis was performed with the obtained miRNA using WizScript™ cDNA Synthesis Kit (High Capacity) W2211. Complementary DNA (cDNA) synthesis was performed using stem-loop primers. Stem-loop primers specific to these miRNAs were designed. These primers are considered the most reliable method since they specifically bind to the miRNA sequence when synthesizing cDNA from miRNA (11). cDNA synthesis was performed using primers specific to each miRNA from the obtained miRNAs. Each sample was cDNAed with its own stem-loop primer. SYBR Green-based Real Time Polymerase Chain Reaction (PCR) was established from the obtained cDNAs. Samples were studied in 2 replicates.

Statistical analysis

Statistical analyses were performed using SPSS version 27 software. After the distribution structures of quantitative

data were evaluated using the Kolmogorov-Smirnov test for normal distribution, independent samples t-test was used in independent groups for comparison of variables that provided the assumption of normal distribution between groups, and descriptive statistics were shown as mean±standard deviation. For quantitative variables that did not meet the assumption of normality, the Mann-Whitney U test or Kruskal-Wallis test was applied depending on the number of groups. Descriptive data were presented as median (25–75 percentiles). Chi-square test was used for analysis of qualitative data, and the results were given as percentages. Receiver Operating Characteristics (ROC) curve analysis was used to evaluate the diagnostic value of serum miRNA-16-5p and miRNA-221-3p levels in predicting thyroid cancer. For the identified significant cutoff values, corresponding sensitivity and specificity were calculated. It was considered statistically significant when the p value was <0.05.

RESULTS

The study included 142 patients scheduled for thyroid surgery at Adnan Menderes University Faculty of Medicine Hospital between November 2019 and November 2020. According to the postoperative pathology results, 68 of the patients were grouped as malignant (56 females, 12 males) and 74 as benign (61 females, 13 males). Both groups were similar in terms of

Table 1. Patient characteristics

	Malign (n=68)	Benign (n=74)
Age (median)	48 (35.5-62)	52 (45.75-61)
Sex	56 female 12 male	61 female 13 male
miRNA-16-5p (median)	17.61 (14.92-19.46)	19.32 (17.68-21.24)
miRNA-221-3p (median)	18.23 (16.30-19.84)	26.13 (20.55-28.67)

gender ($p>0.05$). The median age of all patients was 50 (42-61). The median age of malignant patients was 48 (35.5-62), and the median age of benign patients was 52 (45.75-61), and no significant statistical difference was found between the two groups ($p>0.05$).

According to postoperative pathology results, 38 (55.9%) of the cases with thyroid cancer were diagnosed as micropapillary thyroid cancer, 27 (39.7%) as papillary thyroid cancer, 2 (2.9%) as thyroid medullary cancer, and 1 (1.5%) as follicular thyroid cancer.

miRNA-16-5p level was median 19.32 (17.68-21.24) in benign patients and median 17.61 (14.92-19.46) in malignant patients. miRNA-221-3p level was median 26.13 (20.55-28.67) in benign patients and median 18.23 (16.30-19.84) in malignant patients. miRNA-16-5p and miRNA-221-3p levels of malignant patients were statistically

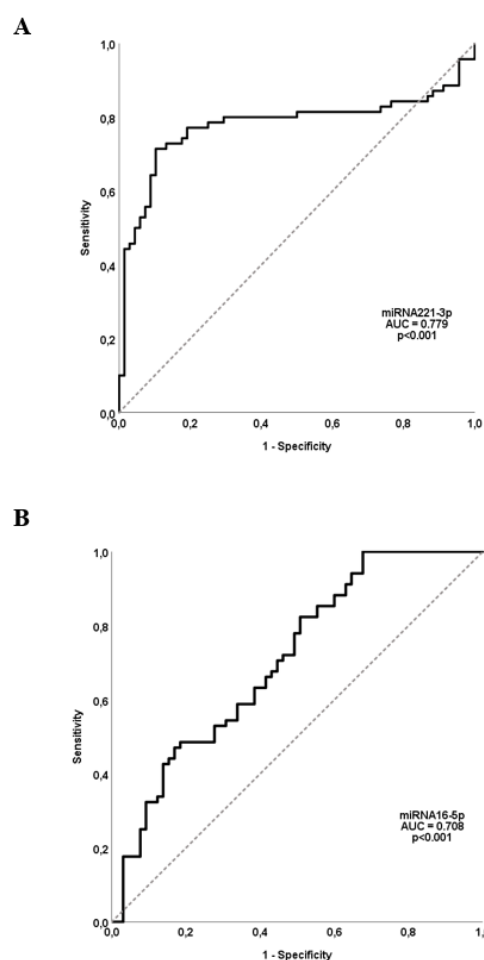


Figure 1. (A) miRNA-221-3p ROC curve. (B) miRNA-16-5p ROC curve.

significantly lower than in benign patients ($p<0.001$). When the echogenicity status was classified as hypoechoic, isoechoic and hyperechoic and miRNA-221-3p levels were examined, a significant difference was found between the 3 groups ($p=0.011$). When post-hoc analysis was performed, the miRNA-221-3p value in isoechoic patients was significantly higher than the values in hypoechoic patients ($p=0.016$). In patients with microcalcification, both miRNA levels were found to be lower than in patients without microcalcification ($p=0.006$ for miRNA-221-3p,

Table 2. ROC Curve Analysis Results

	miRNA-221-3p	miRNA-16-5p
AUC	0.779	0.708
95% Confidence interval	0.700-0.845	0.623-0.784
Cut-off	21.69	15.34
Sensitivity	89.7%	32.3%
Specificity	71.4%	100%
p value	<0.001	<0.001

p=0.016 for miRNA-16-5p). There was no significant difference between the miRNA levels evaluated in our study and other parameters used in the distinction of malignant/benign in ultrasonography such as macrocalcification, halo, periphery calcification, nodule border pattern, nodule size and multinodularity (p>0.05). The analysis showed that miRNA-221-3p and miRNA-16-5p values had diagnostic value in predicting thyroid malignancy. Using a cut-off value of 21.69 for miRNA-221-3p, ROC curve analysis detected 71.4% specificity and 89.7% sensitivity (AUC=0.779, p<0.001). Using a cut-off value of 15.34 for miRNA-16-5p, ROC curve analysis detected 100% specificity and 32.3% sensitivity (AUC=0.708, p<0.001).

DISCUSSION

Thyroid cancer is becoming increasingly common worldwide. While it is usually indolent, it can be aggressive in certain patients. Diagnosis is typically achieved through ultrasound and fine-needle aspiration biopsy, but in some cases, distinguishing between benign and malignant nodules remains challenging.

In recent years, miRNAs have received growing attention due to their potential roles in cancer diagnosis, prognosis, and treatment response. Most studies have investigated miRNA expression in tumor tissues. However, this method is invasive and requires surgical intervention. In contrast, measuring circulating miRNA levels in serum offers several advantages: it is non-invasive, easy to perform, yields rapid results, provides preoperative diagnostic insight, and allows for serial monitoring. Despite these benefits, studies on circulating miRNAs have shown inconsistent results, which may be attributed to individual patient-related factors or external influences such as circadian rhythm (12).

Several studies have shown that miRNA-16-5p and miRNA-221-3p are involved in the molecular mechanisms of thyroid and other cancers. In our study, serum levels of miRNA-16-5p and miRNA-221-3p were significantly lower in malignant cases compared to benign ones. ROC curve analysis demonstrated their diagnostic utility in

detecting thyroid malignancy, suggesting that these miRNAs may serve as valuable serum biomarkers.

miRNA-16-5p has been found to be downregulated in various cancers. For instance, its expression is reduced in osteosarcoma, and its overexpression inhibits cell migration, proliferation, and invasion (13). Ruan et al. reported that miRNA-16-5p expression was significantly lower in breast cancer tissues compared to non-cancerous tissues, with lower expression associated with higher tumor grade (14). Additionally, miRNA-16-5p was shown to inhibit cell proliferation and migration by targeting the actin-binding protein anillin in breast cancer cells (15). Similarly, Feng et al. observed downregulated miRNA-16-5p in PTC tissues compared to normal thyroid tissues (16). Our findings, which show significantly lower serum miRNA-16-5p levels in malignant thyroid nodules, align with previous reports of tissue-level downregulation. This supports the hypothesis that miRNA-16-5p plays a tumor-suppressive role. Importantly, our use of serum—rather than tissue—highlights the potential for a non-invasive, clinically applicable biomarker. However, further studies are needed to confirm whether serum levels accurately reflect intratumoral expression and whether they are sufficiently stable for routine clinical use.

The role of miRNA-221-3p in cancer remains complex, with varying findings reported. Fang et al. found lower levels of miRNA-221-3p in breast cancer tissues compared to normal tissues (17), and reduced expression was also associated with poorer survival in high-risk prostate cancer patients (18). Rogucki et al. supported its potential role in the diagnosis of PTC (19). Conversely, other studies have suggested an oncogenic function for miRNA-221. One study showed that miRNA-221 promotes proliferation and invasion in PTC cells by suppressing TIMP3 expression (20). Furthermore, both miRNA-221-3p and miRNA-222-3p were reported to be upregulated in thyroid cancer cell lines and were associated with treatment response (21).

However, findings on serum miRNA-221-3p levels have been inconsistent. Rosignolo et al. found no significant difference between serum miRNA-221-3p levels in PTC and benign nodule groups (22). Zhang et al. reported elevated serum levels in PTC patients compared to healthy controls, with associations to tumor location, extrathyroidal invasion, stage, and lymph node metastasis (23). Another study also found increased preoperative serum levels in PTC patients, though no correlation with clinical features was observed (24).

In contrast, our study found that serum miRNA-221-3p levels were significantly lower in malignant cases. Using a cut-off value of 21.69, ROC curve analysis showed that miRNA-221-3p could predict thyroid malignancy with a sensitivity of 89.7% and specificity of 71.4% (AUC = 0.779, $p < 0.001$). These results support the potential use of serum miRNA-221-3p as a diagnostic marker.

One of the major factors contributing to inconsistencies in circulating miRNA levels across studies is the variability in RNA isolation techniques. The efficiency and purity of miRNA extraction from serum or plasma samples can vary significantly depending on the kits and protocols employed, directly impacting quantification results. Furthermore, pre-analytical variables such as sample collection, handling, and storage conditions are crucial in preserving miRNA stability. Another critical aspect is the choice of normalization strategy; while some studies utilize endogenous controls like U6 small nuclear RNA, others prefer exogenous spike-in controls such as cel-miR-39. These differing approaches can substantially affect data comparability and interpretation. This heterogeneity in RNA isolation and normalization methods may partly explain the conflicting reports regarding serum miRNA-221-3p expression in thyroid malignancy.

Interestingly, although our study found lower serum levels of miRNA-221-3p in malignant cases, several previous studies have reported increased expression of this miRNA, particularly in thyroid tumor tissues. For example, Zhang et al. demonstrated elevated serum levels in patients with papillary thyroid carcinoma. This discrepancy may arise from differences in sample types (serum versus tissue), ethnic variation, tumor heterogeneity, or methodological differences in RNA quantification. Additionally, the dynamic nature of circulating miRNAs—affected by factors such as degradation, exosomal release, and protein binding—may lead to contrasting serum levels compared to tissue expression. Therefore, further prospective studies are warranted to clarify the context-dependent expression patterns of miRNA-221-3p in thyroid malignancy.

This study has several limitations, including the small sample size, variability in blood collection timing, and the lack of postoperative miRNA follow-up measurements. Moreover, the limited cohort size precluded stratified analyses between thyroid cancer subtypes. To enhance the robustness and generalizability of these findings, future studies should incorporate larger, well-characterized patient populations, employ standardized blood sampling

protocols, and implement longitudinal miRNA monitoring at clearly defined postoperative intervals.

CONCLUSION

Based on the findings of this study, miRNA-221-3p and miRNA-16-5p appear to have diagnostic value in predicting thyroid malignancy and may serve as potential biomarkers. Overall, the results of this study contribute to the growing body of evidence supporting the use of circulating miRNAs as novel biomarkers in thyroid cancer and may provide a foundation for future investigations in this area.

Acknowledgments

Adnan Menderes University Faculty of Medicine Medical Oncology Clinic staff

Authorship contributions

EO, MBA and EG designed the study; EO, MBA, BD, İHE, NKÇ and MGÜ collected the data; İKÖ, MBA and EO carried out statistical analysis; EO, MBA performed the literature search; EG, MGÜ and EO supervised the study; MBA and EO prepared and revised the manuscript. All authors gave the final approval of the version to be published.

Data availability statement

The data that support the findings of this study are available from the corresponding author, [E.O.], upon reasonable request.

Declaration of competing interest

The authors have no conflicts of interest to declare.

Ethics

Ethics committee approval was obtained from the Clinical Research Ethics Committee of Adnan Menderes University Faculty of Medicine Clinical Research Ethics Committee (Date of Approval: 10.10.2019 Protocol No: 2019/120).

Funding

The study was carried out without financial support from any institution.

REFERENCES

1. Haugen BR, Alexander EK, Bible KC, Doherty GM, Mandel SJ, Nikiforov YE, et al. 2015 American Thyroid Association management guidelines for adult patients with thyroid nodules

- and differentiated thyroid cancer: the American Thyroid Association guidelines task force on thyroid nodules and differentiated thyroid cancer. *Thyroid*. 2016;26(1):1-133.
2. Bartel DP. MicroRNAs: genomics, biogenesis, mechanism, and function. *cell*. 2004;116(2):281-97.
3. Boufraquech M, Klubo-Gwiedzinska J, Kebebew E. MicroRNAs in the thyroid. *Best Practice & Research Clinical Endocrinology & Metabolism*. 2016;30(5):603-19.
4. Liang W, Xie Z, Cui W, Guo Y, Xu L, Wu J, et al. Comprehensive gene and microRNA expression profiling reveals a role for miRNAs in the oncogenic roles of SphK1 in papillary thyroid cancer. *Journal of cancer research and clinical oncology*. 2017;143:601-11.
5. Wang Y, Gong W, Yuan Q. Effects of miR-27a upregulation on thyroid cancer cells migration, invasion, and angiogenesis. *Genet Mol Res*. 2016;15(4):1-10.
6. Zhao H, Tang H, Huang Q, Qiu B, Liu X, Fan D, et al. MiR-101 targets USP22 to inhibit the tumorigenesis of papillary thyroid carcinoma. *American journal of cancer research*. 2016;6(11):2575.
7. Cimmino A, Calin GA, Fabbri M, Iorio MV, Ferracin M, Shimizu M, et al. miR-15 and miR-16 induce apoptosis by targeting BCL2. *Proceedings of the National Academy of Sciences*. 2005;102(39):13944-9.
8. Nedaenia R, Manian M, Jazayeri M, Ranjbar M, Salehi R, Sharifi M, et al. Circulating exosomes and exosomal microRNAs as biomarkers in gastrointestinal cancer. *Cancer gene therapy*. 2017;24(2):48-56.
9. Visone R, Croce CM. MiRNAs and cancer. *The American journal of pathology*. 2009;174(4):1131-8.
10. Pallante P, Visone R, Ferracin M, Ferraro A, Berlingieri M, Troncone G, et al. MicroRNA deregulation in human thyroid papillary carcinomas. *Endocrine-related cancer*. 2006;13(2):497-508.
11. Varkonyi-Gasic E, Hellens RP. Quantitative stem-loop RT-PCR for detection of microRNAs. *RNAi and Plant Gene Function Analysis: Methods and Protocols*. 2011:145-57.
12. Suárez B, Solé C, Márquez M, Nanetti F, Lawrie CH. Circulating microRNAs as cancer biomarkers in liquid biopsies. *Systems Biology of MicroRNAs in Cancer*. 2022:23-73.
13. Gu Z, Li Z, Xu R, Zhu X, Hu R, Xue Y, et al. miR-16-5p suppresses progression and invasion of osteosarcoma via targeting at Smad3. *Frontiers in Pharmacology*. 2020;11:1324.
14. Ruan L, Qian X. MiR-16-5p inhibits breast cancer by reducing AKT3 to restrain NF-κB pathway. *Bioscience reports*. 2019;39(8):BSR20191611.
15. Wang Z, Hu S, Li X, Liu Z, Han D, Wang Y, et al. MiR-16-5p suppresses breast cancer proliferation by targeting ANLN. *BMC cancer*. 2021;21:1-12.
16. Feng X, Dong X, Wu D, Zhao H, Xu C, Li H. Long noncoding RNA small nucleolar RNA host gene 12 promotes papillary thyroid carcinoma cell growth and invasion by targeting miR16-5p. 2020.
17. Fang Y, Zhang Q, Chen Z, Guo C, Wu J. Clinical significance and immune characteristics analysis of miR-221-3p and its key target genes related to epithelial-mesenchymal transition in breast cancer. *Aging (Albany NY)*. 2024;16(1):322.
18. Krebs M, Solimando AG, Kalogirou C, Marquardt A, Frank T, Sokolakis I, et al. miR-221-3p regulates VEGFR2 expression in high-risk prostate cancer and represents an escape mechanism from sunitinib in vitro. *Journal of Clinical Medicine*. 2020;9(3):670.
19. Rogucki M, Sidorkiewicz I, Niemira M, Dziecioł JB, Buczyńska A, Adamska A, et al. Expression profile and diagnostic significance of MicroRNAs in papillary thyroid cancer. *Cancers*. 2022;14(11):2679.
20. Diao Y, Fu H, Wang Q. MiR-221 exacerbate cell proliferation and invasion by targeting TIMP3 in papillary thyroid carcinoma. *American Journal of Therapeutics*. 2017;24(3):e317-e28.
21. Ye T, Zhong L, Ye X, Liu J, Li L, Yi H. miR-221-3p and miR-222-3p regulate the SOCS3/STAT3 signaling pathway to downregulate the expression of NIS and reduce radiosensitivity in thyroid cancer. *Experimental and Therapeutic Medicine*. 2021;21(6):652.
22. Rosignolo F, Sponziello M, Giacomelli L, Russo D, Pecce V, Biffoni M, et al. Identification of thyroid-associated serum microRNA profiles and their potential use in thyroid cancer follow-up. *Journal of the Endocrine Society*. 2017;1(1):3-13.
23. Zhang Y, Xu D, Pan J, Yang Z, Chen M, Han J, et al. Dynamic monitoring of circulating microRNAs as a predictive biomarker for the diagnosis and recurrence of papillary thyroid carcinoma. *Oncology letters*. 2017;13(6):4252-66.
24. Verrienti A, Pecce V, Grani G, Del Gatto V, Barp S, Maranghi M, et al. Serum microRNA-146a-5p and microRNA-221-3p as potential clinical biomarkers for papillary thyroid carcinoma. *Journal of Endocrinological Investigation*. 2024:1-13.